

PhD thesis, Doctorate Research Program in Plant Biology
XVII cycle (2002-2005)

[Settore scientifico disciplinare: BIO/01]

THE ELONGATOR COMPLEX: ITS FUNCTION IN GERMINATION AND LEAF DEVELOPMENT

CANDIDATE: FALCONE ANDREA

Supervisor:
Prof. Maria Beatrice Bitonti

Co-supervisor:
Prof. Mieke Van Lijsebettens

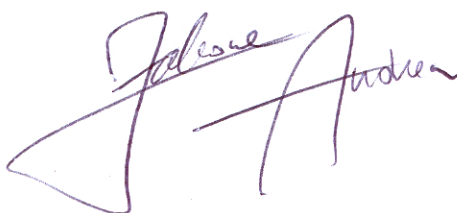
Coordinator: Prof. Anna Maria Innocenti

University of Calabria, Department of Ecology
November 2006

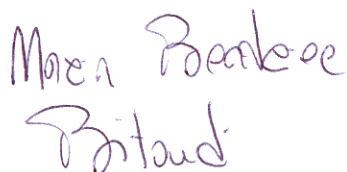
PhD thesis, Doctorate Research Program in Plant Biology,
XVII cycle (2002-2005)

The Elongator complex: its function in leaf development and germination

Candidate: Andrea Falcone



**Tutor: Prof.
Maria Beatrice
Bitonti**



**Co-tutor: Prof.
Mieke
Van Lijsebettens**

**Coordinator: Prof.
Anna Maria
Innocenti**



Settore disciplinare scientifico: BIO/01

**University of Calabria, Department of Ecology
November 2006**

*Alla mia Famiglia
per avermi concesso un altro punto di vista sulla Vita
e a tutti coloro che mi sono fedeli
nell'Amicizia e Amore...*

*Al Governo Berlusconi per aver tagliato i fondi per la Ricerca
e a quello Prodi per averci provato...*

"L'Italia è una Repubblica fondata sul lavoro"

*A tutti coloro che lavorano per passione e necessità o sono in cerca di proposte
e stabilità.*

Graxie.

Viviamo ancora in tempi interessanti? :-)

Andrea Falcone

AIM OF THE WORK	2
INTRODUCTION	3
ARABIDOPSIS THALIANA AS A MODEL PLANT	3
<i>The history of Arabidopsis thaliana</i>	3
<i>Arabidopsis nomenclature, characteristics and ecotypes</i>	6
<i>Timetable for growth-stage based analysis</i>	7
LEAF DEVELOPMENT	8
<i>The maintenance of the SAM's identity and the initiation of leaf primordium</i>	8
<i>Leaf morphogenesis in flowering plants</i>	9
<i>Primary morphogenesis: acquisition of the dorsiventral asymmetry</i>	10
<i>Secondary morphogenesis: acquisition of the proximal-distal and lateral polarity</i>	11
<i>Hormones, light and leaf development</i>	12
<i>Heteroblasty in Arabidopsis</i>	12
THE TRANSCRIPTION MACHINERY OF EUKARYOTES	13
<i>Gene expression in eukaryotes</i>	13
<i>The transcription cycle and the formation of a transcript</i>	13
<i>General transcription factors and the eukaryotic promoters</i>	14
<i>Formation of the PIC (Pre-Initiation Complex) assembly</i>	15
<i>RNAPII initiation regulation</i>	17
<i>RNAPIIa/o, Mediator, Elongator and the transcript elongation</i>	17
<i>The Elongator complex</i>	18
<i>Plant Elongator</i>	18
<i>Transcript termination</i>	19
SUCROSE IN PLANTS	20
<i>General characteristics</i>	20
<i>Sucrose transport</i>	20
<i>Sucrose carriers in Arabidopsis</i>	21
<i>Sucrose synthesis and cleavage: sucrose synthases and invertases</i>	21
<i>Sucrose metabolism</i>	22
<i>Sugar-sensing mechanisms and general gene regulation</i>	23
RESULTS	24
<i>CYTOLOGICAL INVESTIGATIONS OF THE ARABIDOPSIS THALIANA ELO1 MUTANT GIVE NEW INSIGHTS INTO LEAF LATERAL GROWTH AND ELONGATOR FUNCTION</i>	24
CONCLUSION	34
REFERENCES	36
ANNEX: VIB'S WORK	42
RESULTS	42
1. <i>AtELP genes and T-DNA insertion lines</i>	42
2. <i>Morphological comparison between first and third leaves of the DRL1 overexpression line 10B5 (in Ler background) and the wild-type Ler. PCN analysis on RON1 first and third leaves</i>	54
3. <i>Map Based Cloning (MBC): the TRN1 experience</i>	61
4. <i>Bioinformatics: AtELP1p homologue of Saccharomyces cerevisiae ELP1/TOT1/IKI3p</i>	64
MATERIALS AND METHODS	65
REFERENCES	70
PUBLICATIONS, POSTERS AND WORKSHOPS	71

Aim of the work

My PhD work has been focused on the cytophysiological characterization of the Elongator complex in *Arabidopsis thaliana*. The holo-Elongator complex is made of two subcomplexes: ELP1, ELP2 and ELP3 that compose the core-Elongator, and ELP4, ELP5 and ELP6 that constitute the accessory subcomplex. The predicted function of the complex is suggested by ELP3, which contains a HAT domain (histone acetyltransferase activity) that causes chromatin relaxation through histone acetylation and promotes transcription elongation of several genes.

Several experimental approaches have led to a model of Elongator's function in transcription elongation and overall energetic metabolism regulation, in a stage-specific and sucrose-mediated way.

Initially, in my first year work, performed in Ghent (Belgium) under the supervision of Prof. Mieke Van Lijsebettens, several genes presumably involved in the Elongator complex were analyzed for T-DNA insertions and heterozygosity at the locus, to find new alleles for the *Arabidopsis thaliana* homologues of the Yeast Elongator complex.

Phenotype scoring and germination tests were done to further ascertain the mutant genotypes and phenotypes.

In addition, in order to investigate leaf lateral growth and mechanisms such as cell division and expansion, the DRL1ox10B5 (an overexpression line of DEFORMED ROOTS AND LEAVES1) and RON1 (ROTUNDA1) leaf mutants were investigated through morphometric analysis. Finally, under the supervision of Dr. Cnops Gerda, I participated at the final step of the map-based cloning of the TRN1 (TORNADO1), amplifying and sequencing a small genomic region in order to find, through sequence alignment, the putative TRN1 locus.

Next, at the University of Calabria, I investigated the relationships between leaf development, growth conditions and Elongator's function by studying growth responses, under different nutrient and environmental conditions, in both wild type and *elo1* 'narrow leaves' mutants.

These mutants belong to the *elongata* class and have a mutation in one of the components of the histone acetyl transferase Elongator complex. Through germination assays, morphometric analysis and electron microscopy I show that light response, stress tolerance and sucrose metabolism are affected in the Elongator mutant.

Performing an analysis of the genes differentially expressed in the *elo* mutants (data not shown for VIB's patenting reasons), which have been identified by Fleury Delphine (pers. comm.) I propose a functional model for the Elongator complex that is sucrose-dependant and stage-specific.

My PhD work has been achieved through a collaboration with Prof. Mieke Van Lijsebettens, who works at the VIB (Flemish Interuniversity Institute for Biotechnology, Department of Plant Systems Biology, Technologiepark 927, 9052 Ghent, Belgium) and thanks to the supervision of Prof. Maria Beatrice Bitonti of the Università della Calabria (Dipartimento di Ecologia, Via ponte P. Bucci, Cubo 6B, 87036, Arcavacata di Rende, CS, Italia).

This project was funded by the European Union in the frame of the PREDEC project (HPMT-CT-2000 00088) and the MIUR (ex 60% grant).

Introduction

Arabidopsis thaliana as a model plant

The history of *Arabidopsis thaliana*

The flowering dicotyledonous plant named *Arabidopsis thaliana* (mouse-ear cress or wall cress) and ‘Arabetta comune’ in Italian is now widely used as a model system in molecular and developmental biology, as well as in physiology and cell biology. *Arabidopsis* provides an ideal model system for studying genetic and cellular interactions during development, but also genetic basis of species introductions, range expansion and adaptation to broad geographies, all important aspects of modern plant ecology and evolutionary biology.

Indeed, *Arabidopsis* is to plant biologists what the white mouse is to medical researchers. The organism is highly amenable to conventional and molecular genetic approaches [1], its architecture and development are well characterized and the sequence of the entire genome is accessible since year 2000. Since it is currently considered such an important weed for plant research and it is used as a favorite experimental organism for many aspects of plant biology, its history becomes fascinating and necessary to be told [2, 3].

Arabidopsis was first discovered in the 16th century by Johannes Thal (1542-1583) in the Harz Mountains in Germany and was initially named *Pilosella siliquosa*.

In 1753, thanks to the Swedish botanist Carolus Linnaeus (1707-1778) its name became *Arabis thaliana*, in honor of Johannes Thal.

It was only in 1841 that taxonomist Gustav Heynhold changed definitively *Arabis thaliana* in *Arabidopsis thaliana* (L.) Heynh.

In 1873, Alexander Braun (1809-1877) described the first *Arabidopsis* mutant, found in a field near Berlin [4]. Its phenotypical description (lack of pistils and stamens, transformation of stamens to petals and rise of a new flower in place of the gynoeceium) is considered nowadays as the result of a mutation in the AGAMOUS gene, cloned in 1990.

The end of the 19th century became very important for plant biology: in 1894, Eduard Strasburger (1844-1912), who is currently considered the founder of modern cytology, published ‘Lehrbuch der Botanik für Hochschulen’, (‘Textbook of Botany for Universities’, 35th edition still in publication), while other scientists in 1900 rediscovered Mendel’s work on heredity. Cytology and Genetics raised new scientific challenges and for a few decades new suitable animal and plant models were studied to facilitate scientific investigations.

On this basis, Friedrich Laibach (1885–1967), which was a Strasburger's graduate student in Bonn, Germany, accurately observed that *Arabidopsis* had only 5 chromosomes ($2n=10$), the lowest odd number known up at that time for a plant. In 1907 he published his PhD thesis ‘The question of individuality of chromosomes in plant kingdom’ and gave an account of the chromosome number of several plants [5]. Laibach, upon graduation, continued to work intermittently with *Arabidopsis* in the next 30 years, but only in 1943 he described for the first time the potential of this plant as a model organism for genetic studies [6].

Actually, he was in complete disagreement with the Russian genetist N.N. Titova, who went in 1935 on an expedition to find a model plant that could be used in genetics and cytogenetics and finally discarded *Arabidopsis* because of its small chromosome number (incorrectly stated by Titova, who thought that the chromosome haploid number was three, instead of 5), the small size of the plant (which was considered a drawback), and the inability to distinguish different chromosome pairs. It does not appear that *Arabidopsis* was ever used in the laboratory by Titova and her colleagues.

In 1937 F. Laibach, who was particularly interested in natural variation and the effects of light quality and quantity on flowering time and seed dormancy, started to collect *Arabidopsis* ecotypes, being very attracted from the large variation in physiological traits among accessions.

In 1947 Laibach's graduate student E. Reinholz published a detailed study on X-ray mutagenesis, which led to the first collection of *Arabidopsis* mutants. Nonetheless, he also discovered that a late flowering plant could be induced in an early flowering type by those mysterious rays.

Since these first results on mutant plants a large set of new mutant collections was created in the ‘50s and ‘60s. In those years, researchers such as Langridge, Napp-Zinn's, Hussein, Cetl, Rédei, Van der Veen, Veleminsky, Röbbelen, Lawrence and Müller demonstrated the utility of *Arabidopsis* for laboratory studies.

Soon after, it became evident that the *Arabidopsis* research community had to organize a common scientific platform and a conference to exchange information on *Arabidopsis*: in 1964 a newsletter called AIS,

Arabidopsis Information Service was founded by F. Laibach, A. Müller, G. Rédei and J. Veleminsky (constituting the first advisory board, while G. Röbbelen served as first editor) and in 1965, the First International *Arabidopsis* Conference was held in Göttingen, Germany. In the same year, F. Laibach decided to retire and Röbbelen went for the curator role for Laibach's *Arabidopsis* ecotype collection.

In 1976, Bennet and Smith demonstrated that *Arabidopsis* had the smallest nuclear DNA content of all the Angiosperms analyzed.

The widespread adoption of *Arabidopsis* as a model plant, followed by the current revolution in plant genetics, physiology, and molecular genetics, occurred in the 1980s.

The idea that plant biologists should concentrate on a model organism was then under intense discussion and a number of proposals were made such as using petunia because of its ease of transformation and the availability of haploid lines, or using tomato because of the availability of mutants.

One of the most influential *Arabidopsis* papers from the early 1980s was a report from Meyerowitz's lab that *Arabidopsis* had only ~70 Mb of nuclear DNA. Many people were excited by the low DNA content of *Arabidopsis* because of the technical difficulties of doing Southern blots on plants and of cloning genes from organisms with large genomes.

What swung the balance in favor of *Arabidopsis* is not certain, though several contributions can be pointed out. One was the demonstration that mutational analysis could be done to saturation in laboratory conditions, and therefore that informative mutations in any gene could be obtained in screens of a practicable size. Another was the demonstration that *Arabidopsis* has a very small genome and is therefore convenient for gene cloning, which at that time was difficult for large-genome organisms; yet another was the demonstration that *Arabidopsis* could be transformed with exogenous DNA.

These discoveries followed the publication of the first complete linkage map of *Arabidopsis* (a map showing distances between mutated genes in terms of recombination frequency), published by Koorneef and co-workers in 1983. This map had 76 morphological markers. Such maps allowed researchers to see the approximate positions of heritable factors (genes and regulatory elements) on chromosomes. In addition, it was clear from even earlier work that embryo lethals could be produced and studied in detail, and that *Arabidopsis* could be used as a model system for genetic analysis of plant embryo development.

Reasons to adopt *Arabidopsis* as a model system for plant development, physiology, and molecular genetics were published very closely from 1985 to 1987, giving strength and conviction to a fast growing plant researcher community.

Production of tagged mutant collections began and methods were developed making it possible to genetically engineer *Arabidopsis* using *Agrobacterium tumefaciens*.

The first gene sequences were published in 1986 and T-DNA-mediated transformation of *Arabidopsis* was also first established in 1986. This was followed by the first restriction fragment-length polymorphism (RFLP) map in 1988, T-DNA insertional cloning, map-based cloning and the extremely efficient vacuum infiltration method of transformation. Indeed, the production of physical maps based on restriction fragment length polymorphisms (RFLPs) began during this time, allowing genes to be located and characterized even when their identity was unknown.

In 1990, scientists outlined a long-range plan for the Multinational Coordinated *Arabidopsis thaliana* Genome Research Project. The widespread adoption of *Arabidopsis* as a laboratory model system in plant biology has led to additional meetings.

In the fall of 1996, the *Arabidopsis* Genome Initiative began a collaborative effort to determine the complete sequence of the *Arabidopsis thaliana* genome, which finally was completely sequenced in year 2000. The sequencing of the genome has the potential to lead to the understanding of the function of the proteins coded by those genes.

Scientists from the National Science Foundation have collectively set a goal to understand the functions of all 25,000 *Arabidopsis* genes by the year 2010. The publication of this goal has only resulted in the number of labs and institutions growing even more.

Currently, over 11,000 researchers and over 4000 organizations around the world are studying *Arabidopsis*.

The study of this plant has been made so effective partly through the *Arabidopsis* Information Resource (TAIR) [7], an online website where scientists share much experimental information on *Arabidopsis*.

The goal of this website is to facilitate interaction within a research community that aims to understand *Arabidopsis* better.

A summary is presented in Fig.1

PRE-MOLECULAR ERA

- 1570 Johannes Thal first identifies *Pilosella siliquosa*
- 1753 Linnaeus assigns name of *Arabis thaliana* to *Pilosella siliquosa*
- 1873 Alexander Braun publishes first non-taxonomic paper on *A. th.* mutant
- 1841 Gustav Heynhold renames *Arabis thaliana* as *Arabidopsis thaliana* (L.)Heynh.
- 1900 G. Mendel's work on heredity "rediscovered"
- 1907 Friedrich Laibach finds that *Arabidopsis* has only 5 chromosomes;
- 1937 Laibach begins collecting *Arabidopsis* ecotypes
- 1943 Laibach promotes *Arabidopsis* as model system for genetics
- 1947 E. Reinholz publishes first collection of induced mutations by X-rays
- 1964 *Arabidopsis* Information Service newsletter
- 1965 First International *Arabidopsis* Conference
- 1976 Second International *Arabidopsis* Conference

MOLECULAR ERA

- 1983 First detailed genetic map published by Koornneef
- 1985 *A. th.* promoted as model for molecular genetics
- 1986 Transformation with *Agrobacterium tumefaciens* reported
- 1986 First *Arabidopsis* gene sequence published
- 1987 First computerized listing of *Arabidopsis* Information Service
- 1988 Third International *Arabidopsis* Conference; First T-DNA tagged mutant gene cloned
- 1990 Nottingham *Arabidopsis* Stock Centre (NASC) at Nottingham, *Arabidopsis* Biological Resource Centre (ABRC) established at Ohio State
- 1991 *Arabidopsis* Genome Project initiated; AIS newsletter stops
- 1992 First chromosome walk published; North American *Arabidopsis* Steering
- 1993 High-efficiency transformation established
- 1995 Ethylene receptor ETR1 identified; Standard BAC and P1 libraries constructed; Arabidopsis.com goes online
- 1996 *Arabidopsis* Genome Initiative organized
- 1997 Physical maps of all 5 chromosomes completed
- 1999 Chromosomes II and IV sequenced
- 2000 *Arabidopsis* genome sequenced
- 2002 *Arabidopsis* first species whose entire genome placed on a microarray
- 2005 Microarray use matures

Fig.1. A brief summary on *Arabidopsis* history.

Arabidopsis nomenclature, characteristics and ecotypes

Nomenclature: Eukaryota; Viridiplantae; Streptophyta; Streptophytina; Embryophyta; Tracheophyta; Euphyllophyta; Spermatophyta; Magnoliophyta; Eudicotyledons; Core Eudicotyledons; Rosids; Eurosids II; Brassicales; **Brassicaceae**; *Arabidopsis*.

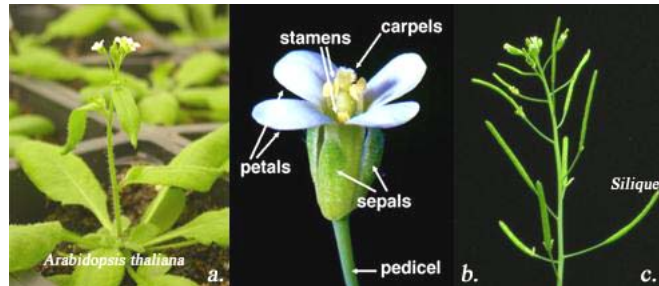


Fig.2. Morphological characteristics of the flowering plant *A. thaliana* (a, b) and its seed production in siliques (c).

Arabidopsis thaliana (Angiosperm, Dicot) is a small (15-30 cm) annual herb, member of the mustard family (Brassicaceae, previously named Cruciferae, which includes cabbage, radish, brussel sprouts) and is self-fertilizing with a short life cycle, from 6 weeks to three months (Fig. 2a).

It has bisexual flowers and is typified by a cross-shaped corolla, tetradynamous stamen (4 long and 2 short ones) (Fig. 2b) and capsular fruits named siliques (Fig. 2c). A single plant can produce 5,000-10,000 seeds in 6-8 weeks. It is a facultative long-day plant (flowering is accelerated when days are long) and even if it has no agronomic significance, it offers important advantages for basic research in genetics and molecular biology.

Indeed, *Arabidopsis* is exceptionally suited to genetic analysis, since its unique characteristics allow for the rapid growth and analysis of a large number of individuals in a minimum of space (100 plants per 0.5 m²) and subsequent amplification of useful genotypes for further study.

Its genome has been entirely sequenced [8], with the exception of some regions around telomeres, centromeres and the ribosomal RNA gene repeat region (115.4 Mbp out of 125 Mbp sequenced).

The plant has five chromosomes, which contain 125 Mbp of DNA and 25,498 identified proteins grouped in 11,000 families.

It has extensive genetic and physical maps of all five chromosomes (the size of the chromosomes vary from 17.5 Mbp to 29.1 Mbp). The genome consists for 80% of single and low-copy DNA. Gene density is one gene every 4.5 Kb, while the average gene length is 2 kb.

Ribosomal DNA accounts for 6% of the genome and is located around the top of chromosomes 2 and 4, while about 60% of plant's genes have a homologous counterpart elsewhere within the genome. 14% of the genome is made up of transposable elements and GC content it up to 35%. Methylation occurs in 6% of the cytosine basis. Plastid and mitochondria genomes are small, and encode a further 79 and 58 protein genes, respectively. Duplications occurred in all five chromosomes.

Most importantly, *Arabidopsis* can be transformed easily and efficiently by simply spraying flowers with bacteria (*Agrobacterium tumefaciens*) that contain a gene of interest in a plasmid. In particular, this has allowed the creation of large collections of insertion mutants based upon a random integration of T-DNA inserts into the plant nuclear genome.

Arabidopsis originated from Eurasia and North Africa; nowadays it is collected from a wide range of habitats distributed primarily over most of the northern hemisphere. It has 750 natural accessions collected from around the world, quite variable in terms of form, development and physiology (e.g. disease resistance, flowering time, etc).

A DNA sequence polymorphism of up to 1.4% in low copy DNA is present between ecotypes, which are nowadays all available from the two major seed stock centers, ABRC (*Arabidopsis* Biological Resource Centre, <http://www.biosci.ohio-state.edu/~plantbio/Facilities/abrc/abrchome.htm>) and NASC (The European - Nottingham- *Arabidopsis* Stock Centre, <http://Arabidopsis.info>).

Researchers around the world are using these differences in natural accessions to uncover the complex genetic interactions such as those underlying plant responses to environment and evolution of morphological traits. While many collections of natural accessions may not meet a strict definition of an ecotype, they are commonly referred to as ecotypes in the scientific literature. Most common accessions are Col-0 (*Columbia-0*), used as standard for the genome sequence, the laboratory strain *Ler* (*Landsberg erecta*) and *Ws* (*Wassilewskija*).

Timetable for growth-stage based analysis

The analysis of *Arabidopsis* growth and development provides a framework methodology for identifying and interpreting phenotypic differences in plants resulting from genetic variation and/or environmental stress. Thirty growth stages cover the development of the plant from seed imbibition through the completion of flowering and seed maturation (Fig.3). These growth stages span the entire life cycle of the plant, thereby maximizing the ability to detect subtle changes that affect only a limited aspect of development. This data set is a robust representation of wild-type development with which all mutants and environmentally stressed plants may be compared [9].

Stage Number	Approx. number of days *	Description
0.0		Seed germination
0.1	3.0 (on plates)	Seed imbibition
0.5	4.3 (on plates)	Radicle emerges from seed coat
0.7	5.5 (on plates)	Hypocotyl and cotyledon emerge from seed coat
1		Rosette growth
1.0	6.0 (on plates)	Cotyledons fully open
1.02	10.3 (on plates) 12.5	2 rosette leaves are greater than 1 mm in length
1.03	14.4 (on plates) 15.9	3 rosette leaves are greater than 1 mm in length
1.04	16.5	4 rosette leaves are greater than 1 mm in length
1.05	17.7	5 rosette leaves are greater than 1 mm
1.06	18.4	6 rosette leaves are greater than 1 mm
1.07	19.4	7 rosette leaves are greater than 1 mm
1.08	20.0	8 rosette leaves are greater than 1 mm
1.09	21.1	9 rosette leaves are greater than 1 mm
1.10	21.6	10 rosette leaves are greater than 1 mm
1.11	22.2	11 rosette leaves are greater than 1 mm
1.12	23.3	12 rosette leaves are greater than 1 mm
1.13	24.8	13 rosette leaves are greater than 1 mm
1.14	25.5	14 rosette leaves are greater than 1 mm
3		Rosette Growth
3.20	18.9	Rosette is 20% of final size
3.50	24.0	Rosette is 50% final size
3.70	27.4	Rosette is 70% final size
3.90	29.3	Rosette growth is complete
5		Inflorescence emergence
5.10	26.0	First flower buds visible in the rosette, plant not yet bolted
6		Flower production
6.00	31.8	First flower open, petals 90 degree angle to pistil
6.10	35.9	10% flowers to be produced are open
6.30	40.1	30% flowers to be produced are open
6.50	43.5	50 % flowers to be produced are open
6.90	49.4	Flowering complete, no more flowers
8		Silique or fruit ripening
8.00	48.0	Seed pods become brown and then shatter. First silique or seed pod shatters.
9		Whole Plant Senescence begins
9.70		Plant starts to lose pigment becoming brownish Senescence complete

* indicates approximate number of days after sowing.

Fig.3. The following growth stages [9] are for Columbia plants grown in soil in 16 hour days/ 8 hour nights with temperatures of 22C during the day and 20°C at night. Lighting was provided with fluorescent bulbs giving an average light intensity of 175 micromoles/meter²*sec. Seeds were cold treated (stratification) for 3 days at 4°C after imbibition to synchronize germination. Days until each stage are approximate and will vary according to growth conditions and genetic background. Approximate dates given include the three day stratification.

Leaf development

The body of Angiosperms is generally constituted of two distinct classes of organs having either an overall radial symmetry (roots and stems) or a distinct asymmetrical development (floral organs and leaves) [10-14]. The leaf is a synchronized medley of developmental domains and is the key unit of the shoot system. Its morphology (Fig. 4) is achieved through an harmonization of processes, cell divisions/enlargements and differentiations [15-17].

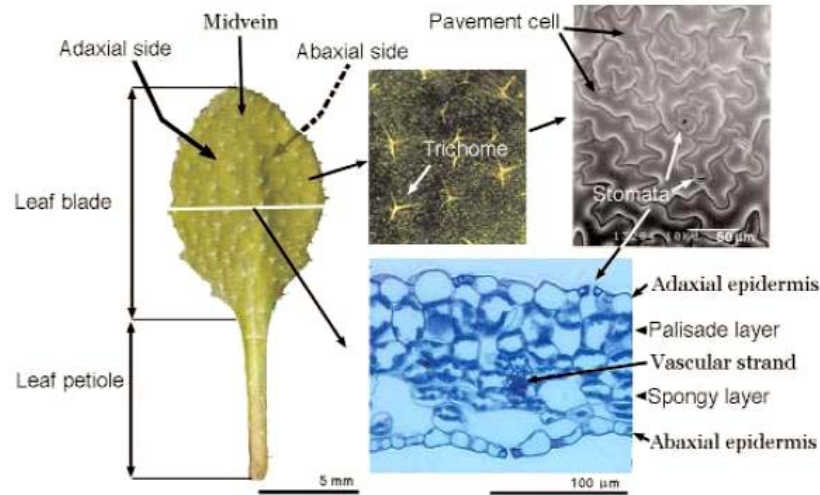


Fig.4. Terminology used for the description of leaf morphology. Left, gross morphology of the fifth rosette leaf of *Arabidopsis*. Upper right, magnified views of the leaf surface. Lower right, magnified view of cross section of the leaf blade. Figure taken from [18].

The capacity of the shoot apical meristem (SAM) to incessantly produce new organs depends on the activity of its stem cell populations, which are located at the meristem tip. In the SAM, leaves arise in succession from organ-founder cells recruited on the flanks of the shoot, a lateral region of relatively high mitotic index called the meristem “peripheral zone” (PZ) [19].

In *Arabidopsis*, leaf development can generally be divided into two main genetically and environmentally regulated processes: initiation of the leaf primordium, starting from the SAM, [15, 20, 21] and leaf morphogenesis, which consists in the acquirement of suborgan identities through tissue differentiation through a dorsal-ventral, proximal-distal and lateral leaf polarity [11, 22] and, finally, the development of a marginal meristem [23-33].

Arabidopsis leaves are very suitable material for studies of leaf morphogenesis because of their simple and stable form and the ease with which genetic analysis can be performed.

The maintenance of the SAM's identity and the initiation of leaf primordium

Primordium initiation in the flowering plant *Arabidopsis* starts soon after embryogenesis from the peripheral zone of the shoot apical meristem. The SAM is characterized by a population of about 1000 cells and is divided into cytologically defined zones (Fig. 5): the central zone (CZ) is at the very apex, the peripheral zone (PZ) where new leaf and flower primordia originate is on the sides, while the rib zone (RZ) is in the central parts of the meristem [34-37].

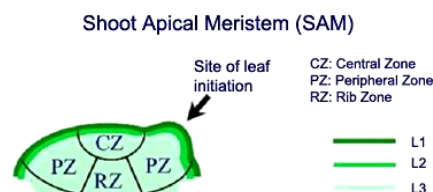


Fig.5. *Arabidopsis* SAM. Cytological domains of the shoot apical meristem. L1 and L2 form the tunica while L3 forms the corpus of the SAM. Figure taken from the web.

The SAM maintains a relatively high rate of cell proliferation [38] and preserves a balance between cell proliferation and commitment to make leaf primordia, between self-renewal and organ initiation. Indeed, the balance of cell production in the SAM and the rate of cell loss through integration of cells into leaves and stem dictate the size of the SAM.

In other words, under the input of key genes, such as the three CLAVATA (CLV) genes [39-55], WUSCHEL (WUS) [56-71], SHOOTMERISTEMLESS (STM) [62, 72-75] or the KNOTTED-like homeobox of *Arabidopsis thaliana*1 (KNAT1) and ASYMMETRIC LEAVES (AS1) genes [24, 27, 30, 75-95], founder cells of SAM's tunica (L1 and L2) [96, 97] and corpus (L3) layers decide whether to start or not periclinal or anticlinal cell division and differentiate into epidermis, mesophyll (palisade and spongy layer) and vascular tissues.

Basically, the maintenance of the SAM is controlled by the opposing functions of two pathways: a WUSCHEL-based and a CLAVATA-based pathway. The positively acting pathway based on the WUS gene promotes meristem growth, acting on the central stem-cell population in the SAM, while the negatively acting pathway based on the CLV gene products suppresses meristem growth. WUS expression downregulates the expression of CLV genes expression and vice versa. Thus, any tendency for increased SAM growth via increased WUS activity leads automatically to suppression of WUS activity via the CLV loop. Mutations at CLV1 and CLV3 lead to enlarged meristems and accumulation of excess undifferentiated cells in the meristems (20, 21).

CLV and WUS genes are necessary for regulating meristem size, but class-I KNOTTED-like homeobox (KNOX) genes, which are expressed in overlapping domains within the SAM and turned off in developing leaves, are required for the maintenance of meristem identity and when downregulated control leaf initiation [24, 75, 92, 98-102]. Loss- and gain-of-function mutations indicate that KNOX (Knotted-like homeobox) genes such as the STM gene [79] are important regulators of the function of the SAM. Indeed, KNOX1 genes, which constitute a gene family in plants, are excluded from the presumptive leaf primordium (P0). The regulation of KNOX gene expression seems to be complex and likely occurs at the level of transcription, translation, alternate splicing, and extracellular trafficking. Analyses of molecular phylogeny, based on the sequences and patterns of expression of transcripts revealed that KNOX genes can be divided into two families in plants: class I KNOX genes, only expressed in the SAM, and class II KNOX genes, which have more diverse patterns of expression and a yet not determined function.

Six KNAT genes have been identified in *Arabidopsis* [27-33, 103, 104].

Leaf morphogenesis in flowering plants

In *Arabidopsis*, leaves initiate post-embryonically in the PZ of the SAM according to a radial pattern. The first two rosette leaves are in opposite positions; the third leaf is perpendicular to the axis between the first two leaves; and the fourth and subsequent leaves are at angles of 137° in a so-called spiral phyllotaxis.

Leaf formation consists in the attainment of suborgan identities through tissue differentiation and the establishment of three leaf axis (Fig. 6): the proximal-distal axis from petiole's base (which is the attached end) to blade's tip (the free end), the dorsal-ventral (or adaxial-abaxial/upper-bottom) axis, with one side forming close to (ad) and the other side away from (ab) the SAM and, finally, the lateral or left-right axis, typical of an expanded lamina around a central midvein.

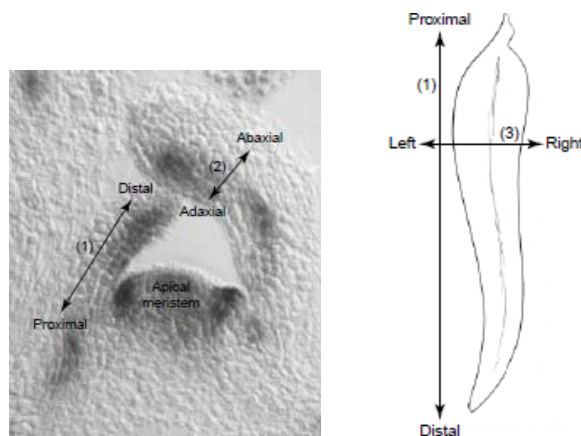


Fig.6. The three symmetry axis of a leaf: 1) proximal-distal, 2) abaxial-adaxial and 3) left-right or lateral. Figure taken from [11].

These asymmetries are important for the function of the leaf, in particular the ad/abaxial axis concerning the two leaf surfaces, since the adaxial surface is optimized for light capture and photosynthesis, while the abaxial surface is fit to exchange gasses and transpire water for plant cooling and circulation.

Primary morphogenesis: acquisition of the dorsiventral asymmetry

Leaves tend to be flattened perpendicular to the stem axis and may show an asymmetric distribution of cell types, with tissues specialised for light harvesting on the 'adaxial' side and those specialised for gas exchange on the 'abaxial' side.

The establishment of dorsiventrality starts in the incipient leaf primordium once class-I KNOX genes, such as KNAT1 or KNAT2 in *Arabidopsis* or KN1 in *Zea*, are downregulated in SAM's peripheral zone.

Four tissues are specified along the dorsiventral axis: the upper epidermis and palisade parenchyma, with dorsal identity; the spongy parenchyma and the lower epidermis, with ventral identity.

In addition, in the mesophyll the vascular bundle has its own asymmetry consisting in an upper xylem and a lower floem.

Nowadays, it is believed that the initial establishment of ad/abaxial polarity may result from a signal deriving from the SAM, which induces or maintains adaxial identity: in the absence of this signal, abaxial identity may be the default.

Waites and Hudson [24] proposed that after primordium initiation, lamina outgrowth requires the juxtaposition of a gradient that generates adaxial and abaxial domains such that leaves lacking one of these domains will necessarily be radial.

Essentially, the future adaxial tissue becomes defined by a set of peculiar transcription factor activities, as does the abaxial tissue, and it is the juxtaposition of these two different tissue identities that triggers lateral growth of the organ to engender the classical flattened and expanded leaf lamina.

Different classes of putative transcription factors and gene families have been shown to be involved in this process: the ARP (AS1, RS2 and PHAN) genes to start leaf differentiation, the PHABULOSA (PHB) [12, 105-115], PHAVOLUTA (PHV) [12, 111, 112, 114, 116, 117] and REVOLUTA (REV) [12, 106, 107, 111] genes of the III HD-ZIP family, to acquire adaxial identity and genes of the KANADI [12-14, 111, 113, 118-122] and YABBY [21, 87, 123-127] families to specify abaxial identity.

These transcripts seem to be uniformly expressed throughout the leaf primordium, but soon after they become limited either to the adaxial domain of the leaf (PHB/PHV/REV) or to the abaxial domain (KANADI, YABBY).

In general, the expression of the adaxial identity genes seems to preclude that of the two abaxial identity family genes and, conversely, ectopic expression of abaxial identity genes leads to suppression of adaxial identity.

The first plant affected in dorsiventral patterning was the cold-sensitive *phantastica* (*phan*) mutant of *Antirrhinum* [24, 25]. The mutations was found in the PHANTASTICA locus, whose product (a MYB transcription factor) is nowadays part of the ARP (ASYMMETRIC LEAVES1/ROUGH SHEATH2/PHANTASTICA) protein class [128], only present in lateral organ primordia. This mutation leads to loss of dorsiventrality in leaves, which were radial and completely abaxialized.

It was observed that the regulation of the knox gene family occurred through the ARP proteins: in *Arabidopsis*, through the AS1 gene [83, 129-131] the ortholog of RS2 [128, 130, 132, 133] and PHAN [134-139], the expression of 2 KNOX genes, KNAT1 and KNAT2 [27, 30, 77], were downregulated in leaf primordia.

Expression of the AS1 gene is, moreover, negatively regulated by the SHOOT MERISTEMLESS gene in the SAM [72, 131].

Soon after new interesting gain-of-function (PHB, PHV) and loss-of-function mutants affected in the establishment of dorsiventrality were studied. The first resulted in adaxialized radial leaves (with similar additional axillary meristems around the base), while the seconds resulted in abaxialized radial cotyledons [114].

McConnell [114, 115] proposed a model wherein the *phb-1d* mutation promotes the development of both the SAM and the adaxial region of a leaf primordium in parallel.

In addition, other gain-of-function alleles (KANADI) resulted also in radial abaxialized leaf primordia [113, 122]

The KAN gene whose transcript encodes a GARP domain, which binds to a specific region of DNA, was originally identified as an enhancer of the abnormal dorsiventrality of carpels associated with the crabs claw (*crc*) mutation [14], [122]. Members of the KANADI gene family in *Arabidopsis thaliana* regulate abaxial identity and laminar growth of lateral organs [118]. Ectopic expression of either KANADI1 (KAN1)

or KAN2 throughout leaf primordia resulted in the transformation of adaxial cell types into abaxial ones and the abolishment of lateral expansion [113, 126].

The partitioning of organ primordia into discrete abaxial and adaxial domains involves gradual separation of the KAN expressing domain from the PHB-like-expressing domain.

The pinhead/zwille mutant exhibits defects in leaf dorsiventrality similar to those of the *phb-1d* mutant, but with more and severe defects ranging from abnormal floral organs, embryos and embryogenesis [140]. PINHEAD (PNH) is expressed in the central domain of the developing plant: the provascular tissue, the shoot apical meristem, and the adaxial (upper) sides of lateral organ primordia. Ectopic expression of PNH on the abaxial (lower) sides of lateral organs results in upward curling of leaf blades. This phenotype correlates with a loss of cell number coordination between the two surfaces of the blade, indicating that ectopic PNH can cause changes in cell division rates.

More strikingly, moving PNH expression from the central to the peripheral domain of the embryo causes transformation of the determinate cotyledon axis to an indeterminate state [141].

Another gene family involved in dorsiventral development and in the abaxialization of lateral organs comprises the YABBY genes [142].

YABBY genes encode a zinc finger and a helix-loop-helix motif, that resembles the first two helices of the high mobility group proteins and are predicted to be transcriptional regulators.

Mutations in members of this family cause abaxial patterning defects that are relatively mild and frequently limited to specific organs (often because of their redundancy).

A schematic representation of several important genes involved in the development of leaf primordium in *Arabidopsis* is presented in Fig. 7.



Fig.7. Genes involved in the development of leaf primordium in *Arabidopsis*. Schematic representation of patterns of expression of genes required for early steps in leaf development. Cross sections of a shoot apex with two young leaf primordia and one predicted area of a leaf primordium are shown. Regions in which the indicated genes are expressed are shaded. Taken and modified from [18].

Secondary morphogenesis: acquisition of the proximal-distal and lateral polarity

The formation of an expanded lamina along the proximal-distal and lateral axis are controlled by a few genes which seem to specify the leaf lamina cell size and number in a polarity-dependent manner [9, 16, 143, 144].

These genes are the AN (ANGUSTIFOLIA) gene [22, 145-151], the ROT3 (ROTUDIFOLIA3) gene [22, 147, 152-156], which encodes a cytochrome P450 and the ELP (Elongator) genes of *Arabidopsis*.

The AN gene is thought to be a key gene in regulation of the polar elongation of leaf cells in the leaf-width direction specifically.

The phenotype, specific to leaves and floral organs (modified leaves), is caused not by a reduction in cell number, but by a specific defect in cell elongation in the transverse (leaf-width) direction of the leaf [22].

The ROT3 gene appears to be the key gene that regulates the elongation of leaf cells (and floral organs cells) in the leaf-length direction, along the proximal-distal axis, without any change in the normal number of cells.

Another class of mutants involved in the expansion of the leaf lamina are the *elo* mutants belonging to the *elongata* class [157, 158]. These mutants show a “narrow leaves” phenotype, not depending on cell expansion polarity but on cell number, which is reduced.

The products of these genes belong to a 6 subunit complex involved in the process of transcription elongation, namely the Elongator complex [159, 160].

The description and function of the Elongator complex will be discussed further on in another paragraph.

Hormones, light and leaf development

Hormones are closely implicated in leaf development and adaptation to changes in environmental factors.

Cytokinins, i.e. are able to organize the development of SAM (through the expression of a subset of KNOX genes [29]), stimulate phyllotaxy and leaf expansion, mainly through action on cell division [161-163].

Leaf initiation involves an increased rate of cell division on the flank of the meristem and the signalling by cytokinins and auxin appears important in this process.

High localized auxin concentrations promote organ initiation, determine the size and position of the future primordium and regulate, in a reiterative process, phyllotaxy. A possible role for an auxin gradient in organ asymmetry patterning is suggested by the dynamic distribution of auxin transporters in the developing organ [164].

Brassinosteroids are important hormones for cell elongation and leaf expansion [165-167]: mutants with an affected brassinosteroid biosynthesis develop smaller leaves than the wild type.

GA dwarf mutants have an overall size reduction, which is evident also for leaves [168].

Abscisic acid (ABA) is recognized as the hormone that controls stomatal closure [169-172].

The PHYTOCHROME (PHY) gene is a light-dependent gene that controls the expansion of leaf blades in *Arabidopsis* [173-175].

Heteroblasty in *Arabidopsis*

Arabidopsis is a heteroblastic or heterophilic plant: it has different leaf morphologies between juvenile, early adult and late adult phase [22, 176].

The *Col* ecotype has 2 small cotyledons, with no trichomes, 11 foliage, rosette leaves of different size, with trichomes and a complex vascular system and, finally, 3 cauline leaves, with no petiole [22, 155], produced later than rosette leaves (Fig. 8).

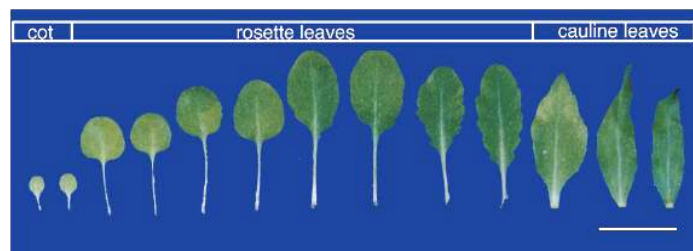


Fig.8. Heteroblasty in *Arabidopsis* (Columbia wild type) under continuous light, 22°C. Reproduced from [177].

The transcription machinery of eukaryotes

Gene expression in eukaryotes

The expression of a gene (Fig. 9) starts with the formation of a copy of a coding DNA sequence into an RNA transcript (Transcription), which itself is afterwards used as the template for the synthesis of a protein (Translation) [178].

Transcription is the first step and a key control point in gene expression, since transcriptional regulation underlies all aspects of cellular metabolism.

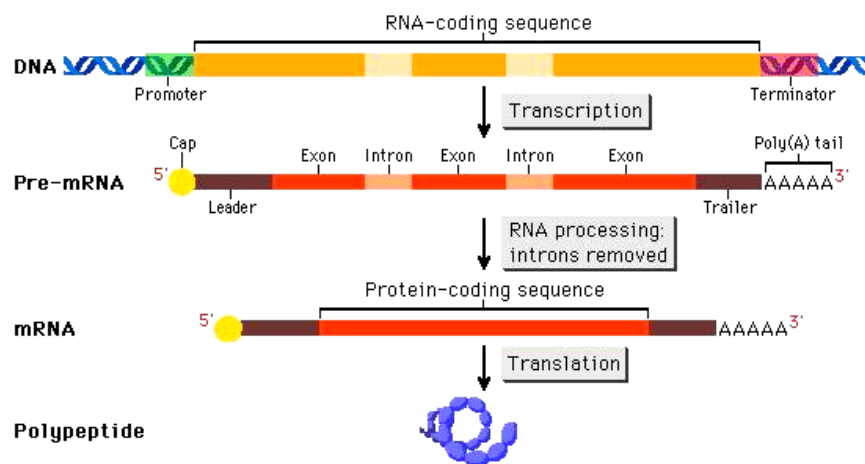


Fig.9. Transcription and translation in eukaryotes. Figure taken from the web.

The transcription machinery of eukaryotes is much more complex than that of prokaryotes or archaea (which have only one polymerase, while eukaryotes use three nuclear enzymes, RNA polymerase I, II, and III to synthesize different classes of RNA), but the general mechanisms of transcription and its regulation are conserved [178].

The transcription of protein-coding genes in eukaryotes is performed by RNA polymerase II (RNAPII).

Transcription is strongly regulated at all levels, including reorganization and modification of the chromatin template. One of these modifications, i.e. histone acetylation, has long been correlated with transcriptional activity, and most known histone acetyltransferases (HATs) are believed to act prior to the initiation of transcription [179, 180].

The transcription cycle and the formation of a transcript

The primary phases of transcript generation constitute a three-step transcription cycle (Fig. 10) including the formation of the Pre-Initiation Complex (PIC) assembly at the promoter, the initiation of transcription, through promoter clearance and, eventually, the reinitiation of a new transcript.

After initiation is achieved, the transcript is elongated in a process named elongation, thanks to the Transcript Elongation Complex (TEC).

Finally, the transcript is terminated in a process named termination.

Current models suggest that during initiation, RNA polymerase II assembles at promoters together with coactivator complexes and general transcription factors.

During elongation, other accessory factors are thought to function as part of the active transcriptional machinery.

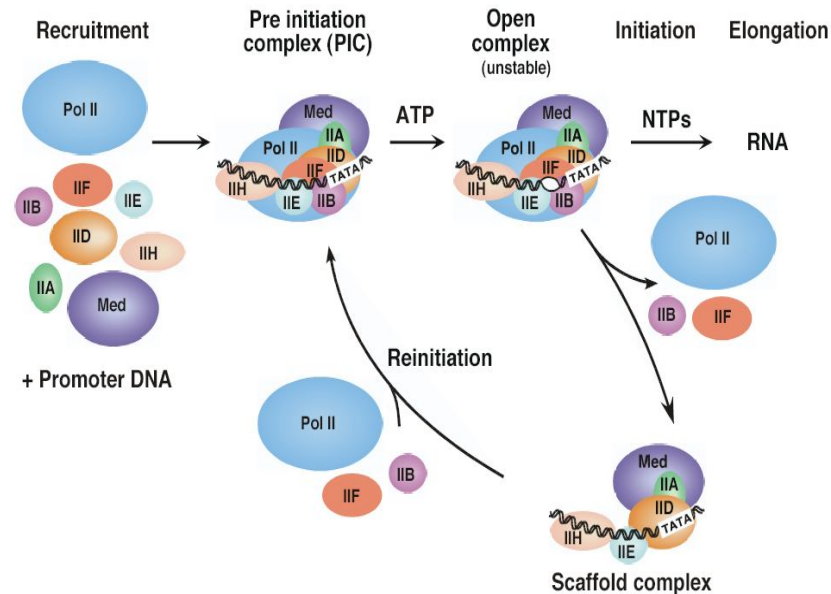


Fig.10. The eukaryotes transcription cycle. Formation of the PIC, initiation, elongation and reinitiation of transcription. Figure taken from the web.

General transcription factors and the eukaryotic promoters

For protein coding genes, transcription by RNAPII requires the function of various accessory factors that associate with the enzyme during initiation and elongation.

Unlike prokaryote polymerase, eukaryote DNA-dependent RNA polymerases are by themselves unable to initiate and complete the transcription of a gene: they're all dependent on the presence of accessory factors and General Transcription Factors (GTFs), required by all promoters (the minimal DNA sequence needed to specify non-regulated or basal transcription) used by RNAPII [181-183].

Eukaryotic RNA polymerases lack the sigma factor found in the prokaryotic enzyme. Therefore, it's not too surprising that promoters in the two groups are different.

Instead of the TATAAT sequence at the -10 location, which is found in prokaryotes, a TATA box, located at approximately -25, is found in eukaryotes. Additional sequences are located upstream of this site, with many promoters having a CAAT box and some containing a GC box, both at around -40 to -110 bases upstream. The location of these elements can vary, and they can be present on either strand.

The nucleation of transcription factors at the core promoter requires a complex network of protein-protein and protein-DNA interactions. Formation of this promoter-bound complex is sufficient for a basal level of transcription. However, for activator-dependent (or regulated) transcription, general cofactors are often required to transmit regulatory signals between gene-specific activators and the general transcription machinery.

The GTFs may activate or repress gene expression and transcription through the modulation of the chromatin structure and binding to a core promoter (Fig. 11).

Enhancer or silencers sequences (cis-acting regulatory sequences, located several thousand bases upstream, downstream, or in the middle of the transcribed region) bind proteins (activators or repressors) which stimulate or repress transcription. These are often tissue- and species-specific, explaining the regulation of genes in some tissues. Activators may bind to coactivators, which directly interact with basal transcription factors (Fig. 11).

GTFs are needed to form the PIC (Pre-Initiation Complex, analogous to the bacterial Closed Complex), which is constituted of almost 60 polypeptides, but also to start the transcript elongation and to terminate and eventually restart the transcription.

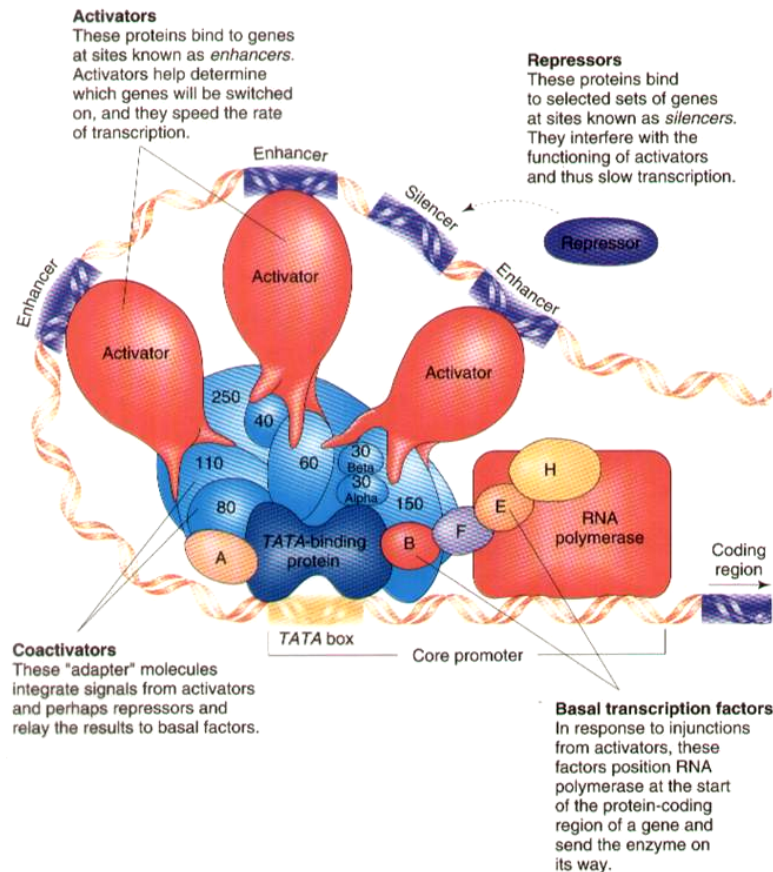


Fig.11. Regulation of transcription at the core promoter through enhancers and silencers, cis-acting regulatory sequences, and formation of the PIC assembly, made by coactivators, basal transcription factors and RNAPII. Figure taken from web.

Formation of the PIC (Pre-Initiation Complex) assembly

The model of PIC assembly starts with promoter binding of TFIID, followed by TFIIA, TFIIB, TFIIE, TFIIH and the remaining GTFs, including RNAPII, plus several additional cofactors (Fig. 12) [184-187].

TFIID is composed of TBP and about 14 TAFs (TBP Associated Factors), nearly all of which have been conserved through evolution, which function in the specific recognition of promoters and activator stimulated transcription [188, 189].

TFIIA and TFIIB are the two general factors that interact specifically and independently with TBP. TFIIA stabilizes TBP-DNA binding and strongly promotes binding of TFIID to DNA through an anti repression mechanism by competing with the TAF1 N-terminal domain (TAND) that occludes the DNA binding surface of TBP when TFIID is not bound to DNA [186, 188]. TFIIB plays a central role in PIC formation, interacting with TBP, RNAPII, TFIIF, and DNA on either side of the TATA box [186, 190-193]. The sequence TATA is located -30' nucleotides upstream of the Transcription Start Point (TSP). In addition, there are also some weakly conserved features including the B-Recognition Element (BRE), approximately five nucleotides upstream of the TATA box. Occasionally there is no TATA box at the promoter. In this case a TAF will bind sequence specifically, and force the TBP to bind non sequence specifically. TAFs are highly variable, and add a level of control to the initiation.

In this state, RNAPII and the general factors are all bound to the promoter but are not in an active conformation to begin transcription. These factors can act indirectly on the transcription machinery by recruiting factors that modify chromatin structure, or directly by interacting with components of the transcription machinery. Not surprisingly, the promoters of class II eukaryotic genes contain elements to direct the binding of GTFs [192].

The transcription start site usually contains a pyrimidine-rich initiator element (INR), with the consensus sequence (Py)₂A+1A/T(Py)₂, that binds TFIID.

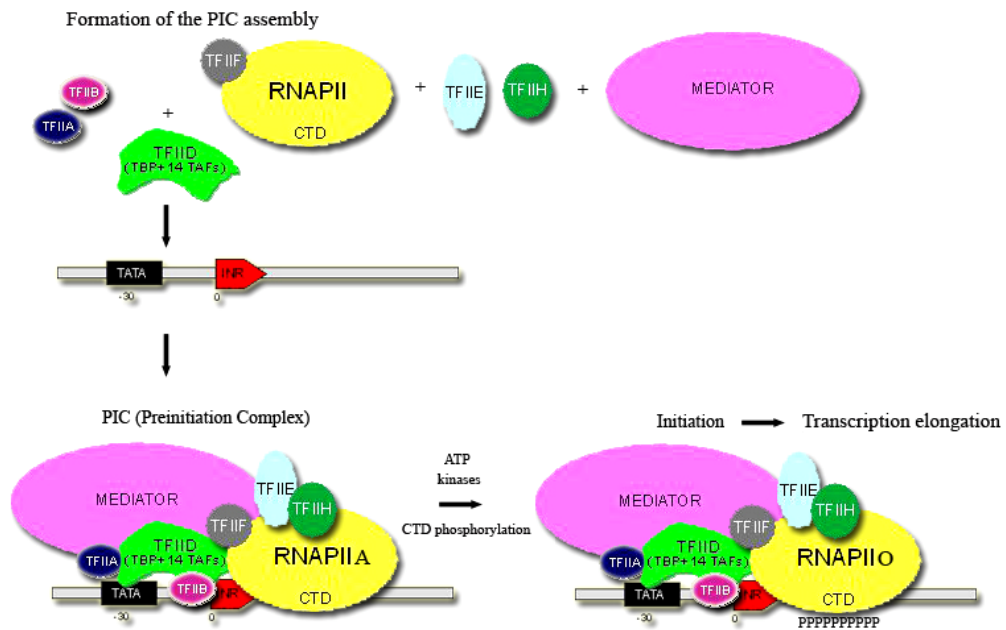


Fig.12. Transcription initiation.

As before mentioned, approximately 25-30 bp upstream from INR lays the TATA box (Consensus sequence TATA A/T A A/T), an element recognised and bound by the TBP (TATA-binding protein) subunit of TFIID. Binding of TFIID to the TATA box causes an 80° kink in the promoter DNA thereby enabling the binding of TFIIB to the adjacent BRE element (Consensus: G/C G/C G/A CGCC), which lies 35 bp upstream from INR. Binding of TFIIB stabilises the binding of TFIID to DNA, forming the interface for recruitment of the RNAPII/TFIIF complex [194].

Upon addition of ATP, the PIC undergoes a large conformational change resulting in separation of the DNA strands surrounding the transcription start site and the insertion of the template DNA strand into the active centre of RNAPII to form the unstable Open Complex [186, 193]. In this step, the general transcription factors TFIIH, TFIIIE and TFIIF are thought to play major roles by inducing torsional strain in the DNA, promoting DNA strand separation, and positioning of the DNA strands within the Open Complex [195, 196]. Indeed, formation of an Open Complex between RNAP II and the DNA template is a prerequisite for transcription initiation.

Melting of the double-stranded DNA into a single-stranded bubble is an ATP-dependent process and requires the action of two GTFs, TFIIIE and TFIIH [197-199].

TFIIIE binds selectively to the nonphosphorylated form of RNAPII (IIa) and this interaction is mediated by the 56-kD subunit of TFIIIE. TFIIIE also interacts with both subunits of TFIIF and with TFIIH, a multisubunit basal factor reported to catalyze RNA polymerase II CTD phosphorylation. Protein affinity assays demonstrate that TFIIIE binds directly to ERCC-3, a DNA repair protein associated with TFIIH [199].

Initiation ends once the open complex is established and the first phosphodiester bonds of the RNA transcript is formed [200].

RNA synthesis begins with DNA-NTP base pairing, phosphodiester bond formation, and movement of the template DNA RNA hybrid within the active centre of RNAPII. Very early transcription complexes are unstable until the nascent transcript is elongated to nine nucleotides, about the length of the RNA-DNA hybrid in the transcription bubble. In many systems, multiple short abortive RNA products of 3–10 bases are synthesized before RNAPII starts transcribing full length RNAs.

RNAPII elongation complexes enter a second period of instability when the nascent transcript is 20–50 nucleotides in length. After synthesis of about 30 bases of RNA, RNAPII is thought to release its contacts with the core promoter and the rest of the transcription machinery and enter the stage of transcription elongation. Elongation complexes lack basal factors, with the exception of TFIIF, which in addition to being required for initiation [201, 202] is also an elongation factor and acts during the early stages of elongation to decrease the frequency of abortive transcription. It has been proposed that TFIIF functions to stabilise the tight interaction of the PIC with promoter DNA and facilitates its unwinding during the formation of the open complex [203, 204].

Before RNAPII becomes engaged into productive transcript elongation, it must pass through a stage known as promoter clearance, which marks the transition between transcription initiation and elongation and phosphorylation of the C-terminal domain (CTD) of Rpb1, the largest subunit of RNAPII [199, 205]. Only non-phosphorylated RNAPII (RNAPIIa) can form initiation complexes. During this stage, the PIC is partially disassembled: a subset of GTFs remains at the promoter in the Scaffold Complex, enabling the fast recruitment of the remaining general factors to speed up a new transcription reinitiation.

RNAPII initiation regulation

Initiation is regulated by many mechanisms. These can be separated into two main categories: protein interference and chromatin structure inhibition.

Protein interference is the process where some signalling protein interacts, either with the promoter or some stage of the partially constructed complex, to prevent further construction of the polymerase complex, so preventing initiation. This is generally a very rapid response and is used for fine level, individual gene control and for 'cascade' processes for a group of genes useful under specific conditions (i.e. DNA repair genes or heat shock genes).

These methods of control can be combined in a modular method, allowing very high specificity in transcription initiation control.

RNAPIIa/o, Mediator, Elongator and the transcript elongation

RNAPII is a 550 Kda complex of 12 subunits. Despite its obvious structural complexity, this multisubunit enzyme requires two groups of auxiliary proteins to solve two critical biochemical problems: the recognition of target promoters and the modulation of the RNA transcripts production of individual genes in response to developmental and environmental signals.

The largest subunit of RNAPII (Rpb1) has a domain at its C-terminus that is called the CTD (carboxy-terminal domain). The CTD can be considered as a platform for transcription factors and is the action site of CTD kinases (two cyclin dependent kinases, namely CDK7 and CDK8 are components of the PIC assembly) and phosphatases, thus allowing attraction and rejection of factors that have a function in the transcription process (elongation, mRNA maturation, surveillance, and export [184]).

The CTD is composed of a tandemly repeated amino acid motif, a heptapeptide consisting of the following consensus sequence: Y¹S²P³T⁴S⁵P⁶S⁷, (Tyr-Ser-Pro-Thr-Ser-Pro-Ser). The amount of the tandem repeats varies between species, ranging from 15 in microsporidia to 26 in yeast, 32 in *Caenorhabditis elegans*, 45 in *Drosophila* and 52 in Mammals [206].

During the transcription cycle, Ser² and Ser⁵ undergo waves of phosphorylation and dephosphorylation. Indeed, many different combinations of phosphorylations are possible along the repeats. Only the phosphorylated (Ilo) form of RNAPII can participate in transcriptional elongation through the RNAPII transcript elongation complex (TEC), which plays important roles in mRNA maturation, pre-mRNA capping, splicing, 3'-end processing and export, while the non-phosphorylated CTD (RNAPIIa) is essential for the formation of a pre-initiation complex (PIC).

The RNAPIIo form marks the transition from initiation to elongation: phosphorylation destabilizes the PIC assembly, leads to the formation of the Scaffold complex and promotes the exchange of factors associated with the polymerase [207].

CTD phosphorylation at Ser⁵ has been correlated with transcription initiation and early elongation (promoter clearance), whereas Ser² phosphorylation is associated with RNAPII already elongating the transcript.

Elongation is stimulated by a large variety of factors (TFIIS, Spt16/Pob3, elongin, ELLs, TFIIF and the Elongator complex) [208-215], of which some prevent pausing or stalling of the RNAPII complex and others model the chromatin for transcription. The degree of chromatin condensation is modulated by histone acetyltransferases and deacetylases [216, 217]. The transition to elongation also involves the replacement of Srb/Mediator, which is tightly associated with RNAPIIa with an elongation complex termed Elongator, associated with the hyperphosphorylated RNAPIIo form [208, 217].

The Mediator complex of about 24 proteins, originally isolated from yeast, but present in all eukaryotes examined, is a coactivator complex limited to initiation complexes [218], essential for both basal and activated transcription [219].

Its subunits are generally divided in 3 domains or modules (head, middle, tail): the products of the five SRB genes, characterized as interacting with the RPB1 CTD; the products of four genes identified as global suppressors, and six members of a new protein family, termed Med, implicated in transcriptional activation.

Reconstitution experiments *in vitro* have shown mediator to stimulate the phosphorylation of CTD by the TFIIF kinase 30- to 50-fold. Since Mediator binds only hypophosphorylated CTD, this function may serve to release itself from the initiation complex once the signal for elongation is received. This is supported by evidence for the recycling of Mediator to initiation complexes and the absence of Mediator from elongating polymerases [220, 221].

The Elongator complex

The elongating RNAPII holoenzyme is copurified with a multisubunit complex, Elongator, whose stable interaction depends on the hyperphosphorylated state of the RNAPII C-terminal domain [208].

Purified holo-Elongator was initially identified in yeast and was found made of 6 proteins organized into 2 subcomplexes [222, 223]. The first one consists of ELP1 [208], ELP2 (a WD40 repeat protein) [222], and ELP3 (a histone acetyltransferase activity directed against histones H3 and H4, highly conserved between yeast and man, that together with other factors facilitates movement of RNA polymerase II through nucleosomes) [217]. The other consists of ELP4 [224], ELP5 [225], and ELP6 [223] constituting the HAP complex, made of HAT Accessory Proteins.

It was suggested that the HAP complex interacts preferentially with the core complex rather than with RNAPII and was therefore proposed to have a regulatory function. The largest subunit, Elp1, was previously isolated from a genetic screen for resistance to *Kluyveromyces lactis* toxin and was initially named TOT1 (Toxin-Target1). Other TOT genes were soon discovered.

Deletion of TOT/ELP genes in yeast cells results in a variety of phenotypes consistent with a role for the factor in transcription elongation, which include slow growth adaptation, delayed gene activation, and temperature sensitivity.

In addition, the *elp* mutants also are delayed in the G1 phase of the cell cycle and are hypersensitive to calcofluor white, 6-azauracil, and caffeine [208, 222-224].

Deletion of ELP3 is synthetically lethal with deletion of the tail of histone H4, or of the Rpb9 subunit of RNA polymerase II and confers a severe growth defect with the gene encoding the Gcn5 subunit of the SAGA complex [213, 226].

It is to be noted however, that despite the growing evidence for Elongator function, recent work in yeast has been unable to detect Elongator associated with RNAPII under any conditions, and revealed that the majority of Elongator is cytoplasmic [220].

Plant Elongator

The Elongator complex has been identified in different species (*Saccharomyces cerevisiae*, *Mus musculus*, *Rattus norvegicus*, *Homo sapiens*, etc) and recently also in Plants [159, 160].

Namely, in *Arabidopsis*, through an initial large-scale screen of EMS (ethane methylsulfonate) leaf mutants of the *elongata* class (*elo1*, *elo2*, *elo3*, and *elo4*) with abnormally shaped leaves were investigated.

Mutations were finally mapped and found to be located in genes constituting the Elongator complex in Plants and involved in its regulation (DRL1) (Table1).

AtELONGATOR genes		
Gene	Ac. number	Protein function/Domains
AtELP1/ELO2	At5g13680	Transcriptional elongation regulator
AtELP2	At1g49540	Unknown - Contains WD40 repeats
AtELP3/ELO3	At5g50320	Histone acetyltransferase/demethylase; Radical SAM proteins
AtELP4/ELO1	At3g11220	Unknown, Paxeb protein-related
AtELP5	At2g18410	Unknown
AtELP6	At4g10090	Unknown
DRL1/ELO4	At1g13870	Unknown - Contains ATP/GTP binding site and CaM binding site

Table1. AtElongator genes. The *A. th.* homologues of the Yeast Elongator genes are presented together with DRL1 (Deformed Root and Leaves1) in the table with their accession number and their function. AtELP3 has recently been colocalized with the *elo3* mutant [160]. AtELP1, AtELP4 and DRL1 have been colocalized respectively as *elo2*, *elo1* and *elo4*.

The *elo1*, *elo2*, and *elo3* mutations colocalized with the genes encoding the ELP4, ELP1, and ELP3 homologues, respectively. Each of the *elo* mutants carried a point mutation in one of these Elongator genes. The sequencing of the ELO2 gene in *elo2* plants revealed a single nucleotide change (G to A) that caused a premature stop codon (TGG to TAG) toward the 3' end of the third exon.

In the *elo3* mutant, a single nucleotide change (G to A) in the fifth exon of the ELO3 gene changed an aspartic acid residue, which is conserved in all ELO3 homologues, into an asparagine (D to N). A single base pair change (G to A) at the acceptor splice site of the third intron of the ELO1 gene caused missplicing in the *elo1* mutant. Three different mRNAs of ELO1 were present in the *elo1* plants, resulting from three different splicing events: exon4 was spliced out, intron3 was spliced out incorrectly using the first AG in exon 4, or intron 3 was not spliced out.

The three splicing events had a similar effect on the formation of the putative protein: at the N terminus, 142 amino acids were identical to those of wild type, followed by divergent amino acids and a stop codon.

The *elo4* mutation colocalized with the gene encoding the DRL1 (Deformed Roots and Leaves1) protein in *Arabidopsis thaliana*, which is the homologue of the Yeast TOT4/KTI12 protein associated with the Elongator complex.

The recessive mutation at the DRL1 locus causes growth defects and general organ disorganization: at the anatomic and cyto-histological level shoot, root, inflorescence and flower meristems were affected.

The leaf phenotype of the *drl1-2* mutant, named “narrow leaves“, has been dissected at different morphological levels: compared to the wild-type *Ler* leaves the *drl1-2* leaf had reduced lamina width and area and an increased lamina/petiole ratio or even an unclear transition between petiole and lamina. The “narrow leaves phenotype” is present in all *elo* mutants (Fig. 13).

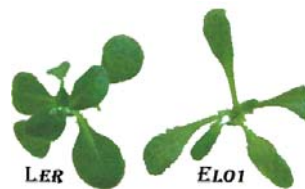


Fig.13. 21 DAV wild-type *Ler* (left) and mutant *elo1* (right) plantlets grown on GM+V+1% sucrose. *Elo1* mutants, belonging to the “elongata” class display a “narrow leaf” phenotype, with a slim lamina.

At a histological level the reduced lateral growth of the lamina has been correlated with a reduced (50%) Palisade Cell Number (PCN). DIC (Differential Interference Contrast) optics analysis showed a reduction in upper epidermis cell-size, but a significant increased palisade cell-size.

In serial transversal sections the palisade cells were larger and more irregularly shaped and intercellular spaces were present all over the mesophyll; the lamina was thicker and the midvein less pronounced, which possibly indicates leaf ventralization, even if marker gene analysis showed that the *drl1-2* leaves had clear dorsal and ventral domains.

Transcript termination

After initiation and elongation, the last step in the transcription cycle is transcript termination. At this stage, the mRNA is cleaved, polyadenylated and transported to the cytoplasm, where it will be translated [227, 228].

Little regulation occurs at termination, although it has been proposed that newly transcribed RNAs are kept in place if proper termination is inhibited, allowing very fast expression of genes given a stimulus, but this has not been demonstrated in eukaryotes yet.

Sucrose in plants

All plants use sucrose, the universal carbohydrate of systemic transport, not only as nutrient but also as general regulator (signal molecule) of growth and development, since it is involved in gene expression through the so-called sugar-sensing pathway [229-234].

General characteristics

Sucrose (common name: table sugar, cane sugar, beet sugar, or maple sugar, depending upon its natural source; also called saccharose; saccarosio in Italian) is a non-reducing L-fructoside disaccharide which is the result of an acetal oxygen bridge in the alpha orientation between an α -D-glucose and a β -D-fructose (Fig.14). The osmotic effect of a substance is tied to the number of particles in solution, so an mL of sucrose solution with the same osmolarity as glucose will have twice the number of carbon atoms and therefore about twice the energy. Thus, for the same osmolarity, twice the energy can be transported per mL. As a non-reducing sugar, sucrose is less reactive and more likely to survive its transport in the phloem. Sucrose has the same molecular formula, $C_{12}H_{22}O_{11}$, as lactose and maltose, but differs from both in structure. Its systematic name is α -D-glucopyranosyl-(1 \rightarrow 2)- β -D-fructofuranose and it melts at 186°C.

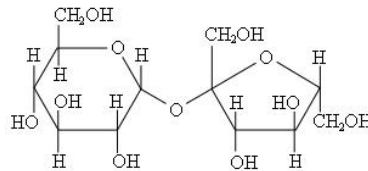


Fig.14. Sucrose molecule: alpha form of D-glucose + beta form of D-fructose

Sucrose transport

Sucrose is an important energy vector for plant sink organs or for fast developing sink tissues unable to perform photosynthesis, like i.e. roots and fruits, where it is stored as sucrose or starch or metabolized. It results either from a surplus of carbohydrates after photosynthesis in mature leaves, which are the predominant sites of photosynthesis in higher plants or from root uptake from soil (but eventually also from a lab germination medium).

Carbohydrate exporting tissues are often referred to as 'source tissues' while importing tissues as 'sink tissues'. Specific plants may also translocate sugar alcohols (polyols like mannitol or sorbitol) or sucrose derivatives, i.e., raffinose, verbascose and stachyose, but these plants simultaneously translocate at least an equal amount of sucrose [235, 236].

Sucrose is transported in solution via a specific part of the vasculature, the phloem, which represents a long distance distribution network for assimilates in order to supply nonphotosynthetic organs with energy and carbon skeletons. It is actively transported into the phloem by the companion cells.

Beginning with the synthesis of sucrose, the first event is the transport of sucrose in the vacuole, which determines the pool of sucrose available for export (sucrose is temporarily stored into the vacuole). Then, sucrose has to exit the mesophyll cell and, from the apoplasm, enter the phloem cells. When sucrose is unloaded into the apoplasmic space, it can then be taken up as sucrose into the sink cells or cleaved by an invertase to hexoses that are transported by specific carriers.

Sucrose diffuses into the neighboring sieve tube cells, through a high number of plasmodesmata [237-239]. Sieve elements lose their nucleus and many organelles during differentiation, but stay connected to companion cells, which have a high metabolic activity. Sieve elements are connected to form sieve tubes that oppose very little resistance to the flow of sap. In most species, at least crop species, the sieve element/companion cell complex (SE-CCC) is symplasmically isolated from the surrounding cells. Water molecules in the xylem diffuse into the sieve tube cells increasing the pressure in these cells. It is this pressure that forces the sugar and water through the phloem.

In addition to diffusion, there are two principal pathways for the delivery of sucrose into the minor vein SE-CCC: symplastic and apoplastic loading, in which sucrose can move from phloem into the cytoplasm of sink cells with or without crossing the plasmamembrane or the cell. In the first way sucrose passes the entire route from the leaf mesophyll cells to the sieve element-companion cell complex in the so-called 'symplast', moving from cell to cell via plasmodesmata while in the second sucrose is released from the

mesophyll cells and then actively taken up by sucrose transporters located in the sieve element–companion cell complex.

An interesting experiment showed that sucrose is also present in plastids [240].

Sucrose carriers in *Arabidopsis*

Three types of sucrose carriers (H^+ /sucrose symporters and antiporters) have been identified in plants:

- 1) plasma membrane influx transporters, responsible for sucrose entry into cells;
- 2) tonoplast (vacuole) transporters which are sucrose/ H^+ antiporters, since the vacuole is acidic compared to the cytoplasm;
- 3) plasma membrane efflux transporters, antiporters responsible for the unloading of sucrose in sink organs or for sucrose exit from the mesophyll cells, in close vicinity to the phloem.

Nine sucrose transporter genes AtSUC1-9 have been identified in *Arabidopsis thaliana* (Fig. 15) [238, 241-243], seven of which encode functional proteins, whereas two genes, AtSUC6 and AtSUC7, are pseudogenes encoding aberrant proteins [241]. Most of these sucrose transporters are localized in the phloem (AtSUC3 and AtSUC5, with AtSUC2 and AtSUC4, predominantly in minor veins), other in cells close to phloem (AtSUC3), but others in flower tissues (AtSUC1, AtSUC8 and atSUC9).

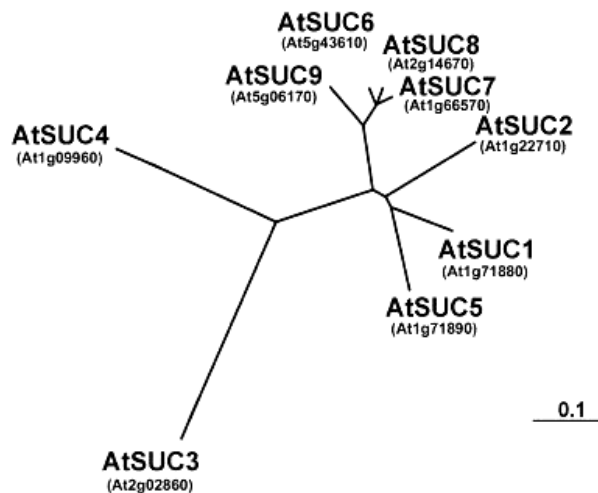


Fig.15. *A. thaliana*'s sucrose carrier's phylogenetic tree.

Sucrose synthesis and cleavage: sucrose synthases and invertases

Free sugars in plants are released from polysaccharides, beginning with disaccharides [244]. In higher plant cells, sucrose synthesis and cleavage are essential reactions for the provision and allocation of carbon resources or initiation of hexose-based sugar signals in importing structures. The breakdown is performed through the regulated activity of three important key enzymes, plus their isoenzymes: acid and alkaline invertases [245-255], also named sucrases, which catalyze the following reaction: sucrose + H_2O = glucose + fructose and sucrose synthases [230, 256], catalyzing the following reaction: sucrose + UDP = UDPglucose + fructose. Sucrose synthases are known to catalyze sucrose synthesis as well as sucrose cleavage.

Plants contain two unrelated families of invertases: acid forms that derive from periplasmic invertases of eubacteria and are found in cell wall and vacuole, and neutral/alkaline forms evolved from the cytosolic invertases of cyanobacteria [257]. Invertases are able to alter sugar signals by producing glucose rather than UDPglucose, thus compared to sucrose synthases two-fold more hexoses. Vacuolar sites of cleavage could allow temporal control via compartmentalization. Together with transcriptional control, the action of invertases may also be regulated at the enzyme level by inhibitor proteins [247, 258].

At the enzyme level, sucrose synthases can be regulated by rapid changes in sub-cellular localization, phosphorylation, and carefully modulated protein turnover [245].

In general, hexoses favor cell division and expansion, whereas sucrose favors differentiation and maturation [259], thus invertases mediate the initiation and expansion of many new sink structures, often with vacuolar activity preceding that in cell walls.

Sucrose metabolism

During the day, plants produce sucrose and starch in their leaves as an energy source for the coming night. Photosynthesis is the main process in leaves, but in higher plants not all cells are photosynthetically active. Indeed, root cells or cells of reproductive structure, developing organs and storage tissue rely entirely on the import of carbohydrates synthesized in leaves. Primary carbon metabolism is divided between the chloroplast and the cytosol. Photosynthesis is regulated as a two-way process by the rate of utilization of photosynthate in the rest of the plant [260-262]. Light regulates the expression of genes for photosynthesis and the activity of the gene products (feedforward control). Other environmental variables such as temperature and nutrition determine the rate at which end-products from the TCA cycle are used (feedback control) [263].

In particular, photosynthesis is inhibited when the production and accumulation of carbohydrates in source leaves exceeds the rate of utilization of these photosynthates by sink organs [264].

Schematically, sucrose metabolism can be summarized as follows: the fixation of CO₂ in the chloroplast yields triose-phosphates, which are needed in the TCA cycle for the regeneration of the ribulose-1,5-bisphosphate (CO₂ acceptor) and for starch synthesis.

All triose-phosphates in excess are used essentially for sucrose formation in the cytosol (through gluconeogenesis to generate fructose, glucose and, finally, through sucrose synthases, sucrose, which is exported to sink tissues where it is stored in the vacuole) and starch synthesis in the chloroplast. Starch and sucrose synthesis must be adjusted to the photosynthetic rate to ensure continuous phosphate recycling. When exported into the cytoplasm from chloroplast. Triose-phosphates can go through glycolysis and respiration, to produce ATP. The fructose-2,6-bisphosphate (Fig.16) is considered a key enzyme in maintaining a balance between glycolysis and gluconeogenesis [265].

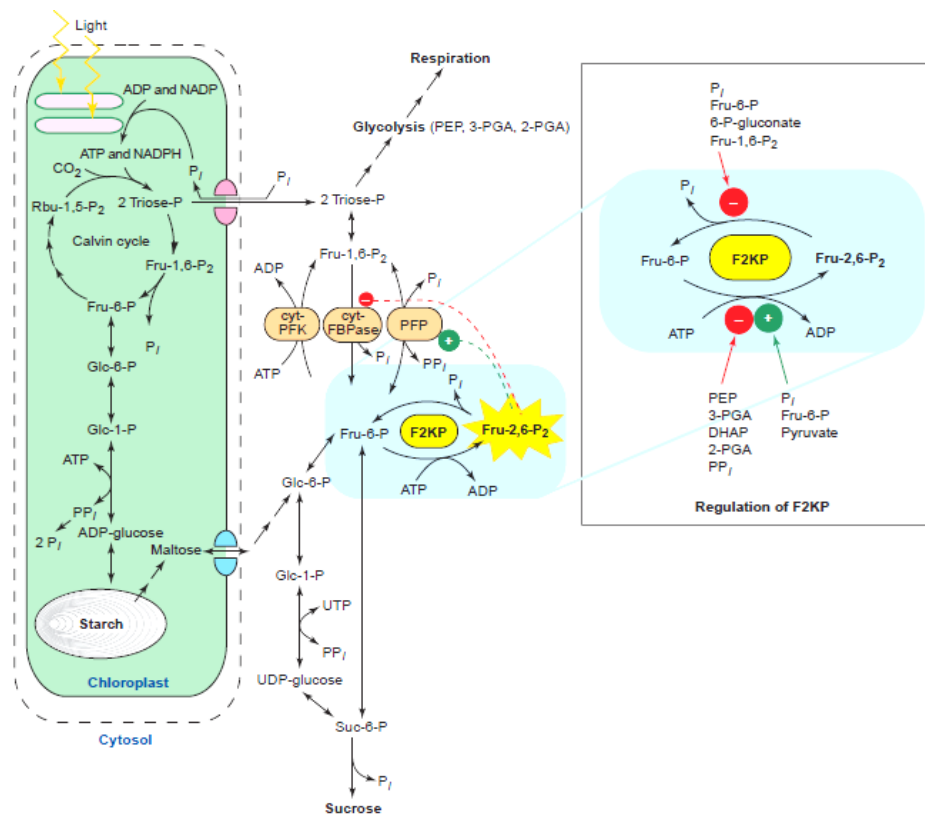


Fig.16. Sucrose metabolism. Taken from [265].

Sugar-sensing mechanisms and general gene regulation

Though lots of sugars and their intermediates have been discovered in plants, only sucrose and hexoses have been found to act as signal molecules. Sugar-induced signals will interact with other sensing and signaling pathways [229, 231].

Three different sugar-sensing systems have been identified in plants:

- (a) an hexokinase-sensing system, similar to the one described for yeast and animals;
- (b) a hexose transport-associated sensor, again similar to the situation in yeast;
- (c) a sucrose-specific pathway, which may involve a signaling sucrose transporter.

These three mechanisms represent the initial step of signal transduction. It is believed that phosphatases and/or kinase may regulate downstream other proteins that directly bind to promoters or coactivators/corepressors of specific set of genes, such as photosynthetic genes. A sucrose cycling through acid invertase and hexokinases may be a fine-tuned mechanism for gene expression regulation [261].

In plants, elevated levels of cellular sugar upregulate genes involved in the synthesis of polysaccharides, storage proteins, pigments, as well as genes associated with defense responses and respiration. Genes that are upregulated when nutrient availability is high are named 'feast' genes, while genes upregulated in nutrient depletion are named 'famine' genes.

Sugar depletion enhances the expression of 'famine' genes involved in photosynthesis and resource remobilization, such as starch, lipid and protein catabolism [256, 266, 267].

It has also been proposed that reduced photosynthesis is the result of increased hexose production and cytosolic phosphate (Pi) depletion or the feedback inhibition of sucrose phosphate synthase that results in the accumulation of phosphorylation intermediates, the depletion of stromal Pi, and the decrease of ATP synthesis [262, 268].

Sugar abundance enhances the expression of 'feast' genes, which in turn enhance gluconeogenesis, fatty acid synthesis, but in general all genes involved in anabolism and storage processes.

Results

Manuscript submitted to *Annals of Botany* (November 2006, personal format)

CYTOLOGICAL INVESTIGATIONS OF THE *ARABIDOPSIS THALIANA* *ELO1* MUTANT GIVE NEW INSIGHTS INTO LEAF LATERAL GROWTH AND ELONGATOR FUNCTION

ANDREA FALCONE^{1,*}, MIEKE VAN LIJSEBETTENS² AND MARIA BEATRICE BITONTI¹

¹ *Università della Calabria, Dipartimento di Ecologia, Via ponte P. Bucci, Cubo 6B, 87036, Arcavacata di Rende, CS, Italia* and ²*VIB (Flanders Interuniversity Institute for Biotechnology), Department of Plant Systems Biology, Technologiepark 927, 9052 Ghent, Belgium*

[*andrea.falcone@unical.it](mailto:andrea.falcone@unical.it)

Running title: CYTOLOGICAL INSIGHTS INTO LEAF LATERAL GROWTH AND ELONGATOR FUNCTION

ABSTRACT

- **Background and Aims** Leaf growth is a complex developmental process controlled by genetic and environmental factors and is determined by a proliferation, expansion and maturation phase. Mutational analysis in *Arabidopsis thaliana* showed that leaf size and shape is dependent on cell division and cell expansion activity. We investigated at the cytophysiological and ultrastructural level the *elo1* mutant of *Arabidopsis thaliana*, which is defective in one of the components of the histone acetyl transferase Elongator complex and displays a distinct ‘narrow leaves’ phenotype, due to a reduced cell number and no transition between petiole and lamina. Our aim was to determine the physiological basis of leaf morphology in this mutant, by investigating the modulatory role of light and sucrose.
- **Methods** The *elo1* mutant was taken as representative of all the *elo* mutations and investigated at cytophysiological level. Germination tests and growth assays were performed on seedlings grown for 21 days at different sucrose concentrations, light conditions and stress variables. Leaf morphometric and ultrastructural features were also investigated by image analysis and electronical microscopy, respectively.
- **Key results** *elo1* plants exhibited different responses to sucrose, light and stress variables and at high sucrose concentrations showed an enhancement of germination and inhibition of leaf growth as compared to wild type. Furthermore, electron microscopical analysis provided the first ultrastructural description of an *elo* mutant, which showed a hypotonic vacuole, alterations in the size of grana and starch grains in the chloroplasts and the massive presence of Golgi’s vesicles in the cytoplasm.
- **Conclusions** Based on the obtained results we propose that mechanisms which produce carbon assimilates or import sucrose could be affected in *elo1* plants and could account for the observed differences, implying a role of Elongator in the regulation of these processes.

Key words: Elongator complex, *elo1*, leaf development, germination, cell division, cell expansion, morphometric analysis, electron microscopy, *Arabidopsis thaliana*, sucrose.

INTRODUCTION

Leaf morphogenesis is a complex developmental process, controlled by genetic and environmental factors. Finally, it results into a functional photosynthetic organ, able to capture light, produce carbon metabolites, exchange gasses and transpire water for plant cooling and circulation [16, 18, 157, 269-271]. Leaf growth is determined by cell division and expansion. According to the “neo cell theory” [16], the size and shape of leaves is secondarily affected by the size and shape of each leaf cell, which is considered the unit of all tissues and organs. Both final cell number and cell polarity have a genetic basis, thus controlling tissue organization and, finally, leaf shape. Indeed the manipulation of cell cycle or cell wall extensibility resulted in different leaf shapes [272]. Peculiarly, in plant leaf an inter-reliant cellular compensatory mechanism can deliver the same morphological output in different ways: for instance, a specific lamina width can be achieved with lots of small palisade cells or vice versa with a smaller amount of large palisade cells. However this so-called compensation mechanism does not always occur. Furthermore, environmental variables, such as light, temperature or nutrients, play a modulatory role and can modify an established morphogenetic program [144].

In this context, an important role is played by sucrose, which is an important metabolite for plant growth, tissue differentiation and maturation. Namely, its import and cleavage, via invertases and sucrose synthases, into signal hexoses (glucose, fructose, UDP-glucose) is known to act at the cellular level, controlling cell division and expansion [238, 245, 256, 273-275].

In the present work a “narrow leaf” *elo1* mutant of *Arabidopsis thaliana*, which displays a slim lamina (Fig. 1a), the so-called “narrow leaves” phenotype was taken as representative of all the *elo* mutations and investigated at cytophysiological level. *elo1* belongs to the *elongata* class [158] and has a mutation in the At3g11220 gene which is homologous to the yeast ELP4 component of the Elongator complex (Fig. 1b) [159, 160, 208, 222, 224, 276-282].

In yeast, the holo-Elongator complex, which contains histone acetyltransferase (HAT) activity [226] consists of 2 subcomplexes: ELP1, ELP2 and ELP3 (HAT) that compose the core-Elongator, and ELP4, ELP5 and ELP6 that constitute the accessory subcomplex. The *ELP* genes are the homologues of the TOxin Target (*TOT*) genes of *Saccharomyces cerevisiae*, that upon mutation slowly adapt growth to changing conditions and resistance to the zymocin toxin (Fig. 1b) [278]. KTI12 is a putative regulator of Elongator and its respective mutants display a

similar phenotype as the *elp/tot* mutants. DRL1 is the homologue of KTI12 in *Arabidopsis* and its mutant alleles have a narrow leaves phenotype.

Our aim was to determine the physiological basis of the leaf morphology of the *elo1* mutant. In addition, we show through germination assays that light response, stress tolerance and sucrose metabolism are affected in the Elongator mutant.

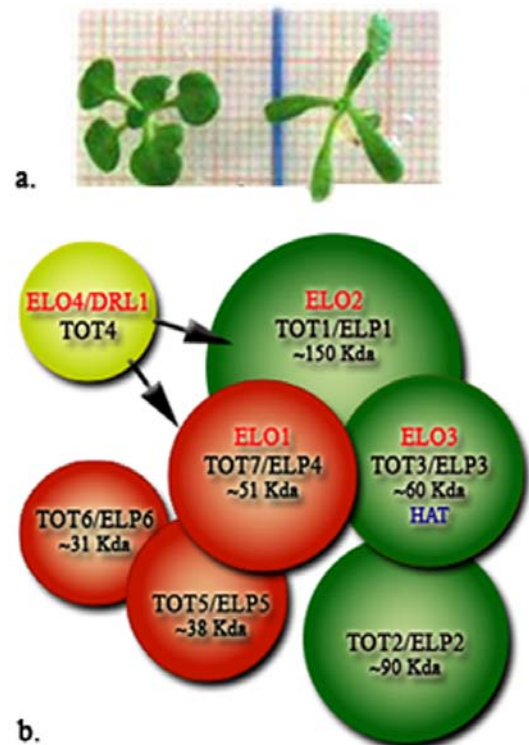


Fig.1. (a) 21 DAV wild type *Ler* (left) and mutant *elo1* (right) plantlets grown under standard condition 21 DAV. (b) The holo-Elongator complex. Red = accessory complex; green = core-Elongator; yellow = DRL1, interacts with the holo-Elongator complex. Red codes (*ELO1* to *ELO4*) refer to plant *elongata* genes [158], while black codes refer to Yeast Elongator genes (*TOT1* to *TOT7*) and their plant homologues (*ELP1* to *ELP6*) [160].

MATERIALS AND METHODS

Plant material and in vitro growth conditions

Seeds of *Arabidopsis thaliana* (L.) Heynh ecotype *Ler* (*Landsberg erecta*) and *elongata1* (*elo1*) have been described previously [159, 160]. For standard growth conditions, seeds were strongly sterilized by incubation for 2 min in ethanol 100% and for 12' in 1.75% hypochlorite solution (NaClO). Thereafter seeds were

germinated on plates using germination medium (GM) at 1% sucrose [283] and 0.7% agar (Sigma-Aldrich). Plates were kept 3 days overnight at 4°C for seed vernalization prior to be transferred to the germination chamber, where plants were grown under sterile conditions in a 16-h-light/8-h-dark regime at 22°C, with light intensity of 150 $\mu\text{mol}/\text{m}^2\cdot\text{sec}$ and 60% relative humidity. Plant age was estimated after completion of the 3-day-vernalization period and the first day of the plant corresponds to 1 day after vernalization (DAV). Different growth conditions were tested as described below.

Germination analysis

Germination tests performed at standard growth conditions were used as control. Different sterilization (water, 100% ethanol, 7%, 5.25%, 3.5%, sodium hypochlorite solution %), light (0 and 50 $\mu\text{mol}/\text{m}^2\cdot\text{sec}$) and nutrient (0-3% sucrose concentration) conditions were independently tested. Three replicates were done; for each replica, $n > 50$ seeds were germinated for each sample.

Morphological analysis

Analysis was performed on first and third expanded leaves of 24-day-old (21 DAV) *Ler* and *elo1* plantlets, grown at standard conditions on GM, supplemented with three different sucrose concentrations (0.5%, 1% or 2%). Entire leaves were excised at the basis of the petiole, mounted onto a microscope slide, put on a millimeter paper and photographed with a fixed 6.3 Mp Fuji Finepix S7000 digital camera. Image analysis was done using the ImageJ 1.032j software (Wayne Rasband, National Institutes of Health, USA) after pixel/mm conversion. Four parameters were measured: lamina length, width and area, petiole length. Three different replicas were done and $n > 10$ leaves were utilised for each sample.

Histological analysis

Analysis was performed on first and third fully expanded leaves of 24-day-old (21 DAV) *Ler* and *elo1* seedlings, grown at the standard conditions on GM, supplemented with three different sucrose concentrations (0.5%, 1% or 2%). From each collected leaf a median sector was excised under a stereomicroscope and immediately fixed either in paraformaldehyde 4% overnight or in a glutaraldehyde 3%-paraformaldehyde 0.5%-phosphate buffered

saline solution at 4°C, for 3 h. After dehydration samples were embedded in Tecnovitt 8100 resin and cross sectioned at 4 μm using a LEICA RM 2155 Microtome; other samples were embedded in paraplast embedding media (Sigma-Aldrich) and cross sectioned at 10 μm . Sections were stained for 10' with either toluidine blue (0.05% in phosphate buffer 0.1M pH 6.7) or Periodic Acid Schiff (PAS) and mounted with Canada balsam. Screenshots of transversal sections were consecutively acquired using a LEICA DMRB Microscope and the LEICA IM50 software under a 200X magnification. Palisade Cell Number (PCN) [284] and Palisade Cell/Gap Number (PCGN) were estimated on the three widest sections of each leaf. PCGN analysis takes into account gaps present in the palisade layer. One gap corresponds to one "virtual" palisade cell with the same mean area of the 2 cells that are adjacent to the gap. PCGN analysis was necessary in the case of *elo1* mutants, characterized by high number of gaps in the palisade layer (>5%), in order to obtain a more significant correlation with lamina width. Stomatal chambers were not taken into account. The screenshots of the transversal sections were merged together with the Adobe Photoshop CS2 "photomerge" function and cell area measurements on digital images were done with the freely available IMAGEJ software, after pixel/ μm conversion. Three different replicas were done and $n > 20$ leaves were taken for each sample. Cell area analysis ($n > 600$ for each sample) was performed on the same sections. In addition, cell area was also measured from the adaxial side through differential interference contrast optics. Cleared first leaves were used to measure the cell area from the adaxial side. The cells seen under the microscope were digitalized and analyzed with the IMAGEJ software, after pixel/ μm conversion. Other parameters, such as cell length (along the proximal-distal axis of the leaf) and width (along the lateral axis of the leaf) were measured on the same pictures.

Statistical Analysis

All data were evaluated statistically with the SPSS software (Statistical Package for the Social Sciences, version 11.0.0, SPSS, Inc., Chicago, IL). In order to verify whether the distribution was normal or left/right skewed, a "descriptive statistics" was performed. In case of skewed distribution, a logarithmic transformation ($\ln X$) of the data was applied, thus transforming it into a normal distribution. Thereafter a Student t-test between two set of data was calculated to obtain a significance value p of the mean differences. In our case the

null (H_0) hypothesis of “equality of means” is rejected if $p \leq 0.05$.

Electron microscopy

Analysis was performed on first and third fully expanded leaves of 24-day-old (21 DAV) *Ler* and *elo1* seedlings, grown at the standard conditions on GM, supplemented with three different sucrose concentrations (0.5%, 1% or 2%). Slices ($n > 5$ for each sample) were fixed overnight at 4°C in 3% glutaraldehyde in 0,1 M cacodylate buffer (pH 6.9) and post-fixed for 2h in 15% osmium tetroxide in the same buffer and at the same temperature. Specimens were dehydrated in a graded series of ethyl alcohol and propylene oxide solutions and embedded in araldite. Staining with uranyl acetate was carried out while dehydrating with 75% alcohol. Ultrathin sections (0.06 μm) were cut with a Leica Ultracut UCT, stained with lead citrate and observed with a transmission electron microscope (Zeiss EM900) operating at 50 kV.

RESULTS

elo1 seed germination is more efficient under stress conditions

As expected, washing and only ethanol sterilization were ineffective in avoiding contaminations for both *elo1* and *Ler* seeds. By contrast, 14' treatment with NaClO solutions suppressed any contamination whatever concentration was applied. However, after treatment with 7% NaClO solution seed germination was completely inhibited for *Ler* seeds (0%) and drastically reduced for *elo1* seeds (<10% germination) (Fig. 2a).

Treatments with serial dilutions (25%, 50% and 75%) of NaClO solution showed that *elo1* seeds were more resistant to hypochlorite than *Ler* seeds, being able to maintain good germination rates (>60%) at higher bleach concentrations (5.25%) compared to wild type (3.5%), (Fig. 2a). Subsequently, the effects of low light intensity (50 $\mu\text{mol}/\text{m}^2 \cdot \text{sec}$) and dark conditions on seed germination were also tested (Fig. 2b). Results showed that in absence of light, both *Ler* and *elo1* seeds had a significant decreased germination rate compared to standard light conditions (150 $\mu\text{mol}/\text{m}^2 \cdot \text{sec}$). Interestingly, under “strong shadow” conditions, *Ler* seeds had a low germination rate of about 50%, whereas *elo1* seeds maintained a high

germination rate (>80%). Finally (Fig. 2c), a nutrient test was done, using sucrose concentration (ranging from 0 to 3%) as variable. It was ascertained that germination of *Ler* seeds was always affected when standard sucrose concentrations were varied from sucrose depletion to sucrose abundance. By contrast, *elo1* seeds exhibited a reduced germination rate only at the highest sucrose concentrations (3%).

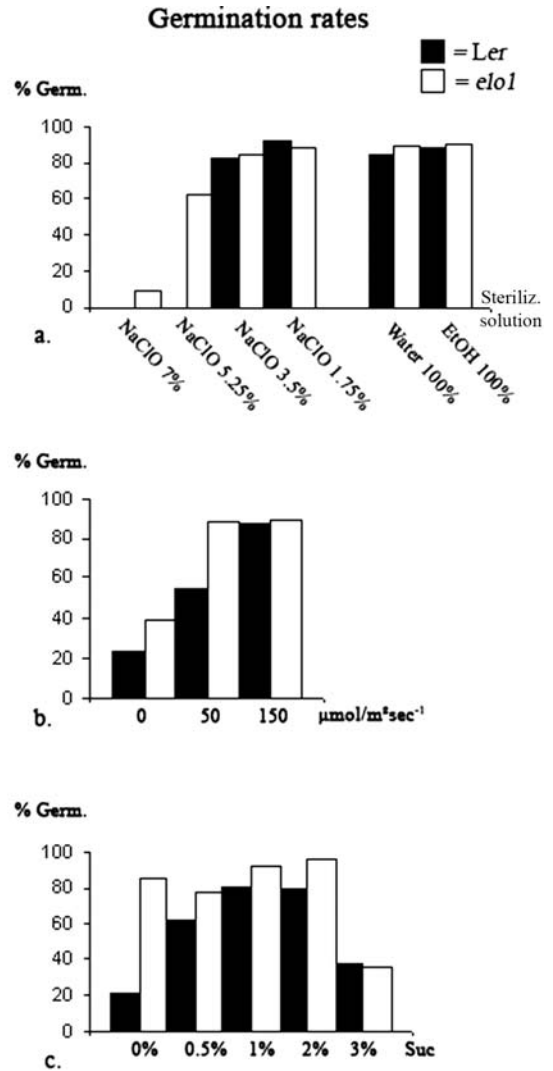


Fig.2 Seed germination rates under different environmental conditions dealing with: (a) sodium hypochlorite solutions concentration, (b) light intensity and (c) sucrose concentrations.

Sucrose-dependent differences in growth stage exist between elo1 and Ler plants

Growth stage-based analysis of *Ler* and *elo1* plants (Table 1) cultured for 24 days in standard *in vitro* conditions on germination medium supplied with different sucrose

concentrations (0.5%, 1% and 2%) was done. Seeds were synchronized by means of a 3-DAV period, but radicle appearance and cotyledon emergence from seed coat were not synchronized (data not shown). However, 7 DAV both wild type and mutant plantlets reached stage 1.00 [9], with the 2 cotyledons fully open. Since then, plant growth proceeded dissimilarly between mutants and wild types. At 12 DAV sucrose starvation (0.5%) had clearly a macroscopic and visible effect on *elo1* plants, which displayed a one-leaf delay as compared to those grown in standard conditions (1% sucrose) and in sucrose abundance (2%). Namely, the former exhibited only three rosette leaves bigger than 1 mm (stage 1.03), while these latter were able to produce four rosette leaves bigger than 1 mm (stage 1.04). This delay was kept until 21 DAV where stages 1.05 and 1.06 were reached, respectively. No visible differences were induced by sucrose treatment in *Ler* plants until 15 DAV. From this point on, sucrose abundance transiently accelerated leaf emergence (stage 1.07) compared to standard conditions (stage 1.06).

More precisely, at 21 DAV *Ler* plants grown in standard conditions and in sucrose abundance reached the same stage (stage 1.07, with 7 rosette leaves bigger than 1 mm), because of a faster growth in standard conditions than in sucrose abundance. In addition, at 18 DAV *Ler* plants cultured either in sucrose starvation or standard conditions displayed no growth differences and the one-leaf delay was observed only at 21 DAV.

Taken all together these observations showed that *elo1* plants had a final one-stage retard compared to *Ler* plants grown in the same nutrient conditions, but also that growth dynamics of wild type and mutant plants are differentially driven by sucrose availability. Namely, sucrose abundance had no effect on *elo1* plants and early effects of sucrose starvation were observed in *elo1* plants with respect to wild type, in such a way the delay in leaf emergence was anticipated.

Under different sucrose concentrations Ler and elo1 leaves exhibit opposite lamina growth dynamics

Leaf morphometric parameters were measured of the fully expanded first and third leaves of 21 DAV plants grown on media supplemented with 0.5%, 1% and 2% sucrose. Four parameters were taken into account: petiole length, lamina length, width, and area (Fig. 3). In *elo1* plants grown at 2% sucrose, petiole and lamina length were not evaluated, due to the absence of transition between lamina and petiole; in this case the whole leaf length was measured.

Our data showed that, with the exception of the first leaf at 0.5% sucrose concentration, *elo1* leaves were always significantly narrower than *Ler* leaves (Fig. 3a). Secondly, in *Ler* and *elo1* plants leaf growth responded to sucrose concentration in opposite ways: high sucrose concentrations enlarged *Ler* leaves, namely lamina width and area, whereas narrowed *elo1* leaves (Fig. 3a and e). Notably, the differences in lamina width and area were statistically significant at 2% sucrose concentration and especially for the third leaf.

PC(G)N analysis show different cell division number at increasing sucrose concentrations

In order to investigate whether sucrose treatments induced variations in lamina width by cell division number, we evaluated the number of cells and gaps in the palisade layer PC(G)N of leaf mesophyll. The analysis was performed on transversal sections of fully expanded first and third leaves of *Ler* and *elo1* plants grown 21 DAV on media supplemented with 0.5%, 1% and 2% sucrose (Fig. 4a).

Mutants had a significantly reduced PCN compared to *Ler* plants, while PCGN was reduced at almost all sucrose conditions, with the exception of first leaves in sucrose starvation and abundance. PCN sensibly increased for *Ler* first leaves from 0.5% sucrose to 1% and for *Ler* third leaves from 1 to 2%.

Table.1 Growth stage-based analysis [33] of *Ler* and *elo1* plants grown in standard in vitro conditions on germination medium supplied with different sucrose concentrations

Phenotype	% Sucrose	7 DAV	12 DAV	15 DAV	18 DAV	21 DAV
<i>Ler</i>	0.5	1	1.04	1.05	1.06	1.06
<i>Ler</i>	1	1	1.04	1.05	1.06	1.07
<i>Ler</i>	2	1	1.04	1.05	1.07	1.07
<i>elo1</i>	0.5	1	1.02	1.03	1.04	1.05
<i>elo1</i>	1	1	1.02	1.04	1.05	1.06
<i>elo1</i>	2	1	1.02	1.04	1.05	1.06

DAV= Days After Vernalization; growth stages: 1 = 2 cotyledons fully open, 1.02 - 1.07 = plantlets with 2 - 7 rosette leaves bigger than 1 mm

These results are consistent with a clear effect of sucrose concentrations on cell division. On the other hand, PCGN values showed that the reduction of cell number was accompanied by the presence of several gaps (Fig. 4b) that, at 0.5% and 2% sucrose concentrations, for first leaves, partially compensate the reduction of cells in the mutant.

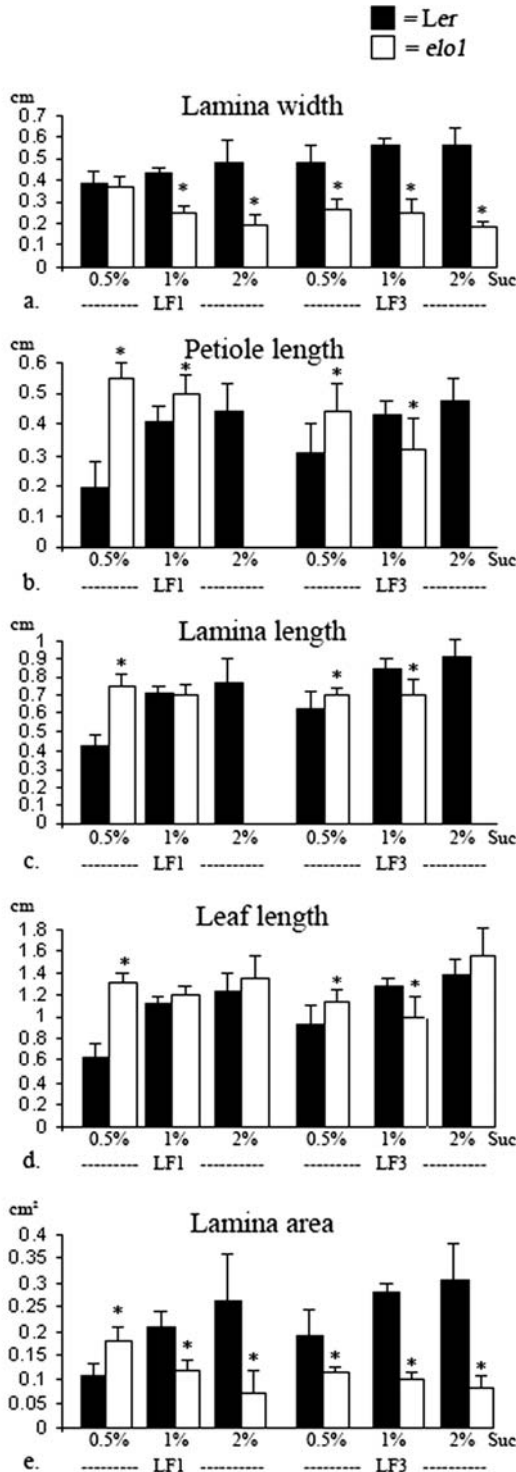


Fig.3. Mean values and standard deviation of lamina width (a), petiole length (b), lamina length (c), leaf

length (d) and lamina area (e) of 21 DAV *Ler* and *elo1* first and third leaves, grown in standard *in vitro* conditions, but with different sucrose concentrations (0.5%, 1% and 2%) in the medium. Asterisks indicate a statistically significant difference between *elo1* and *Ler* values (t-test, $P < 0.05$).

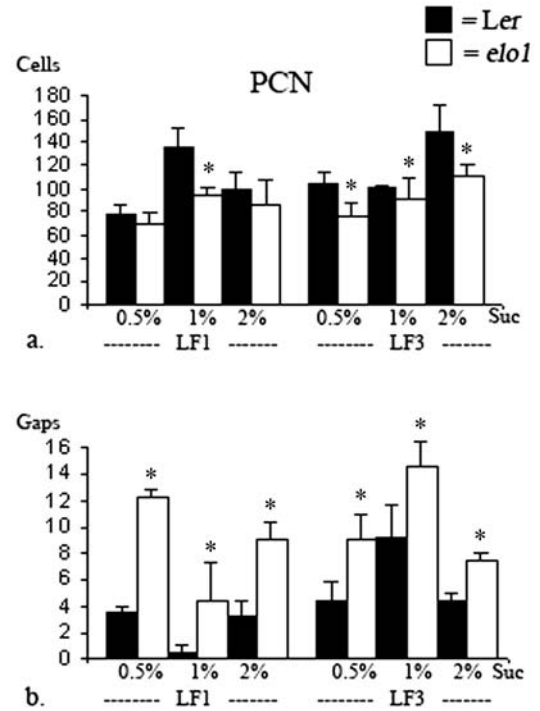


Fig.4. (a) Mean and standard deviation values of Palisade Cell Number (PCN) and (b) gaps of 21 DAV *Ler* and *elo1* first and third (a) leaves, grown in standard *in vitro* conditions, but with different sucrose concentrations (0.5%, 1% and 2%) in the medium. Asterisks indicate a statistically significant difference between *elo1* and *Ler* values (t-test, $P < 0.05$).

Sucrose concentrations differentially affected cell expansion in *elo1* and wild type plants

In order to have a complete overview on lamina growth, the area of palisade cells was evaluated on paradermal and transversal leaf sections (Fig. 5a).

In standard conditions, from paradermal microscopic observations, *elo1* cells showed an increased area compared to *Ler* cells. Furthermore, wild type cells increased their area when sucrose concentration was enhanced, while at the same condition cell expansion was reduced in the mutant. Vice versa, in sucrose starvation, *elo1* cells increased their area and *Ler* cells reduced theirs.

Cell dimensions were also measured along the two main axes of the leaf, the proximal-distal X-axis and the lateral Y-axis. No significant polarity was found in cell growth

along these two axes (data not shown) and such condition was not affected by sucrose concentration.

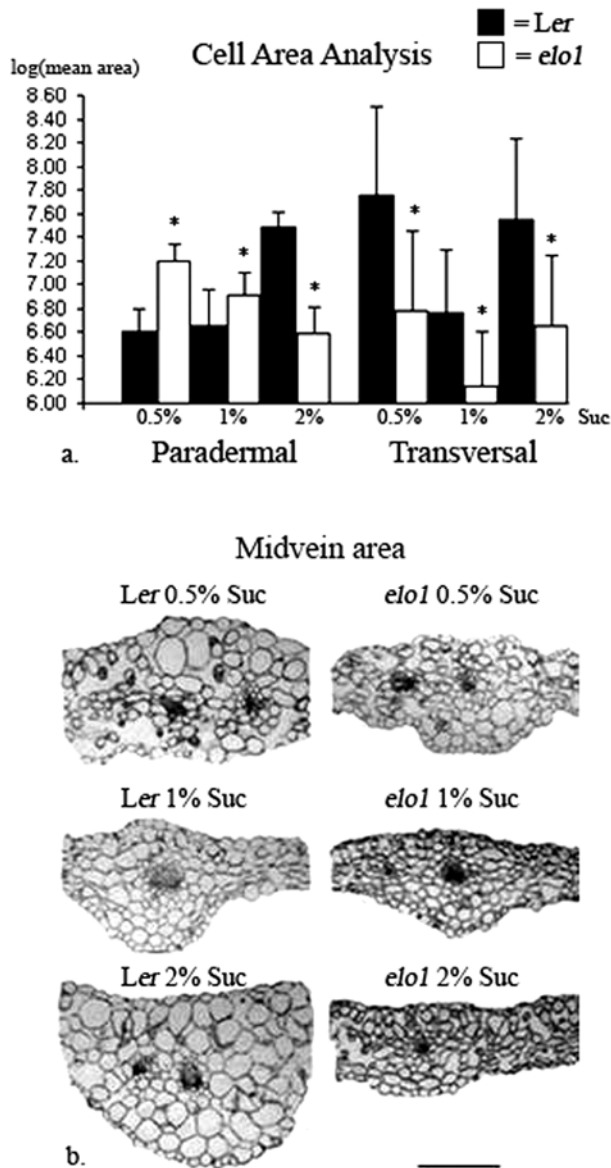


Fig.5. (a) Logarithmic mean and standard deviation values of paradermal (measured from the adaxial face of the leaf) and transversal cell area of 21 DAV *Ler* and *elo1* first leaves, grown in standard *in vitro* conditions, but with different sucrose concentrations (0.5%, 1% and 2%) in the medium. Asterisks indicate a statistically significant difference between *elo1* and *Ler* values (t-test, $P < 0.05$). (b) Transversal sections of 21 DAV *Ler* and *elo1* first leaves grown on different germination media with 0.5%, 1% and 2% sucrose showing the midvein and cell area differences. All sections are at the same magnification (bar = 500 μ m).

The palisade cell area was furthermore estimated on transversal sections. Surprisingly, compared to controls grown under different sucrose concentrations, mutants exhibited an overall reduced cell area (Fig. 5b). When the effects of different sucrose concentrations were analyzed, it was evident that high sucrose concentration induced a significant increase of cell area in *Ler* leaves, whereas *elo1* cell area stayed relatively constant and small. These results suggest clearly that cell expansion along the dorsal-ventral axis (Z-axis) is affected in mutants and that an opposite behaviour is active in *elo1* and *Ler* plants, in a sucrose-dependent way.

Finally, in the *elo1* mutant, sucrose starvation induced cells to become smaller along Z-axis and larger in the XY lamina, thus showing the establishment of a compensatory polarity in cell growth.

***elo1* plants have less stacked grana, a hypotonic vacuole and an active exocytosis**

TEM (Transmission Electron Microscopy) was carried out on ultrathin sections of *Ler* and *elo1* first leaves harvested at 21 DAV (Fig. 6).

Plants were grown on germination media with different sucrose concentrations.

Comparing wild type and mutant plants grown at standard conditions (1% sucrose), it was evident that chloroplast were well differentiated in *Ler* (Fig. 6a), with abundant grana and thylakoids distributed in the stroma (Fig. 6c), whereas *elo1* chloroplasts (Fig.6b) had long double interconnecting thylakoids and less stacked granal thylakoids (Fig. 6d). Furthermore, *Ler*'s chloroplasts preferentially accumulated lipids and proteins, evidenced by the presence of numerous plastoglobules (Fig. 6a), as compared to the reduced number or complete absence of primary starch. By contrast, in *elo1* primary starch was frequently visible in addition to few plastoglobules (Fig. 6b).

In both *Ler* and *elo1* seedlings grown on GM at 2% sucrose concentration, cells exhibited chloroplasts with large starch grains (Fig. 6e and f). In addition, a peculiar feature of *elo1* (Fig. 6g) cells, compared to control (Fig. 6h), was a hypotonic vacuole, likely related to a reduced turgor pressure. The vacuole consisted of a dense matrix in *elo1* cells grown on 2% sucrose media (Fig. 6h). Such a matrix is possibly a mixture of intravacuolar components and glycosides, as supported by eosine staining (data not shown). As a consequence of a lower vacuole/cytoplasm ratio nuclei were more easily detectable in *elo1* cells.

Mitochondria and peroxisomes were normally distributed in both mutant and wild type

cells, associated with chloroplast (data not shown).

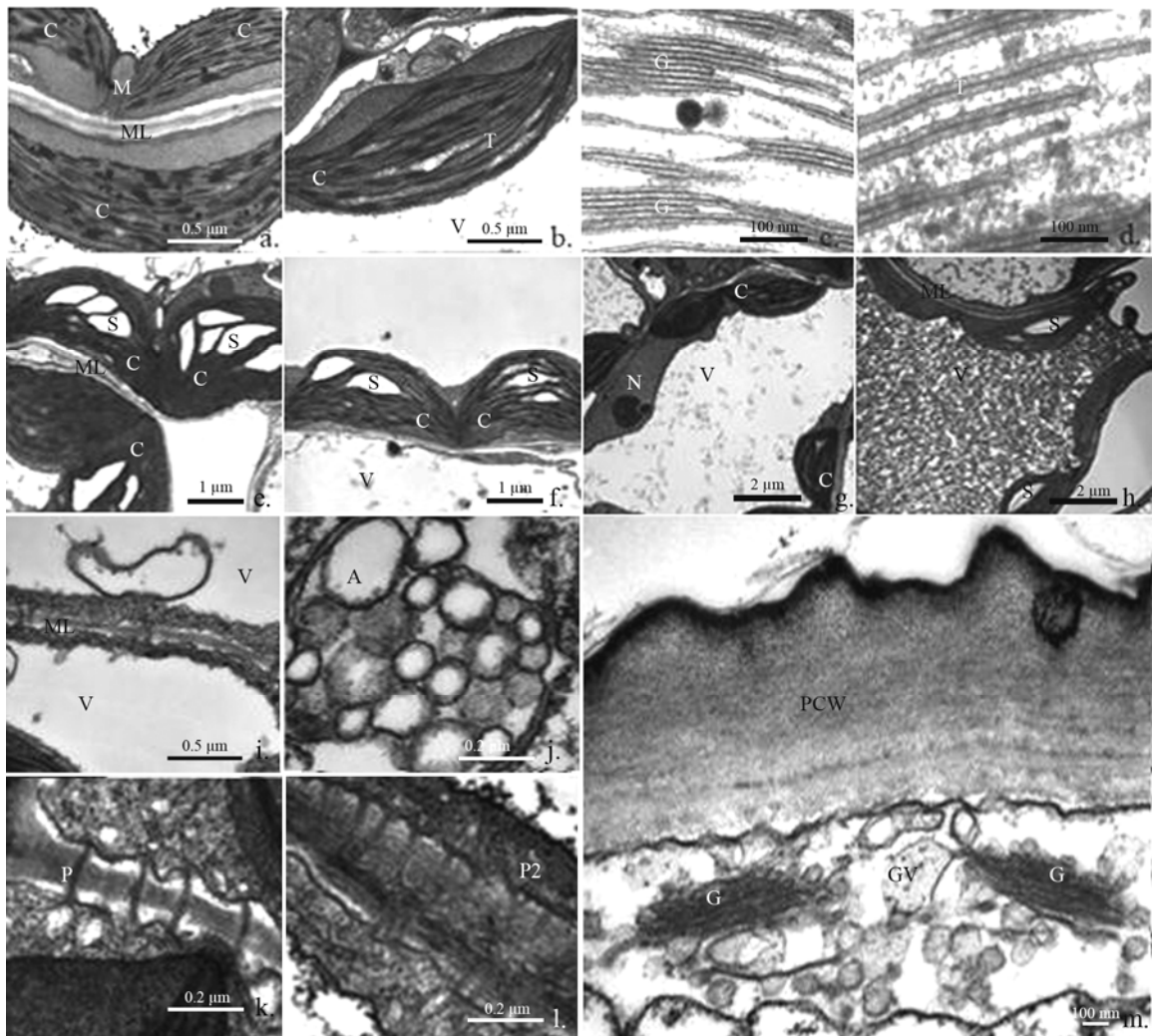


Fig.6. Chloroplasts of (a) *Ler* and (b) *elo1* cells at standard conditions. Chloroplast thylakoids of *Ler* (c) and *elo1* (d). Chloroplast of *Ler* (e) and *elo1* (f) plants grown on 2% sucrose medium, showing a strong starch accumulation in the stroma. (g, h) *elo1* cells of plants grown on 0.5% (g) and 2% (h) sucrose concentration medium. (i, j) Autophagy in *Ler* (i) cells grown under sucrose starvation and *elo1* (j) cells grown in standard conditions. (k, l) Plasmodesmata of *elo1* cells of plants grown in standard conditions (k) and in sucrose abundance (l). (m) Golgi of *elo1* cells of plants grown in standard conditions. Magnifications: (a,b,i)= 20000X; (c,d) 85000X; (e,f)= 7000X; (g,h)= 4400X; (j,k,l) = 50000X; (m)= 30000X. C=chloroplast, M= Mithochondrion, N=Nucleus, S=Starch, ML=Median lamella, V=Vacuole, A=Autofagic products, P=Simple plasmodesma, P2=Y plasmodesma, G=Golgi apparatus, GV=Golgi's vesicles, PCW= Primary cell wall.

We observed autophagy in *Ler* cells grown in sucrose starvation (Fig. 6i) and in *elo1* cells grown in standard conditions (Fig. 6j).

Dense plasmodesmata were present in *elo1* cells of plants grown on 1% (Fig. 6k, simple plasmodesmata) and 2% (l, Y plasmodesmata) sucrose media, indicating functional and active symplastic cooperation between cells. Finally, the Golgi apparatus (Fig. 6m) had a high number of exocytosis vesicles and a large primary cell wall formation.

DISCUSSION

In the present work a clear relationship between leaf development, growth conditions and Elongator function has been detected by investigating growth responses, under different nutrient and environmental conditions, in both wild type and an *Arabidopsis* "narrow leaves" mutant (*elo1*), belonging to the *elongata* class (Berna *et al.*, 1999), which has a mutation in one of the components of the histone acetyl transferase Elongator complex.

Leaf morphology is the result of endogenous and exogenous factors [285], which act in a coordinated manner to optimize leaf functions [144]. Favourable environmental conditions, ranging from nutrients availability to physic and biotic factors, and active sensing mechanisms working in the plants can cooperatively enhance leaf growth, which is achieved through cell division initially, but prominently through cell expansion afterwards [143].

The “narrow leaves” phenotype of *Arabidopsis elo1* mutant is mainly the result of, at cytological level, a reduced number of palisade cells [159, 160] which also showed an altered pattern of cell expansion. During leaf growth cell division and cell expansion may spatially and temporally overlap and normally, both events are tightly related to carbohydrate availability. Among them a relevant role is played by sucrose [233, 256, 263, 286]. It has been widely demonstrated that sucrose depletion or abundance triggers enormous metabolic changes in order to reach a new equilibrium in nutrient balance and that sucrose plays important roles in gene expression, metabolic pathways and, finally, plant growth and differentiation [235, 256, 263, 265, 287, 288]. For instance, glucose and fructose, which originate from sucrose cleavage, are able to modulate gene expression by inducing/repressing so-called “famine” and “feast” genes [235]. In this context we may recall that in hexose depletion, genes involved in photosynthesis and nutrient mobilization are upregulated in “source” cells, while genes involved in storage and utilization are inhibited. Vice versa, in hexose abundance, storage and utilization genes are upregulated, in order to keep apart nutrients as much as possible and free energy for optimum metabolic processes (Volkenburgh, 1999; Roitsch and Gonzalez, 2004).

Using several cytological approaches we showed that *elo1* seeds, compared to *Ler* seeds, had higher germination rates in sucrose depletion. Our data also showed that *elo1* seeds had higher germination rates at low light intensities and at higher NaClO concentrations when compared to wild type. Furthermore, plant growth is differentially affected in *Ler* ecotype and *elo1* mutant following changes in sucrose concentrations of growth medium.

In particular, growth-stage based analysis showed that no sucrose effects were evident during the first week after vernalization, thus suggesting a late stage-specific action mechanism of sucrose. In addition, sucrose-dependent differences in leaf growth were detected between the two samples. Indeed, even if strong sucrose abundance (>3%) or sucrose depletion (0%), greatly inhibited or limited general plant growth,

under different sucrose concentrations lamina growth showed opposite patterns in the two phenotypes: increasing sucrose concentration from 0.5% to 2% narrowed leaf lamina in *elo1* mutants as compared to standard condition; by contrast, in wild type lamina growth was enhanced by increasing sucrose concentrations, mainly as a consequence of an increased cell area. Thus, it was assessed that in *elo1* mutants increasing sucrose concentrations inhibited faster general growth and especially leaf expansion than wild type plants.

A second peculiar aspect of our results dealt with the inhibitory action of high sucrose concentrations on cell expansion in *elo1* mutant. According to data in literature [159, 160], at standard conditions the reduction of palisade cell number in *elo1* first leaf was accompanied by numerous cell gaps. However, due to a partial compensatory mechanism, the paradermal area of these cells was larger than in the wild type. High sucrose concentrations strongly affected cell division, resulting in an even more reduced cell number in both phenotypes, but compensatory mechanism, leading to an enhancement of cell expansion, was active only in wild type. Namely, *elo1* cells reduced and *Ler* cells increased their paradermal cell area, respectively. In addition, whatever sucrose concentrations were tested, dorsal-ventral expansion of palisade cells was reduced, thus showing that in *elo1* mutants cell expansion is polarly affected. These different sucrose-related effects on *elo1* and wild type plants clearly indicate that sucrose and Elongator activity are mutually related to leaf growth.

In line with the cell area results, at ultrastructural level, *elo1* cells exhibited a hypotonic vacuole filled with a dense matrix, thus indicating an impairment of water influx, which in turn could account for the lack of cell expansion. In this context, we speculate that, because of the mutation in the At3g11220 gene, the *elo1* mutant plants don't sense anymore sucrose as an active metabolite or osmotic product, even if cellular concentrations are elevated. On the other hand, other ultrastructural differences, dealing with the size of grana and starch grains in the chloroplasts and the massive presence of Golgi's vesicles in the cytoplasm, which have been detected between *Ler* and *elo1* plants, were all related to either sucrose accumulation, or catabolism or export. Based on these observations, it can be suggested that mechanisms which produce carbon assimilates or import sucrose could be differentially regulated in *elo1* plants as compared to the wild type. These results are consistent with the upregulation of genes involved in sucrose cleavage and accumulation such as sucrose synthase and invertase inhibitor, detected in the *elo1* mutant

compared to wild type, in an AFFYMETRIX microarray analysis (D. Fleury, personal communication).

During germination sucrose formation and reallocation are necessary for all processes that lead to radicle emergence [289, 290]. We may postulate that the enhancement of peculiar metabolic pathways leading to sucrose formation gives raise to higher germination rates and stress tolerance mechanisms in the *elo1* mutant seed. Conversely, in wild types, a functional Elongator is able to “sense” intracellular sucrose levels and adjust transcription of genes involved in sucrose cleavage and hexose formation, which are known to favour cell division and are important for ATP formation, thus avoiding the establishment of inhibitory levels that may affect general growth.

Further speculation may suggest a stage-specific action of Elongator at the critical switch germination-seedling growth, when photosynthesis becomes the main metabolic way that leads to sucrose formation. Elongator could “sense” the intracellular energetic status and control important pathways leading to sucrose synthesis or sucrose cleavage, thus adjusting intracellular respiratory ratios.

In conclusion, we demonstrated that sucrose and light sensing mechanisms but also stress tolerance mechanisms of *elo1* plants were not comparable to those of the wild type. Based on the above mentioned microarray data, we propose that in *elo1* mutants high sucrose concentration, due to both enhanced endogenous biosynthesis and exogenous supply, could account for the stimulation of germination and inhibition of leaf growth.

Acknowledgments

We thank Dr. Enrico Perrotta and Dr. Enza Tenzi for technical support, and Dr. Delphine Fleury for providing unpublished information on microarray analysis. This project was funded by the European Union in the frame of the PREDEC project (HPMT-CT-2000 00088) and the MIUR (ex 60% grant).

Conclusion

Our data showed that *elo1* seeds had higher germination rates at low light intensities and at higher NaClO concentrations when compared to wild type.

Although our experimental approach does not allow identifying the direct mechanisms underlying Elongator functions, the discussed results show that in *Arabidopsis thaliana* leaf formation (i.e. lamina width) and seed germination is Elongator-dependent in a sucrose, light and stress-mediated way.

These results are supported by a recently published microarray experiment on *elo* genes ([16]; ArrayExpress: E-MEXP-300) and personal communication of Delphine Fleury. This Affymetrix ATH1 microarray experiment identified 2897 differentially ($P \leq 0.05$) expressed genes between genotypes, wt *Ler* and at least one mutant (*elo2*, *elo3*, *elo4* and *ang4*). A further “narrow leaf”-type phenotype (*Ang4*) was also included to distinguish the differentially expressed genes that were not a direct consequence of *elo* and *dr1-2* mutations but, rather, a secondary effect of the leaf phenotype. Among these genes, 469 resulted upregulated while 371 downregulated.

The organization of these genes into metabolic pathways has brought to interesting metabolic features, which support our results. Namely, in addition to other metabolic pathways, *elo* mutant plants exhibited upregulation of genes involved in gluconeogenesis (GNG), TCA cycle, pentose phosphate shunt, protein catabolism and β -oxidation.

On the other hand, genes related to glycolysis, photosynthesis, sucrose breakdown and fatty acid synthesis resulted downregulated.

In this context we may recall that during the first stages of germination, β -oxidation pathway and protein degradation are active in producing sucrose via GNG, which is important to undergo cell division and growth [291, 292]. At these initial stages a large amount of ATP is necessary for supporting anabolic processes leading to carbohydrate and especially sucrose formation [293].

After radicle emergence (end of germination) and first leaf formation, carbohydrate allocation is mainly due to photosynthesis, which produces ATP and NADPH and promotes starch storage and fatty acid synthesis. Notably, in *elo* mutants the processes of carbohydrate formation through photosynthesis is downregulated, while the β -oxidation/GNG pathway remains upregulated throughout growth.

Thus, from our results and microarray data it seems that in *elo* mutants a germination-like metabolism is permanently active.

Based on these overall evidences a model of Elongator's function in regulating differential set of genes in plants is proposed (Fig. 17).

Elongator, through histone acetylation and chromatin relaxation, may promote in a growth stage-specific way, the transcription of two peculiar set of genes, regulating the switch GNG-germination/photosynthesis-postgermination. According to this model, during germination Elongator could facilitate gene expression for sucrose synthesis, through GNG and β -oxidation, while in later stages it could promote sucrose formation through photosynthesis. In mutant plants, the switch from GNG to photosynthesis could be affected resulting in a scarce availability of ATP which in turn reduces general metabolism and growth (cell division and expansion, storage, etc.), causing the ‘narrow leaves’ phenotype, but also explaining the reduced root development of *elo* mutants. The ‘sensing’ mechanism could involve the intracellular respiratory ratio or the cytoplasmic Ca^{2+} concentration, both related to an ATP cycle: in such a way high ATP levels induce higher intracellular cytoplasmic Ca^{2+} levels [294], which enable metabolic responses, such as exocytosis, and finally lead to a reduction of intracellular ATP levels and Ca^{2+} sequestration in different cell compartments.

In our model, Elongator in the embryo, is active in promoting only the transcription of GNG and β -oxidation, which require a favourable respiratory ratio ($[ATP]/[ADP] > 1$). By contrast, when this ratio is unfavourable Elongator changes its conformation, thus promoting the transcription of another set of genes (i.e. genes involved in photosynthesis and fatty acid biosynthesis). In the mutant, Elongator is likely unable to “sense” anymore a low respiratory ratio, thus remaining constantly active in transcribing GNG and β -oxidation genes.

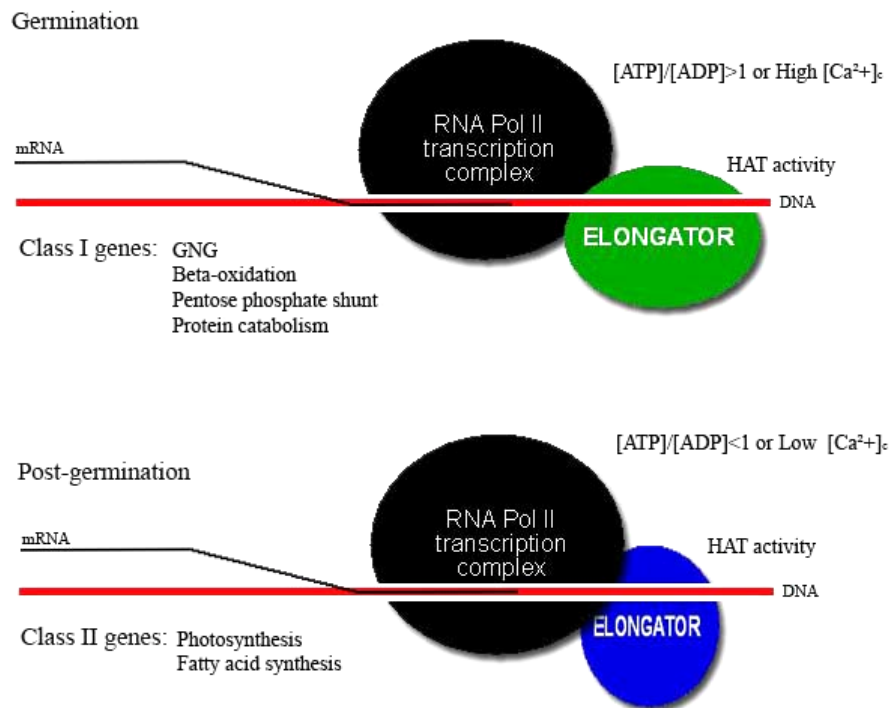


Fig.17. Model on the function of the Elongator complex. In the first stages of germination $[ATP]/[ADP]>1$, Elongator facilitates transcription through its HAT activity of a peculiar set of genes involved in storage mobilization, β -oxidation, GNG, pentose phosphate shunt, etc, which enhances sucrose formation, needed for radicle emergence and other metabolic processes. After germination, the respiratory ratio is low $[ATP]/[ADP]<1$. Elongator switches to another set of genes and facilitates their transcription in order to enhance photosynthesis and ATP, NADPH production and, consequently, fatty acid synthesis. The respiratory ratio or Ca^{2+} levels (strictly related to ATP concentrations) may regulate the holo-modifications of the Elongator complex and dictate the switch from catabolic to anabolic processes.

However, in this context, we have to consider that the Elongator complex is also present in Mammals [295, 296], which do not perform germination and photosynthesis. Still, the regulation of the Elongator complex could have been maintained throughout evolution and only the classes of genes differentially transcribed may have slightly changed. In Human, mutations in *IKBKAP*, encoding a subunit of Elongator, causes a severe neurodevelopmental disease named familial dysautonomia [297]; we may postulate that this disease could still be due to a defect in the switch of some differentially transcribed classes of genes, assessed in plants, like i.e. the downregulation of glycolysis and fatty acid biosynthesis and upregulation of GNG, pentose phosphate shunt and β -oxidation.

In conclusion, we demonstrated that sucrose and light sensing mechanisms but also stress tolerance mechanisms of *elo1* plants were not comparable to those of wild type. On the basis of the above model, in *elo1* mutants high sucrose concentration, due to both enhanced endogenous biosynthesis and exogenous supply, could account for the stimulation of germination and inhibition of leaf growth. Concerning Elongator's mechanism our hypothesis is that the holo-complex is able to sense the energetic state of cell through a direct binding of ADP or ATP or even Ca^{2+} to one of its subunits, which all together are necessary for its conformational status and allow transcription elongation of peculiar set of genes. Interactions with other proteins, such as *DRL1-2*, which contains ATP/GTP and calmoduline binding domains, could allow fine-tuning of Elongator regulation.

References

- Meinke, D.W., et al., *Arabidopsis thaliana: a model plant for genome analysis*. Science, 1998. **282**(5389): p. 662, 679-82.
- Meyerowitz, E.M., *Prehistory and history of Arabidopsis research*. Plant Physiol, 2001. **125**(1): p. 15-9.
- Somerville, C. and M. Koornneef, *A fortunate choice: the history of Arabidopsis as a model plant*. Nat Rev Genet, 2002. **3**(11): p. 883-9.
- Braun, A., *Freunde Zu Berlin*, 1873: p. p75.
- Laibach, F., *Zur frage nach der individualitat der chromosomen im pflanzenreich*. Beih. Bot. Zentralbl., 1907. **22**: p. 191-210.
- Laibach, F., *Arabidopsis thaliana (L.) Heynh, als object fur genetische und entwicklungsphysiologische untersuchungen*. Beih. Bot. Zentralbl., 1943. **44**: p. 439-455.
- Garcia-Hernandez, M., et al., *TAIR: a resource for integrated Arabidopsis data*. Funct Integr Genomics, 2002. **2**(6): p. 239-53.
- Initiative, T.A.G., *Analysis of the genome sequence of the flowering plant Arabidopsis thaliana*. Nature, 2000. **408**: p. 796-815.
- Boyes, D.C., et al., *Growth stage-based phenotypic analysis of Arabidopsis: a model for high throughput functional genomics in plants*. Plant Cell, 2001. **13**(7): p. 1499-510.
- Medford, J.I., et al., *Normal and Abnormal Development in the Arabidopsis Vegetative Shoot Apex*. Plant Cell, 1992. **4**(6): p. 631-643.
- Hudson, A., *Development of Symmetry in Plants*. Annu Rev Plant Physiol Plant Mol Biol, 2000. **51**: p. 349-370.
- Emery, J.F., et al., *Radial patterning of Arabidopsis shoots by class III HD-ZIP and KANADI genes*. Curr Biol, 2003. **13**(20): p. 1768-74.
- Hudson, A., *Plant development: Two sides to organ asymmetry*. Curr Biol, 2001. **11**(18): p. R756-8.
- Eshed, Y., S.F. Baum, and J.L. Bowman, *Distinct mechanisms promote polarity establishment in carpels of Arabidopsis*. Cell, 1999. **99**(2): p. 199-209.
- SurrIDGE, C., *Plant development: leaves by number*. Nature, 2003. **426**(6964): p. 237.
- Tsukaya, H., *Organ shape and size: a lesson from studies of leaf morphogenesis*. Curr Opin Plant Biol, 2003. **6**(1): p. 57-62.
- Kerstetter, R.A. and R.S. Poethig, *The specification of leaf identity during shoot development*. Annu Rev Cell Dev Biol, 1998. **14**: p. 373-98.
- Tsukaya, H., *Leaf development*. The Arabidopsis Book, 2002. **published online** <http://www.aspb.org/publications/Arabidopsis>.
- Scanlon, M.J., *Developmental complexities of simple leaves*. Curr Opin Plant Biol, 2000. **3**(1): p. 31-6.
- Bowman, J.L. and Y. Eshed, *Formation and maintenance of the shoot apical meristem*. Trends Plant Sci, 2000. **5**(3): p. 110-5.
- Bowman, J.L., *The YABBY gene family and abaxial cell fate*. Curr Opin Plant Biol, 2000. **3**(1): p. 17-22.
- Tsuge, T., H. Tsukaya, and H. Uchimiya, *Two independent and polarized processes of cell elongation regulate leaf blade expansion in Arabidopsis thaliana (L.) Heynh*. Development, 1996. **122**(5): p. 1589-600.
- Yu, Q., et al., *Cloning and characterization of a FLORICAULA/LEAFY ortholog, PFL, in polygamous papaya*. Cell Res, 2005. **15**(8): p. 576-84.
- Sano, R., et al., *KNOX homeobox genes potentially have similar function in both diploid unicellular and multicellular meristems, but not in haploid meristems*. Evol Dev, 2005. **7**(1): p. 69-78.
- Heisler, M.G., et al., *SPATULA, a gene that controls development of carpel margin tissues in Arabidopsis, encodes a bHLH protein*. Development, 2001. **128**(7): p. 1089-98.
- van der Graaff, E., et al., *Activation tagging of the LEAFY PETIOLE gene affects leaf petiole development in Arabidopsis thaliana*. Development, 2000. **127**(22): p. 4971-80.
- Chuck, G., C. Lincoln, and S. Hake, *KNAT1 induces lobed leaves with ectopic meristems when overexpressed in Arabidopsis*. Plant Cell, 1996. **8**(8): p. 1277-89.
- Serikawa, K.A. and P.C. Zambryski, *Domain exchanges between KNAT3 and KNAT1 suggest specificity of the kn1-like homeodomains requires sequences outside of the third helix and N-terminal arm of the homeodomain*. Plant J, 1997. **11**(4): p. 863-9.
- Rupp, H.M., et al., *Increased steady state mRNA levels of the STM and KNAT1 homeobox genes in cytokinin overproducing Arabidopsis thaliana indicate a role for cytokinins in the shoot apical meristem*. Plant J, 1999. **18**(5): p. 557-63.
- Pautot, V., et al., *KNAT2: evidence for a link between knotted-like genes and carpel development*. Plant Cell, 2001. **13**(8): p. 1719-34.
- Frugis, G., et al., *Overexpression of KNAT1 in lettuce shifts leaf determinate growth to a shoot-like indeterminate growth associated with an accumulation of isopentenyl-type cytokinins*. Plant Physiol, 2001. **126**(4): p. 1370-80.
- Douglas, S.J., et al., *KNAT1 and ERECTA regulate inflorescence architecture in Arabidopsis*. Plant Cell, 2002. **14**(3): p. 547-58.
- Venglat, S.P., et al., *The homeobox gene BREVIPEDICELLUS is a key regulator of inflorescence architecture in Arabidopsis*. Proc Natl Acad Sci U S A, 2002. **99**(7): p. 4730-5.
- Meyerowitz, E.M., *Genetic control of cell division patterns in developing plants*. Cell, 1997. **88**(3): p. 299-308.
- Barton, M.K., *Cell type specification and self renewal in the vegetative shoot apical meristem*. Curr Opin Plant Biol, 1998. **1**(1): p. 37-42.
- Evans, M.M. and M.K. Barton, *Genetics of Angiosperm Shoot Apical Meristem Development*. Annu Rev Plant Physiol Plant Mol Biol, 1997. **48**: p. 673-701.
- Barton, M.K.a.P.R.S., *Formation of the shoot apical meristem in Arabidopsis thaliana: an analysis of development in the wild type and in the shoot meristemless mutant*. Development, 1993(119): p. 823-831.
- Veit, B., *Determination of cell fate in apical meristems*. Curr Opin Plant Biol, 2004. **7**(1): p. 57-64.
- Brand, U., et al., *Dependence of stem cell fate in Arabidopsis on a feedback loop regulated by CLV3 activity*. Science, 2000. **289**(5479): p. 617-9.
- Fletcher, J.C., et al., *Signaling of cell fate decisions by CLAVATA3 in Arabidopsis shoot meristems*. Science, 1999. **283**(5409): p. 1911-4.
- Clark, S.E., et al., *The CLAVATA and SHOOT MERISTEMLESS loci competitively regulate meristem activity in Arabidopsis*. Development, 1996. **122**(5): p. 1567-75.
- Trotochaud, A.E., S. Jeong, and S.E. Clark, *CLAVATA3, a multimeric ligand for the CLAVATA1 receptor-kinase*. Science, 2000. **289**(5479): p. 613-7.
- Trotochaud, A.E., et al., *The CLAVATA1 receptor-like kinase requires CLAVATA3 for its assembly into a signaling complex that includes KAPP and a Rho-related protein*. Plant Cell, 1999. **11**(3): p. 393-406.
- Cock, J.M. and S. McCormick, *A large family of genes that share homology with CLAVATA3*. Plant Physiol, 2001. **126**(3): p. 939-42.
- Olsen, A.N. and K. Skriver, *Ligand mimicry? Plant-parasitic nematode polypeptide with similarity to CLAVATA3*. Trends Plant Sci, 2003. **8**(2): p. 55-7.
- Lenhard, M. and T. Laux, *Stem cell homeostasis in the Arabidopsis shoot meristem is regulated by intercellular movement of CLAVATA3 and its sequestration by CLAVATA1*. Development, 2003. **130**(14): p. 3163-73.
- Dievart, A., et al., *CLAVATA1 dominant-negative alleles reveal functional overlap between multiple receptor kinases that regulate meristem and organ development*. Plant Cell, 2003. **15**(5): p. 1198-211.
- Searle, I.R., et al., *Long-distance signaling in nodulation directed by a CLAVATA1-like receptor kinase*. Science, 2003. **299**(5603): p. 109-12.
- DeYoung, B.J. and S.E. Clark, *Signaling through the CLAVATA1 receptor complex*. Plant Mol Biol, 2001. **46**(5): p. 505-13.
- Jeong, S., A.E. Trotochaud, and S.E. Clark, *The Arabidopsis CLAVATA2 gene encodes a receptor-like protein required for the stability of the CLAVATA1 receptor-like kinase*. Plant Cell, 1999. **11**(10): p. 1925-34.
- Williams, R.W., S.E. Clark, and E.M. Meyerowitz, *Genetic and physical characterization of a region of Arabidopsis chromosome 1 containing the CLAVATA1 gene*. Plant Mol Biol, 1999. **39**(1): p. 171-6.
- Stone, J.M., et al., *Control of meristem development by CLAVATA1 receptor kinase and kinase-associated protein phosphatase interactions*. Plant Physiol, 1998. **117**(4): p. 1217-25.
- Williams, R.W., J.M. Wilson, and E.M. Meyerowitz, *A possible role for kinase-associated protein phosphatase in the Arabidopsis CLAVATA1 signaling pathway*. Proc Natl Acad Sci U S A, 1997. **94**(19): p. 10467-72.
- Clark, S.E., R.W. Williams, and E.M. Meyerowitz, *The CLAVATA1 gene encodes a putative receptor kinase that controls shoot and floral meristem size in Arabidopsis*. Cell, 1997. **89**(4): p. 575-85.

55. Clark, S.E., M.P. Running, and E.M. Meyerowitz, *CLAVATA1, a regulator of meristem and flower development in Arabidopsis*. Development, 1993. **119**(2): p. 397-418.
56. Zuo, J., et al., *The WUSCHEL gene promotes vegetative-to-embryonic transition in Arabidopsis*. Plant J, 2002. **30**(3): p. 349-59.
57. Xu, Y.Y., et al., *Activation of the WUS Gene Induces Ectopic Initiation of Floral Meristems on Mature Stem Surface in Arabidopsis thaliana*. Plant Mol Biol, 2005. **58**(6): p. 915.
58. Baurle, I. and T. Laux, *Regulation of WUSCHEL transcription in the stem cell niche of the Arabidopsis shoot meristem*. Plant Cell, 2005. **17**(8): p. 2271-80.
59. Jonsson, H., et al., *Modeling the organization of the WUSCHEL expression domain in the shoot apical meristem*. Bioinformatics, 2005. **21 Suppl 1**: p. i232-i240.
60. Kwon, C.S., C. Chen, and D. Wagner, *WUSCHEL is a primary target for transcriptional regulation by SPLAYED in dynamic control of stem cell fate in Arabidopsis*. Genes Dev, 2005. **19**(8): p. 992-1003.
61. Kamiya, N., et al., *Isolation and characterization of a rice WUSCHEL-type homeobox gene that is specifically expressed in the central cells of a quiescent center in the root apical meristem*. Plant J, 2003. **35**(4): p. 429-41.
62. Gallois, J.L., et al., *Combined SHOOT MERISTEMLESS and WUSCHEL trigger ectopic organogenesis in Arabidopsis*. Development, 2002. **129**(13): p. 3207-17.
63. Lenhard, M., G. Jurgens, and T. Laux, *The WUSCHEL and SHOOTMERISTEMLESS genes fulfil complementary roles in Arabidopsis shoot meristem regulation*. Development, 2002. **129**(13): p. 3195-206.
64. Brand, U., et al., *Regulation of CLV3 expression by two homeobox genes in Arabidopsis*. Plant Physiol, 2002. **129**(2): p. 565-75.
65. Gross-Hardt, R., M. Lenhard, and T. Laux, *WUSCHEL signaling functions in interregional communication during Arabidopsis ovule development*. Genes Dev, 2002. **16**(9): p. 1129-38.
66. Otsuga, D., et al., *REVOLUTA regulates meristem initiation at lateral positions*. Plant J, 2001. **25**(2): p. 223-36.
67. Hamada, S., et al., *Mutations in the WUSCHEL gene of Arabidopsis thaliana result in the development of shoots without juvenile leaves*. Plant J, 2000. **24**(1): p. 91-101.
68. Yu, L.P., et al., *POLTERGEIST functions to regulate meristem development downstream of the CLAVATA loci*. Development, 2000. **127**(8): p. 1661-70.
69. Schoof, H., et al., *The stem cell population of Arabidopsis shoot meristems is maintained by a regulatory loop between the CLAVATA and WUSCHEL genes*. Cell, 2000. **100**(6): p. 635-44.
70. Mayer, K.F., et al., *Role of WUSCHEL in regulating stem cell fate in the Arabidopsis shoot meristem*. Cell, 1998. **95**(6): p. 805-15.
71. Laux, T., et al., *The WUSCHEL gene is required for shoot and floral meristem integrity in Arabidopsis*. Development, 1996. **122**(1): p. 87-96.
72. Endrizzi, K., et al., *The SHOOT MERISTEMLESS gene is required for maintenance of undifferentiated cells in Arabidopsis shoot and floral meristems and acts at a different regulatory level than the meristem genes WUSCHEL and ZWILLE*. Plant J, 1996. **10**(6): p. 967-79.
73. Groot, E.P., N. Sinha, and S. Gleissberg, *Expression patterns of STM-like KNOX and Histone H4 genes in shoot development of the dissected-leaved basal eudicot plants Chelidonium majus and Eschscholzia californica (Papaveraceae)*. Plant Mol Biol, 2005. **58**(3): p. 317-31.
74. Yanai, O., et al., *Arabidopsis KNOXI proteins activate cytokinin biosynthesis*. Curr Biol, 2005. **15**(17): p. 1566-71.
75. Jasinski, S., et al., *KNOX action in Arabidopsis is mediated by coordinate regulation of cytokinin and gibberellin activities*. Curr Biol, 2005. **15**(17): p. 1560-5.
76. Matsuoka, M., et al., *Expression of a rice homeobox gene causes altered morphology of transgenic plants*. Plant Cell, 1993. **5**(9): p. 1039-48.
77. Lincoln, C., et al., *A knotted1-like homeobox gene in Arabidopsis is expressed in the vegetative meristem and dramatically alters leaf morphology when overexpressed in transgenic plants*. Plant Cell, 1994. **6**(12): p. 1859-76.
78. Meisel, L. and E. Lam, *The conserved ELK-homeodomain of KNOTTED-1 contains two regions that signal nuclear localization*. Plant Mol Biol, 1996. **30**(1): p. 1-14.
79. Long, J.A., et al., *A member of the KNOTTED class of homeodomain proteins encoded by the STM gene of Arabidopsis*. Nature, 1996. **379**(6560): p. 66-9.
80. Sundas-Larsson, A., et al., *A homeobox gene with potential developmental control function in the meristem of the conifer Picea abies*. Proc Natl Acad Sci U S A, 1998. **95**(25): p. 15118-22.
81. Goliber, T., et al., *Genetic, molecular, and morphological analysis of compound leaf development*. Curr Top Dev Biol, 1999. **43**: p. 259-90.
82. Bellaoui, M., et al., *The Arabidopsis BELL1 and KNOX TALE homeodomain proteins interact through a domain conserved between plants and animals*. Plant Cell, 2001. **13**(11): p. 2455-70.
83. Byrne, M.E., J. Simorowski, and R.A. Martienssen, *ASYMMETRIC LEAVES1 reveals knox gene redundancy in Arabidopsis*. Development, 2002. **129**(8): p. 1957-65.
84. Golz, J.F., E.J. Keck, and A. Hudson, *Spontaneous mutations in KNOX genes give rise to a novel floral structure in Antirrhinum*. Curr Biol, 2002. **12**(7): p. 515-22.
85. Hamant, O., et al., *The KNAT2 homeodomain protein interacts with ethylene and cytokinin signaling*. Plant Physiol, 2002. **130**(2): p. 657-65.
86. Barley, R. and R. Waites, *Plant meristems: the interplay of KNOX and gibberellins*. Curr Biol, 2002. **12**(20): p. R696-8.
87. Kumaran, M.K., J.L. Bowman, and V. Sundaresan, *YABBY polarity genes mediate the repression of KNOX homeobox genes in Arabidopsis*. Plant Cell, 2002. **14**(11): p. 2761-70.
88. Kim, J.Y., Z. Yuan, and D. Jackson, *Developmental regulation and significance of KNOX protein trafficking in Arabidopsis*. Development, 2003. **130**(18): p. 4351-62.
89. Engstrom, E.M., A. Izhaki, and J.L. Bowman, *Promoter bashing, microRNAs, and Knox genes. New insights, regulators, and targets-of-regulation in the establishment of lateral organ polarity in Arabidopsis*. Plant Physiol, 2004. **135**(2): p. 685-94.
90. Kim, J.Y., et al., *A novel cell-to-cell trafficking assay indicates that the KNOX homeodomain is necessary and sufficient for intercellular protein and mRNA trafficking*. Genes Dev, 2005. **19**(7): p. 788-93.
91. Postma-Haarsma, A.D., et al., *Characterization of the KNOX class homeobox genes Oskn2 and Oskn3 identified in a collection of cDNA libraries covering the early stages of rice embryogenesis*. Plant Mol Biol, 1999. **39**(2): p. 257-71.
92. Burglin, T.R., *Analysis of TALE superclass homeobox genes (MEIS, PBC, KNOX, Iroquois, TGIF) reveals a novel domain conserved between plants and animals*. Nucleic Acids Res, 1997. **25**(21): p. 4173-80.
93. Chen, H., A.K. Banerjee, and D.J. Hannapel, *The tandem complex of BEL and KNOX partners is required for transcriptional repression of ga20ox1*. Plant J, 2004. **38**(2): p. 276-84.
94. Kuijt, S.J., et al., *Different subcellular localization and trafficking properties of KNOX class 1 homeodomain proteins from rice*. Plant Mol Biol, 2004. **55**(6): p. 781-96.
95. Hay, A., et al., *Analysis of the competence to respond to KNOTTED1 activity in Arabidopsis leaves using a steroid induction system*. Plant Physiol, 2003. **131**(4): p. 1671-80.
96. Lu, P., et al., *Identification of a meristem L1 layer-specific gene in Arabidopsis that is expressed during embryonic pattern formation and defines a new class of homeobox genes*. Plant Cell, 1996. **8**(12): p. 2155-68.
97. Abe, M., T. Takahashi, and Y. Komeda, *Identification of a cis-regulatory element for L1 layer-specific gene expression, which is targeted by an L1-specific homeodomain protein*. Plant J, 2001. **26**(5): p. 487-94.
98. Chen, J.J., et al., *A gene fusion at a homeobox locus: alterations in leaf shape and implications for morphological evolution*. Plant Cell, 1997. **9**(8): p. 1289-304.
99. Langdale, J.A., *Plant morphogenesis. More knots untied*. Curr Biol, 1994. **4**(6): p. 529-31.
100. Ito, Y., M. Eiguchi, and N. Kurata, *KNOX homeobox genes are sufficient in maintaining cultured cells in an undifferentiated state in rice*. Genesis, 2001. **30**(4): p. 231-8.
101. Sakamoto, T., et al., *KNOX homeodomain protein directly suppresses the expression of a gibberellin biosynthetic gene in the tobacco shoot apical meristem*. Genes Dev, 2001. **15**(5): p. 581-90.
102. Ito, M., Y. Sato, and M. Matsuoka, *Involvement of homeobox genes in early body plan of monocot*. Int Rev Cytol, 2002. **218**: p. 1-35.
103. Dean, G., S. Casson, and K. Lindsey, *KNAT6 gene of Arabidopsis is expressed in roots and is required for correct lateral root formation*. Plant Mol Biol, 2004. **54**(1): p. 71-84.

104. Serikawa, K.A., A. Martinez-Laborda, and P. Zambryski, *Three knotted1-like homeobox genes in Arabidopsis*. Plant Mol Biol, 1996. **32**(4): p. 673-83.
105. Grigg, S.P., et al., *SERRATE coordinates shoot meristem function and leaf axial patterning in Arabidopsis*. Nature, 2005. **437**(7061): p. 1022-6.
106. Williams, L., et al., *Regulation of Arabidopsis shoot apical meristem and lateral organ formation by microRNA miR166g and its AtHD-ZIP target genes*. Development, 2005. **132**(16): p. 3657-68.
107. Prigge, M.J., et al., *Class III homeodomain-leucine zipper gene family members have overlapping, antagonistic, and distinct roles in Arabidopsis development*. Plant Cell, 2005. **17**(1): p. 61-76.
108. Bao, N., K.W. Lye, and M.K. Barton, *MicroRNA binding sites in Arabidopsis class III HD-ZIP mRNAs are required for methylation of the template chromosome*. Dev Cell, 2004. **7**(5): p. 653-62.
109. Sieber, P., et al., *Pattern formation during early ovule development in Arabidopsis thaliana*. Dev Biol, 2004. **273**(2): p. 321-34.
110. Mallory, A.C., et al., *MicroRNA control of PHABULOSA in leaf development: importance of pairing to the microRNA 5' region*. Embo J, 2004. **23**(16): p. 3356-64.
111. Juares, M.T., et al., *microRNA-mediated repression of rolled leaf1 specifies maize leaf polarity*. Nature, 2004. **428**(6978): p. 84-8.
112. Kidner, C.A. and R.A. Martienssen, *Spatially restricted microRNA directs leaf polarity through ARGONAUTE1*. Nature, 2004. **428**(6978): p. 81-4.
113. Eshed, Y., et al., *Establishment of polarity in lateral organs of plants*. Curr Biol, 2001. **11**(16): p. 1251-60.
114. McConnell, J.R., et al., *Role of PHABULOSA and PHAVOLUTA in determining radial patterning in shoots*. Nature, 2001. **411**(6838): p. 709-13.
115. McConnell, J.R. and M.K. Barton, *Leaf polarity and meristem formation in Arabidopsis*. Development, 1998. **125**(15): p. 2935-42.
116. McHale, N.A. and R.E. Koning, *MicroRNA-directed cleavage of Nicotiana sylvestris PHAVOLUTA mRNA regulates the vascular cambium and structure of apical meristems*. Plant Cell, 2004. **16**(7): p. 1730-40.
117. Tang, G., et al., *A biochemical framework for RNA silencing in plants*. Genes Dev, 2003. **17**(1): p. 49-63.
118. Pekker, I., J.P. Alvarez, and Y. Eshed, *Auxin Response Factors Mediate Arabidopsis Organ Asymmetry via Modulation of KANADI Activity*. Plant Cell, 2005.
119. Carlsbecker, A. and Y. Helariutta, *Phloem and xylem specification: pieces of the puzzle emerge*. Curr Opin Plant Biol, 2005. **8**(5): p. 512-7.
120. Zhao, C., et al., *The xylem and phloem transcriptomes from secondary tissues of the Arabidopsis root-hypocotyl*. Plant Physiol, 2005. **138**(2): p. 803-18.
121. Hawker, N.P. and J.L. Bowman, *Roles for Class III HD-Zip and KANADI genes in Arabidopsis root development*. Plant Physiol, 2004. **135**(4): p. 2261-70.
122. Kerstetter, R.A., et al., *KANADI regulates organ polarity in Arabidopsis*. Nature, 2001. **411**(6838): p. 706-9.
123. Meister, R.J., et al., *Multiple protein regions contribute to differential activities of YABBY proteins in reproductive development*. Plant Physiol, 2005. **137**(2): p. 651-62.
124. Yamaguchi, T., et al., *The YABBY gene DROOPING LEAF regulates carpel specification and midrib development in Oryza sativa*. Plant Cell, 2004. **16**(2): p. 500-9.
125. Golz, J.F. and A. Hudson, *Plant development: YABBYs claw to the fore*. Curr Biol, 1999. **9**(22): p. R861-3.
126. Eshed, Y., et al., *Asymmetric leaf development and blade expansion in Arabidopsis are mediated by KANADI and YABBY activities*. Development, 2004. **131**(12): p. 2997-3006.
127. Watanabe, K. and K. Okada, *Two discrete cis elements control the Abaxial side-specific expression of the FILAMENTOUS FLOWER gene in Arabidopsis*. Plant Cell, 2003. **15**(11): p. 2592-602.
128. Timmermans, M.C., et al., *ROUGH SHEATH2: a Myb protein that represses knox homeobox genes in maize lateral organ primordia*. Science, 1999. **284**(5411): p. 151-3.
129. Byrne, M.E., et al., *Asymmetric leaves1 mediates leaf patterning and stem cell function in Arabidopsis*. Nature, 2000. **408**(6815): p. 967-71.
130. Theodoris, G., N. Inada, and M. Freeling, *Conservation and molecular dissection of ROUGH SHEATH2 and ASYMMETRIC LEAVES1 function in leaf development*. Proc Natl Acad Sci U S A, 2003. **100**(11): p. 6837-42.
131. Ori, N., et al., *Mechanisms that control knox gene expression in the Arabidopsis shoot*. Development, 2000. **127**(24): p. 5523-32.
132. Tsiantis, M., et al., *The maize rough sheath2 gene and leaf development programs in monocot and dicot plants*. Science, 1999. **284**(5411): p. 154-6.
133. Schneeberger, R., et al., *The rough sheath2 gene negatively regulates homeobox gene expression during maize leaf development*. Development, 1998. **125**(15): p. 2857-65.
134. Luo, J.H., et al., *Different expression patterns of duplicated PHANTASTICA-like genes in Lotus japonicus suggest their divergent functions during compound leaf development*. Cell Res, 2005. **15**(8): p. 665-77.
135. Tattersall, A.D., et al., *The mutant crisper reveals multiple roles for PHANTASTICA in pea compound leaf development*. Plant Cell, 2005. **17**(4): p. 1046-60.
136. McHale, N.A. and R.E. Koning, *PHANTASTICA regulates development of the adaxial mesophyll in Nicotiana leaves*. Plant Cell, 2004. **16**(5): p. 1251-62.
137. Kim, M., et al., *The expression domain of PHANTASTICA determines leaflet placement in compound leaves*. Nature, 2003. **424**(6947): p. 438-43.
138. Koltai, H. and D.M. Bird, *Epistatic repression of PHANTASTICA and class 1 KNOTTED genes is uncoupled in tomato*. Plant J, 2000. **22**(5): p. 455-9.
139. Waites, R., et al., *The PHANTASTICA gene encodes a MYB transcription factor involved in growth and dorsoventrality of lateral organs in Antirrhinum*. Cell, 1998. **93**(5): p. 779-89.
140. Lynn, K., et al., *The PINHEAD/ZWILLE gene acts pleiotropically in Arabidopsis development and has overlapping functions with the ARGONAUTE1 gene*. Development, 1999. **126**(3): p. 469-81.
141. Newman, K.L., A.G. Fernandez, and M.K. Barton, *Regulation of axis determinacy by the Arabidopsis PINHEAD gene*. Plant Cell, 2002. **14**(12): p. 3029-42.
142. Siegfried, K.R., et al., *Members of the YABBY gene family specify abaxial cell fate in Arabidopsis*. Development, 1999. **126**(18): p. 4117-28.
143. Dale, J.E., *The control of leaf expansion*. Annual Review of Plant Physiology and Plant Molecular Biology, 1988. **39**: p. 267-295.
144. Volkenburgh, E.V., *Leaf expansion - an integrating plant behaviour*. Plant, Cell and Environment, 1999. **22**: p. 1463-1473.
145. Cho, K.H., et al., *Characterization of a member of the AN subfamily, IAN, from Ipomoea nil*. Plant Cell Physiol, 2005. **46**(1): p. 250-5.
146. de Lanerolle, P. and A.B. Cole, *Cytoskeletal proteins and gene regulation: form, function, and signal transduction in the nucleus*. Sci STKE, 2002. **2002**(139): p. PE30.
147. Tsukaya, H., *The leaf index: heteroblasty, natural variation, and the genetic control of polar processes of leaf expansion*. Plant Cell Physiol, 2002. **43**(4): p. 372-8.
148. Folkers, U., et al., *The cell morphogenesis gene ANGUSTIFOLIA encodes a CtBP/BARS-like protein and is involved in the control of the microtubule cytoskeleton*. Embo J, 2002. **21**(6): p. 1280-8.
149. Kim, G.T., et al., *The ANGUSTIFOLIA gene of Arabidopsis, a plant CtBP gene, regulates leaf-cell expansion, the arrangement of cortical microtubules in leaf cells and expression of a gene involved in cell-wall formation*. Embo J, 2002. **21**(6): p. 1267-79.
150. Kim, G.T., H. Tsukaya, and H. Uchimiya, *The CURLY LEAF gene controls both division and elongation of cells during the expansion of the leaf blade in Arabidopsis thaliana*. Planta, 1998. **206**(2): p. 175-83.
151. Tsukaya, H. and H. Uchimiya, *Genetic analyses of the formation of the serrated margin of leaf blades in Arabidopsis: combination of a mutational analysis of leaf morphogenesis with the characterization of a specific marker gene expressed in hydathodes and stipules*. Mol Gen Genet, 1997. **256**(3): p. 231-8.
152. Kim, G.T., et al., *CYP90C1 and CYP90D1 are involved in different steps in the brassinosteroid biosynthesis pathway in Arabidopsis thaliana*. Plant J, 2005. **41**(5): p. 710-21.
153. Kim, G.T., et al., *Changes in the shapes of leaves and flowers upon overexpression of cytochrome P450 in Arabidopsis*. Proc Natl Acad Sci U S A, 1999. **96**(16): p. 9433-7.
154. Kim, G.T., H. Tsukaya, and H. Uchimiya, *The ROTUNDIFOLIA3 gene of Arabidopsis thaliana encodes a new member of the cytochrome P-450 family that is required for the regulated polar elongation of leaf cells*. Genes Dev, 1998. **12**(15): p. 2381-91.
155. Tsukaya, H., T. Kozuka, and G.T. Kim, *Genetic control of petiole length in Arabidopsis thaliana*. Plant Cell Physiol, 2002. **43**(10): p. 1221-8.

156. Bancos, S., et al., *Regulation of transcript levels of the Arabidopsis cytochrome p450 genes involved in brassinosteroid biosynthesis*. Plant Physiol, 2002. **130**(1): p. 504-13.
157. Micol, J.L. and S. Hake, *The development of plant leaves*. Plant Physiol, 2003. **131**(2): p. 389-94.
158. Berna, G., P. Robles, and J.L. Micol, *A mutational analysis of leaf morphogenesis in Arabidopsis thaliana*. Genetics, 1999. **152**(2): p. 729-42.
159. Nelissen, H., et al., *DRL1, a homolog of the yeast TOT4/KTI12 protein, has a function in meristem activity and organ growth in plants*. Plant Cell, 2003. **15**(3): p. 639-54.
160. Nelissen, H., et al., *The elongata mutants identify a functional Elongator complex in plants with a role in cell proliferation during organ growth*. Proc Natl Acad Sci U S A, 2005. **102**(21): p. 7754-9.
161. Stoyanova-Bakalova, E. and P. Petrov, *Control by cytokinins of the cellular behavior in the plate meristem of zucchini cotyledons*. Planta, 2006. **223**(6): p. 1256-62.
162. Giulini, A., J. Wang, and D. Jackson, *Control of phyllotaxy by the cytokinin-inducible response regulator homologue ABPHYLL1*. Nature, 2004. **430**(7003): p. 1031-4.
163. Moore, B., et al., *Role of the Arabidopsis glucose sensor HXK1 in nutrient, light, and hormonal signaling*. Science, 2003. **300**(5617): p. 332-6.
164. Reinhardt, D., et al., *Regulation of phyllotaxis by polar auxin transport*. Nature, 2003. **426**(6964): p. 255-60.
165. Altmann, T., *Recent advances in brassinosteroid molecular genetics*. Curr Opin Plant Biol, 1998. **1**(5): p. 378-83.
166. Catterou, M., et al., *Brassinosteroids, microtubules and cell elongation in Arabidopsis thaliana. II. Effects of brassinosteroids on microtubules and cell elongation in the bul1 mutant*. Planta, 2001. **212**(5-6): p. 673-83.
167. Karlova, R. and S.C. de Vries, *Advances in understanding brassinosteroid signaling*. Sci STKE, 2006. **2006**(354): p. pe36.
168. Hedden, P. and W.M. Proebsting, *Genetic analysis of gibberellin biosynthesis*. Plant Physiol, 1999. **119**(2): p. 365-70.
169. Yang, S., et al., *Stomatal movement in response to long distance-communicated signals initiated by heat shock in partial roots of Commelina communis L.* Sci China C Life Sci, 2006. **49**(1): p. 18-25.
170. Yan, C., et al., *A novel ABA-hypersensitive mutant in Arabidopsis defines a genetic locus that confers tolerance to xerothermic stress*. Planta, 2006. **224**(4): p. 889-99.
171. Prokic, L., et al., *Species-dependent changes in stomatal sensitivity to abscisic acid mediated by external pH*. J Exp Bot, 2006. **57**(3): p. 675-83.
172. Chen, Z., et al., *Mutations in ABO1/ELO2, a subunit of holo-Elongator, increase abscisic acid sensitivity and drought tolerance in Arabidopsis thaliana*. Mol Cell Biol, 2006. **26**(18): p. 6902-12.
173. Quail, P.H., *Phytochrome: a light-activated molecular switch that regulates plant gene expression*. Annu Rev Genet, 1991. **25**: p. 389-409.
174. Luzardo, A.D., F.X. Niell, and F. Lopez-Figueroa, *[Photocontrol of the synthesis of chlorophyll a and phycocyanin in the cyanobacterium Calothrix crustacea Schousboe]*. Rev Esp Fisiol, 1991. **47**(3): p. 109-14.
175. Haas, C.J., R. Scheuerlein, and S.J. Roux, *Phytochrome-mediated germination and early development in spores of Dryopteris filix-mas L.: phase-specific and non phase-specific inhibition by staurosporine*. J Plant Physiol, 1991. **138**(6): p. 747-51.
176. Telfer, A., K.M. Bollman, and R.S. Poethig, *Phase change and the regulation of trichome distribution in Arabidopsis thaliana*. Development, 1997. **124**(3): p. 645-54.
177. Tsukaya, H., et al., *Heteroblasty in Arabidopsis thaliana (L.) Heynh*. Planta, 2000. **210**(4): p. 536-42.
178. Thomas, M.C. and C.M. Chiang, *The general transcription machinery and general cofactors*. Crit Rev Biochem Mol Biol, 2006. **41**(3): p. 105-78.
179. Pandey, R., et al., *Analysis of histone acetyltransferase and histone deacetylase families of Arabidopsis thaliana suggests functional diversification of chromatin modification among multicellular eukaryotes*. Nucleic Acids Res, 2002. **30**(23): p. 5036-55.
180. Pugh, B.F., *HATs off to PIC assembly*. Mol Cell, 2006. **23**(6): p. 776-7.
181. Gill, G., *Regulation of the initiation of eukaryotic transcription*. Essays Biochem, 2001. **37**: p. 33-43.
182. Breiling, A., et al., *General transcription factors bind promoters repressed by Polycomb group proteins*. Nature, 2001. **412**(6847): p. 651-5.
183. Wassarman, D.A. and F. Sauer, *TAF(II)250: a transcription toolbox*. J Cell Sci, 2001. **114**(Pt 16): p. 2895-902.
184. Orphanides, G., T. Lagrange, and D. Reinberg, *The general transcription factors of RNA polymerase II*. Genes Dev, 1996. **10**(21): p. 2657-83.
185. Friedrich, J.K., et al., *TBP-TAF complex SL1 directs RNA polymerase I pre-initiation complex formation and stabilizes upstream binding factor at the rDNA promoter*. J Biol Chem, 2005. **280**(33): p. 29551-8.
186. Chen, H.T. and S. Hahn, *Mapping the location of TFIIB within the RNA polymerase II transcription preinitiation complex: a model for the structure of the PIC*. Cell, 2004. **119**(2): p. 169-80.
187. Qiu, H., et al., *An array of coactivators is required for optimal recruitment of TATA binding protein and RNA polymerase II by promoter-bound Gcn4p*. Mol Cell Biol, 2004. **24**(10): p. 4104-17.
188. Komarnitsky, P.B., B. Michel, and S. Buratowski, *TFIID-specific yeast TAF40 is essential for the majority of RNA polymerase II-mediated transcription in vivo*. Genes Dev, 1999. **13**(19): p. 2484-9.
189. Virbasius, C.M., et al., *Promoter-specific activation defects by a novel yeast TBP mutant compromised for TFIIB interaction*. Curr Biol, 2001. **11**(22): p. 1794-8.
190. Hampsey, M., *Molecular genetics of the RNA polymerase II general transcriptional machinery*. Microbiol Mol Biol Rev, 1998. **62**(2): p. 465-503.
191. Makino, Y., et al., *TATA-Binding protein-interacting protein 120, TIP120, stimulates three classes of eukaryotic transcription via a unique mechanism*. Mol Cell Biol, 1999. **19**(12): p. 7951-60.
192. Huh, J.R., et al., *Recruitment of TBP or TFIIB to a promoter proximal position leads to stimulation of RNA polymerase II transcription without activator proteins both in vivo and in vitro*. Biochem Biophys Res Commun, 1999. **256**(1): p. 45-51.
193. Ranish, J.A., N. Yudkovsky, and S. Hahn, *Intermediates in formation and activity of the RNA polymerase II preinitiation complex: holoenzyme recruitment and a postrecruitment role for the TATA box and TFIIB*. Genes Dev, 1999. **13**(1): p. 49-63.
194. Zhang, D.Y., D.J. Carson, and J. Ma, *The role of TFIIB-RNA polymerase II interaction in start site selection in yeast cells*. Nucleic Acids Res, 2002. **30**(14): p. 3078-85.
195. Liu, Y., et al., *Two cyclin-dependent kinases promote RNA polymerase II transcription and formation of the scaffold complex*. Mol Cell Biol, 2004. **24**(4): p. 1721-35.
196. Tan, S., R.C. Conaway, and J.W. Conaway, *Dissection of transcription factor TFIIF functional domains required for initiation and elongation*. Proc Natl Acad Sci U S A, 1995. **92**(13): p. 6042-6.
197. Laine, J.P., V. Mocquet, and J.M. Egly, *TFIIH enzymatic activities in transcription and nucleotide excision repair*. Methods Enzymol, 2006. **408**: p. 246-63.
198. Sarker, A.H., et al., *Recognition of RNA polymerase II and transcription bubbles by XPG, CSB, and TFIIH: insights for transcription-coupled repair and Cockayne Syndrome*. Mol Cell, 2005. **20**(2): p. 187-98.
199. Maxon, M.E., J.A. Goodrich, and R. Tjian, *Transcription factor IIE binds preferentially to RNA polymerase IIa and recruits TFIIH: a model for promoter clearance*. Genes Dev, 1994. **8**(5): p. 515-24.
200. Kugel, J.F. and J.A. Goodrich, *Translocation after synthesis of a four-nucleotide RNA commits RNA polymerase II to promoter escape*. Mol Cell Biol, 2002. **22**(3): p. 762-73.
201. Dvir, A., J.W. Conaway, and R.C. Conaway, *Mechanism of transcription initiation and promoter escape by RNA polymerase II*. Curr Opin Genet Dev, 2001. **11**(2): p. 209-14.
202. Spangler, L., et al., *TFIIH action in transcription initiation and promoter escape requires distinct regions of downstream promoter DNA*. Proc Natl Acad Sci U S A, 2001. **98**(10): p. 5544-9.
203. Yan, Q., et al., *Dual roles for transcription factor IIF in promoter escape by RNA polymerase II*. J Biol Chem, 1999. **274**(50): p. 35668-75.
204. Moreland, R.J., et al., *A role for the TFIIH XPB DNA helicase in promoter escape by RNA polymerase II*. J Biol Chem, 1999. **274**(32): p. 22127-30.
205. Goodrich, J.A. and R. Tjian, *Transcription factors IIE and IIH and ATP hydrolysis direct promoter clearance by RNA polymerase II*. Cell, 1994. **77**(1): p. 145-56.
206. Payne, J.M. and M.E. Dahmus, *Partial purification and characterization of two distinct protein kinases that differentially*

- phosphorylate the carboxyl-terminal domain of RNA polymerase subunit IIa. *J Biol Chem*, 1993. **268**(1): p. 80-7.
207. Cadena, D.L. and M.E. Dahmus, Messenger RNA synthesis in mammalian cells is catalyzed by the phosphorylated form of RNA polymerase II. *J Biol Chem*, 1987. **262**(26): p. 12468-74.
208. Otero, G., et al., *Elongator*, a multisubunit component of a novel RNA polymerase II holoenzyme for transcriptional elongation. *Mol Cell*, 1999. **3**(1): p. 109-18.
209. Hartzog, G.A., et al., Evidence that *Spt4*, *Spt5*, and *Spt6* control transcription elongation by RNA polymerase II in *Saccharomyces cerevisiae*. *Genes Dev*, 1998. **12**(3): p. 357-69.
210. Wada, T., et al., *DSIF*, a novel transcription elongation factor that regulates RNA polymerase II processivity, is composed of human *Spt4* and *Spt5* homologs. *Genes Dev*, 1998. **12**(3): p. 343-56.
211. Fish, R.N., et al., Genetic interactions between *TFIIF* and *TFIIS*. *Genetics*, 2006. **173**(4): p. 1871-84.
212. Oh, Y., et al., Promoter analysis of the *Drosophila melanogaster* gene encoding transcription elongation factor *TFIIS*. *Biochim Biophys Acta*, 2001. **1518**(3): p. 276-81.
213. Van Mullem, V., et al., The *Rpb9* subunit of RNA polymerase II binds transcription factor *TFIIE* and interferes with the SAGA and *Elongator* histone acetyltransferases. *J Biol Chem*, 2002. **277**(12): p. 10220-5.
214. Schneider, D.A., et al., RNA polymerase II elongation factors *Spt4p* and *Spt5p* play roles in transcription elongation by RNA polymerase I and rRNA processing. *Proc Natl Acad Sci U S A*, 2006. **103**(34): p. 12707-12.
215. Qiu, H., et al., The *Spt4p* subunit of yeast *DSIF* stimulates association of the *Pafl* complex with elongating RNA polymerase II. *Mol Cell Biol*, 2006. **26**(8): p. 3135-48.
216. Wittschleben, B.O., et al., Overlapping roles for the histone acetyltransferase activities of SAGA and *Elongator* in vivo. *Embo J*, 2000. **19**(12): p. 3060-8.
217. Wittschleben, B.O., et al., A novel histone acetyltransferase is an integral subunit of elongating RNA polymerase II holoenzyme. *Mol Cell*, 1999. **4**(1): p. 123-8.
218. Johnson, K.M. and M. Carey, Assembly of a mediator/*TFIID*/*TFIIA* complex bypasses the need for an activator. *Curr Biol*, 2003. **13**(9): p. 772-7.
219. Wang, G., et al., Mediator requirement for both recruitment and postrecruitment steps in transcription initiation. *Mol Cell*, 2005. **17**(5): p. 683-94.
220. Pokholok, D.K., N.M. Hannett, and R.A. Young, Exchange of RNA polymerase II initiation and elongation factors during gene expression in vivo. *Mol Cell*, 2002. **9**(4): p. 799-809.
221. Svestrup, J.Q., et al., Evidence for a mediator cycle at the initiation of transcription. *Proc Natl Acad Sci U S A*, 1997. **94**(12): p. 6075-8.
222. Fellows, J., et al., The *Elp2* subunit of *Elongator* and elongating RNA polymerase II holoenzyme is a WD40 repeat protein. *J Biol Chem*, 2000. **275**(17): p. 12896-9.
223. Winkler, G.S., et al., RNA polymerase II *Elongator* holoenzyme is composed of two discrete subcomplexes. *J Biol Chem*, 2001. **276**(35): p. 32743-9.
224. Krogan, N.J. and J.F. Greenblatt, Characterization of a six-subunit holo-*Elongator* complex required for the regulated expression of a group of genes in *Saccharomyces cerevisiae*. *Mol Cell Biol*, 2001. **21**(23): p. 8203-12.
225. Li, Y., et al., A multiprotein complex that interacts with RNA polymerase II *Elongator*. *J Biol Chem*, 2001. **276**(32): p. 29628-31.
226. Winkler, G.S., et al., *Elongator* is a histone H3 and H4 acetyltransferase important for normal histone acetylation levels in vivo. *Proc Natl Acad Sci U S A*, 2002. **99**(6): p. 3517-22.
227. Proudfoot, N. and J. O'Sullivan, Polyadenylation: a tail of two complexes. *Curr Biol*, 2002. **12**(24): p. R855-7.
228. Alen, C., et al., A role for chromatin remodeling in transcriptional termination by RNA polymerase II. *Mol Cell*, 2002. **10**(6): p. 1441-52.
229. Smeekens, S., Sugar regulation of gene expression in plants. *Curr Opin Plant Biol*, 1998. **1**(3): p. 230-4.
230. Chiou, T.J. and D.R. Bush, Sucrose is a signal molecule in assimilate partitioning. *Proc Natl Acad Sci U S A*, 1998. **95**(8): p. 4784-8.
231. Smeekens, S. and F. Rook, Sugar Sensing and Sugar-Mediated Signal Transduction in Plants. *Plant Physiol*, 1997. **115**(1): p. 7-13.
232. Jang, J.C., et al., Hexokinase as a sugar sensor in higher plants. *Plant Cell*, 1997. **9**(1): p. 5-19.
233. Wobus, U. and H. Weber, Sugars as signal molecules in plant seed development. *Biol Chem*, 1999. **380**(7-8): p. 937-44.
234. Pego, J.V., et al., Photosynthesis, sugars and the regulation of gene expression. *J Exp Bot*, 2000. **51 Spec No**: p. 407-16.
235. Koch, K.E., Carbohydrate-Modulated Gene Expression in Plants. *Annu Rev Plant Physiol Plant Mol Biol*, 1996. **47**: p. 509-540.
236. Dijkwel, P.P., et al., Sucrose control of phytochrome A signaling in *Arabidopsis*. *Plant Cell*, 1997. **9**(4): p. 583-95.
237. Williams, L.E., R. Lemoine, and N. Sauer, Sugar transporters in higher plants--a diversity of roles and complex regulation. *Trends Plant Sci*, 2000. **5**(7): p. 283-90.
238. Lemoine, R., Sucrose transporters in plants: update on function and structure. *Biochim Biophys Acta*, 2000. **1465**(1-2): p. 246-62.
239. Li, Z.S., et al., The sucrose carrier of the plant plasmalemma. III. Partial purification and reconstitution of active sucrose transport in liposomes. *Biochim Biophys Acta*, 1992. **1103**(2): p. 259-67.
240. Gerrits, N., et al., Sucrose metabolism in plastids. *Plant Physiol*, 2001. **125**(2): p. 926-34.
241. Sauer, N., et al., *AtSUC8* and *AtSUC9* encode functional sucrose transporters, but the closely related *AtSUC6* and *AtSUC7* genes encode aberrant proteins in different *Arabidopsis* ecotypes. *Plant J*, 2004. **40**(1): p. 120-30.
242. Meyer, S., et al., Wounding enhances expression of *AtSUC3*, a sucrose transporter from *Arabidopsis* sieve elements and sink tissues. *Plant Physiol*, 2004. **134**(2): p. 684-93.
243. Initiative, T.A., Analysis of the genome sequence of the flowering plant *Arabidopsis thaliana*. *Nature*, 2000. **408**(6814): p. 796-815.
244. Farrar, J., C. Pollock, and J. Gallagher, Sucrose and the integration of metabolism in vascular plants. *Plant Science*, 2000. **154**(1): p. 1-11.
245. Roitsch, T. and M.C. Gonzalez, Function and regulation of plant invertases: sweet sensations. *Trends Plant Sci*, 2004. **9**(12): p. 606-13.
246. Sergeeva, L.I., et al., Vacuolar invertase regulates elongation of *Arabidopsis thaliana* roots as revealed by *QTL* and mutant analysis. *Proc Natl Acad Sci U S A*, 2006. **103**(8): p. 2994-9.
247. Link, M., T. Rausch, and S. Greiner, In *Arabidopsis thaliana*, the invertase inhibitors *AtCNIF1* and 2 exhibit distinct target enzyme specificities and expression profiles. *FEBS Lett*, 2004. **573**(1-3): p. 105-9.
248. Heyer, A.G., et al., Cell wall invertase expression at the apical meristem alters floral, architectural, and reproductive traits in *Arabidopsis thaliana*. *Plant J*, 2004. **39**(2): p. 161-9.
249. Mitsuhashi, W., et al., Differential expression of acid invertase genes during seed germination in *Arabidopsis thaliana*. *Biosci Biotechnol Biochem*, 2004. **68**(3): p. 602-8.
250. Sherson, S.M., et al., Roles of cell-wall invertases and monosaccharide transporters in the growth and development of *Arabidopsis*. *J Exp Bot*, 2003. **54**(382): p. 525-31.
251. Tymowska-Lalanne, Z. and M. Kreis, Expression of the *Arabidopsis thaliana* invertase gene family. *Planta*, 1998. **207**(2): p. 259-65.
252. Haouazine-Takvorian, N., et al., Characterization of two members of the *Arabidopsis thaliana* gene family, *At beta fruct3* and *At beta fruct4*, coding for vacuolar invertases. *Gene*, 1997. **197**(1-2): p. 239-51.
253. Tang, X., et al., Purification and characterisation of soluble invertases from leaves of *Arabidopsis thaliana*. *Planta*, 1996. **198**(1): p. 17-23.
254. Konishi, T., Y. Ohmiya, and T. Hayashi, Evidence that sucrose loaded into the phloem of a poplar leaf is used directly by sucrose synthase associated with various beta-glucan synthases in the stem. *Plant Physiol*, 2004. **134**(3): p. 1146-52.
255. Kutschera, U. and A. Heiderich, Sucrose metabolism and cellulose biosynthesis in sunflower hypocotyls. *Physiol Plant*, 2002. **114**(3): p. 372-379.
256. Koch, K., Sucrose metabolism: regulatory mechanisms and pivotal roles in sugar sensing and plant development. *Curr Opin Plant Biol*, 2004. **7**(3): p. 235-46.
257. Ji, X., et al., Structure, evolution, and expression of the two invertase gene families of rice. *J Mol Evol*, 2005. **60**(5): p. 615-34.
258. Rausch, T. and S. Greiner, Plant protein inhibitors of invertases. *Biochim Biophys Acta*, 2004. **1696**(2): p. 253-61.
259. Tomlinson, K.L., et al., Evidence that the hexose-to-sucrose ratio does not control the switch to storage product accumulation in oilseeds: analysis of tobacco seed development and effects of overexpressing apoplastic invertase. *J Exp Bot*, 2004. **55**(406): p. 2291-303.
260. Jang, J.C. and J. Sheen, Sugar sensing in higher plants. *Plant Cell*, 1994. **6**(11): p. 1665-79.

261. Stessman, D., et al., *Regulation of photosynthesis during Arabidopsis leaf development in continuous light*. Photosynth Res, 2002. **72**(1): p. 27-37.
262. Goldschmidt, E.E. and S.C. Huber, *Regulation of Photosynthesis by End-Product Accumulation in Leaves of Plants Storing Starch, Sucrose, and Hexose Sugars*. Plant Physiol, 1992. **99**(4): p. 1443-1448.
263. Paul, M.J. and T.K. Pellny, *Carbon metabolite feedback regulation of leaf photosynthesis and development*. J Exp Bot, 2003. **54**(382): p. 539-47.
264. Paul, M.J. and C.H. Foyer, *Sink regulation of photosynthesis*. J Exp Bot, 2001. **52**(360): p. 1383-400.
265. Nielsen, T.H., J.H. Rung, and D. Villadsen, *Fructose-2,6-bisphosphate: a traffic signal in plant metabolism*. Trends Plant Sci, 2004. **9**(11): p. 556-63.
266. Koch, K.E., et al., *Multiple paths of sugar-sensing and a sugar/oxygen overlap for genes of sucrose and ethanol metabolism*. J Exp Bot, 2000. **51 Spec No**: p. 417-27.
267. Li, C.Y., D. Weiss, and E.E. Goldschmidt, *Effects of carbohydrate starvation on gene expression in citrus root*. Planta, 2003. **217**(1): p. 11-20.
268. Foyer, C.H., *Evidence for different kinases in thylakoid protein phosphorylation*. Biochem J, 1987. **248**(1): p. 103-8.
269. Kessler, S. and N. Sinha, *Shaping up: the genetic control of leaf shape*. Curr Opin Plant Biol, 2004. **7**(1): p. 65-72.
270. Pozzi, C., L. Rossini, and F. Agosti, *Patterns and symmetries in leaf development*. Semin Cell Dev Biol, 2001. **12**(5): p. 363-72.
271. Fleming, A.J., *Formation of primordia and phyllotaxy*. Curr Opin Plant Biol, 2005. **8**(1): p. 53-8.
272. Fleming, A.J., *The mechanism of leaf morphogenesis*. Planta, 2002. **216**(1): p. 17-22.
273. Weschke, W., et al., *The role of invertases and hexose transporters in controlling sugar ratios in maternal and filial tissues of barley caryopses during early development*. Plant J, 2003. **33**(2): p. 395-411.
274. Sturm, A., *Invertases. Primary structures, functions, and roles in plant development and sucrose partitioning*. Plant Physiol, 1999. **121**(1): p. 1-8.
275. Weber, H., et al., *A role for sugar transporters during seed development: molecular characterization of a hexose and a sucrose carrier in fava bean seeds*. Plant Cell, 1997. **9**(6): p. 895-908.
276. Slangenaupt, S.A. and J.F. Gusella, *Familial dysautonomia*. Curr Opin Genet Dev, 2002. **12**(3): p. 307-11.
277. Kim, J.H., W.S. Lane, and D. Reinberg, *Human Elongator facilitates RNA polymerase II transcription through chromatin*. Proc Natl Acad Sci U S A, 2002. **99**(3): p. 1241-6.
278. Frohloff, F., et al., *Saccharomyces cerevisiae Elongator mutations confer resistance to the Kluyveromyces lactis zymocin*. Embo J, 2001. **20**(8): p. 1993-2003.
279. Gilbert, C., et al., *Elongator interactions with nascent mRNA revealed by RNA immunoprecipitation*. Mol Cell, 2004. **14**(4): p. 457-64.
280. Fichtner, L., et al., *Elongator's toxin-target (TOT) function is nuclear localization sequence dependent and suppressed by post-translational modification*. Mol Microbiol, 2003. **49**(5): p. 1297-307.
281. Jablonowski, D., et al., *Kluyveromyces lactis zymocin mode of action is linked to RNA polymerase II function via Elongator*. Mol Microbiol, 2001. **42**(4): p. 1095-105.
282. Jablonowski, D. and R. Schaffrath, *Saccharomyces cerevisiae RNA polymerase II is affected by Kluyveromyces lactis zymocin*. J Biol Chem, 2002. **277**(29): p. 26276-80.
283. Valvekens, D., M.V. Montagu, and M.V. Lijsebettens, *Agrobacterium tumefaciens-mediated transformation of Arabidopsis thaliana root explants by using kanamycin selection*. Proc Natl Acad Sci U S A, 1988. **85**(15): p. 5536-5540.
284. Cnops, G., et al., *The rotunda2 mutants identify a role for the LEUNIG gene in vegetative leaf morphogenesis*. J Exp Bot, 2004. **55**(402): p. 1529-39.
285. Tsukaya, H., *Leaf shape: genetic controls and environmental factors*. Int J Dev Biol, 2005. **49**(5-6): p. 547-55.
286. Gibson, S.I., *Sugar and phytohormone response pathways: navigating a signalling network*. J Exp Bot, 2004. **55**(395): p. 253-64.
287. Loreti, E., et al., *A genome-wide analysis of the effects of sucrose on gene expression in Arabidopsis seedlings under anoxia*. Plant Physiol, 2005. **137**(3): p. 1130-8.
288. Li, H., et al., *The Rop GTPase switch controls multiple developmental processes in Arabidopsis*. Plant Physiol, 2001. **126**(2): p. 670-84.
289. Aoki, N., et al., *Pathway of sugar transport in germinating wheat seeds*. Plant Physiol, 2006. **141**(4): p. 1255-63.
290. Gupta, A.K. and N. Kaur, *Sugar signalling and gene expression in relation to carbohydrate metabolism under abiotic stresses in plants*. J Biosci, 2005. **30**(5): p. 761-76.
291. Pinfield-Wells, H., et al., *Sucrose rescues seedling establishment but not germination of Arabidopsis mutants disrupted in peroxisomal fatty acid catabolism*. Plant J, 2005. **43**(6): p. 861-72.
292. Job, C., et al., *Patterns of protein oxidation in Arabidopsis seeds and during germination*. Plant Physiol, 2005. **138**(2): p. 790-802.
293. Penfield, S., S. Graham, and I.A. Graham, *Storage reserve mobilization in germinating oilseeds: Arabidopsis as a model system*. Biochem Soc Trans, 2005. **33**(Pt 2): p. 380-3.
294. Fridlyand, L.E., L. Ma, and L.H. Philipson, *Adenine nucleotide regulation in pancreatic beta-cells: modeling of ATP/ADP-Ca²⁺ interactions*. Am J Physiol Endocrinol Metab, 2005. **289**(5): p. E839-48.
295. Li, F., et al., *[The Elp4 subunit of human Elongator complex partially complements the growth defects of yeast ELP4 deletion strain]*. Yi Chuan Xue Bao, 2004. **31**(7): p. 668-74.
296. Mezey, E., et al., *Of splice and men: what does the distribution of IKAP mRNA in the rat tell us about the pathogenesis of familial dysautonomia?* Brain Res, 2003. **983**(1-2): p. 209-14.
297. Close, P., et al., *Transcription impairment and cell migration defects in Elongator-depleted cells: implication for familial dysautonomia*. Mol Cell, 2006. **22**(4): p. 521-31.

Annex: VIB's work

Results

1. AtELP genes and T-DNA insertion lines

1.1 Introduction

Mutant alleles, containing a single locus-specific T-DNA insertion, have been ordered and obtained via the SIGnAL (Salk Institute Genomic Analysis Laboratory) 'T-DNA Express' *Arabidopsis* Gene Mapping Tool (<http://signal.salk.edu/cgi-bin/tdnaexpress>) and the FST Projects (Flanking Sequence Tags; INRA Versailles, http://flagdb-genoplante-info.infobiogen.fr/projects/fst/DocsIntro/Page_accueil.html) for all the AtELP genes. These 2 sites are to be found at the TAIR (The *Arabidopsis* Information Resource; <http://www.Arabidopsis.org/home.html>) web site under the "Insertions, Knockout and Other Mutations" link. The AtELP genes were identified based on homology with Yeast and are named according to Nelissen *et al.* (2003), (Table1).

Table1. AtELONGATOR genes						
Gene	Accession Nr.	Protein function	EMS	Ds	SALK	INRA
AtELP1	At5g13680	putative	elo2		SALK_011529	
					SALK_085928	
					SALK_005153	
					SALK_004690	
					SALK_004693	
					SALK_004682	
					SALK_122379	
					SALK_084199	
AtELP2	At1g49540	hypothetical			SALK_106485	
					SALK_027091	
					SALK_072288	
					SALK_119384	
AtELP3	At5g50320	(contains WD-40 repeats) histone acetyltransferase and demethylase	elo3?		/	219E08
AtELP4	At3g11220	unknown	elo1		/	220B03
AtELP5	At2g18410	hypothetical			SALK_079193	
AtELP6	At4g10090	hypothetical			SALK_003541	
					SALK_003548	
DRL1	At1g13870	hypothetical (contains ATP/GTP binding site and a CaM binding site)	elo4	dr11-1 dr11-2 dr11-3	SALK_143430	
					SALK_100099	
					SALK_028216	
					SALK_027093	
					SALK_071178	
					SALK_071179	
					SALK_056915	
					SALK_069191	

Table1. AtElongator genes. The *A. th.* homologues of the Yeast Elongator genes are presented together with DRL1 (Deformed Root and Leaves1) in the table with their accession number, their function, their colocalization with the EMS induced elo mutants of the elongata class, (Bernà *et al.*, 1999), the ds alleles identified and finally the codes of the SALK and INRA lines containing a T-DNA insertion, available at the Salk Institute Genomic Analysis Laboratory and INRA Versailles for reverse genetics analysis. AtELP3 has not been colocalized with the elo3 mutant. AtELP1, AtELP4 and DRL1 have been colocalized respectively as elo2, elo1 and elo4.

1.2 Mutant alleles for AtELP1

At this time, 8 different SALK-lines are present in the SIGnAL collection for AtELP1 (Fig.1). 2 of these SALK-lines were selected for analysis: SALK_004690 (N004690) and SALK_011529 (N011529).

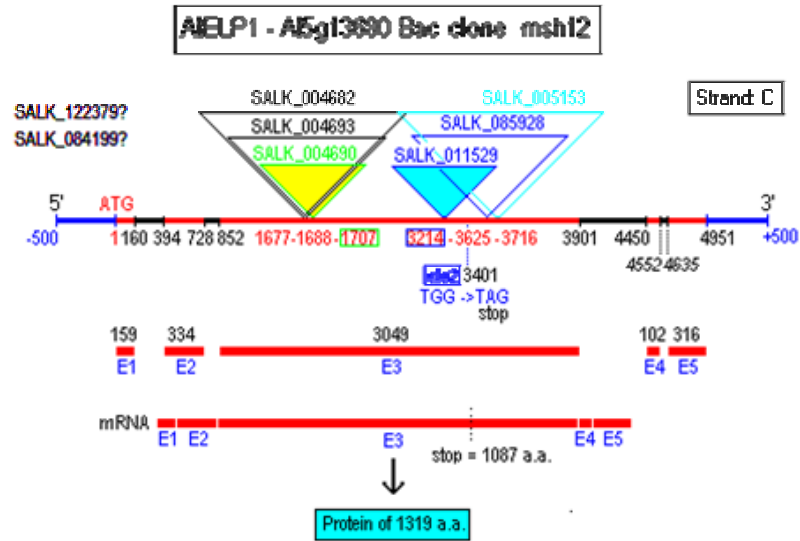


Fig.1. AtELP1 structure and position of the 8 T-DNA insertions (6 were identified by blasting the T-DNA left border SIGnAL sequence; 2 are not yet blasted). The gene has 5 exons that encode a protein of 1319 AA. The 2 SALK-lines on a colored triangle were selected for reverse genetics analysis. In the *elo2* allele due to a point mutation, which changes a G into an A, a stop codon is created at position 3041 and a truncated protein of 1087 AA is formed, lacking 232 AA at the C-terminus.

1.2.1 Phenotypic analysis in subsequent generations

Two AtELP1 SALK-lines (SALK_004690 and SALK_011529), with the T-DNA located in E3, exon3, were ordered and the obtained seeds were germinated *in vitro* on germination medium containing vitamins (GM+V) in order to increase the seed stock. These F2 lines were checked for the segregation of a phenotype due to T-DNA insertion in the AtELP1 gene. The F2 seed population was sowed out on the same type of medium and then transferred to soil where the phenotype of the seedlings was analysed in order to distinguish between mutants and wild-type (Table1). Mutants have been identified with the “Narrow leaves” phenotype, peculiar to the well-known *dr11-2* mutant (Fig.2).

Table1. AtELP1

	F2 Plant Nr.	F3 Mutants	F3 Wild-type
SALK_004690	7	5	42
SALK_011529	10	2	11
	14	25	0
	15	3	10

Table1. AtELP1 SALK-lines. Phenotype analysis of the *in vitro* grown F3 seedlings of AtELP1.



Fig.2. Comparison between a wild-type Col-0 seedling and a “Narrow leaves” mutant (*elp1-2*, SALK_004690).

All the 35 mutant and 15 wild-type randomly chosen F3 seedlings were harvested in liquid nitrogen for fast plant DNA extraction (Fig.2), using the Edwards protocol (Edwards et al., 1991), in order to define via PCR and specific primer combinations the genotype of the seedling.

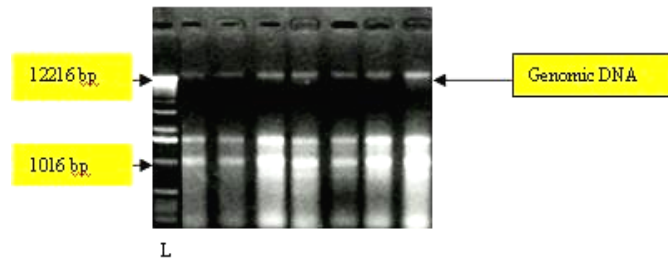


Fig.3. Example of a 0.8% agarose gel showing the high molecular weight genomic DNA band extracted from AtELP1 tissue.

1.2.2 T-DNA position and homo- or heterozygosity

With the OLIGO4 software (Rychlik, 1989) 4 Gene-Specific Primers (GSP) were designed so as to amplify with different primer combinations 4 different genomic fragments present in the AtELP1 locus (Fig.3): P1 (Hinel-146), P1' (Hinel-105), P3 (Hinel-147) and P3' (Hinel-106) and a T-DNA specific primer P2 (Lba1).

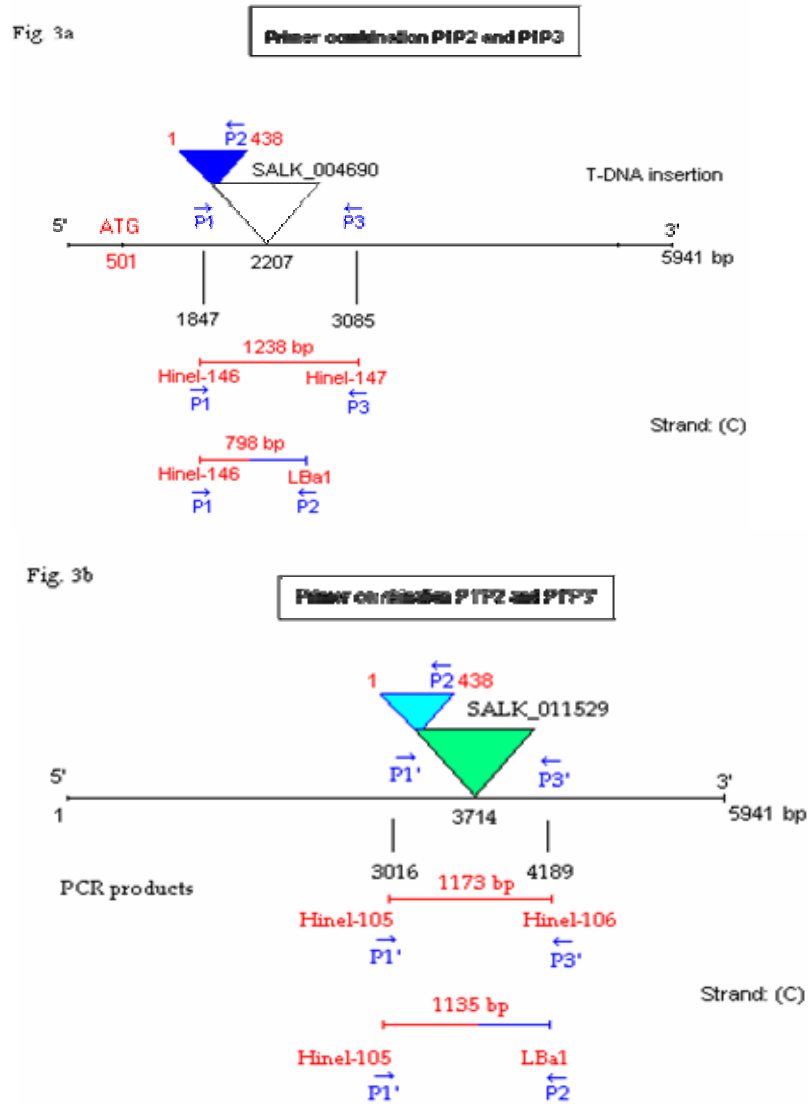


Fig.3. The AtELP1 gene structure is shown twice with its different T-DNA insertion, the primer combinations and the expected genomic fragment size after PCR amplification. The numeration is shown as reported in the unspliced version of the gene, having in addition 500 bp in the promoter region and 500 bp after the stop codon. The SALK_004690 line (Fig.3a) has the insertion in position 2207 (1707 without the promoter region); the 2 primer combinations P1-P2 and P1-P3 give fragments of 1238 bp and 798 bp respectively. The SALK_011529 line (Fig.3b) has the T-DNA insert in position 3714 (3214 without the promoter region) and the 2 primer combinations P1'-P2 and P1'-P3' give fragments of 1173 bp and 1135 bp respectively.

With the P1-P2 and P1'-P2 primer combination the presence of the T-DNA is checked: presence of the band means presence of the insertion (Fig.4). In Fig.4, for example, the insert is present in lane 7, 8 and 9 but not in lane 10. With the GSP-GSP P1-P3 and P1'-P3' primer combination (Fig.5) the heterozygosity at the locus is tested: a band indicates the absence of the T-DNA. If the T-DNA is present in a homozygous state the fragment is not amplified under the PCR conditions because of its increased size. If the T-DNA is present in a heterozygous state a fragment is obtained with the GSP-T-DNA primer combination and another fragment with the GSP-GSP-primers. Combining the data of Fig.4 and 5, for example, it is possible to conclude that the sample in lane 7 and 8 are homozygous "narrow leaves" mutants, the sample in lane 9 is a heterozygous wild-type and the sample in lane 10 is a homozygote wild-type. Amplified fragments have been sequenced and the position of the T-DNA as published on TAIR was confirmed, i.e. position 1707 for SALK_004690 or position 3214 for SALK_011529 (D. Fleury & H. Nelissen, pers. comm.).

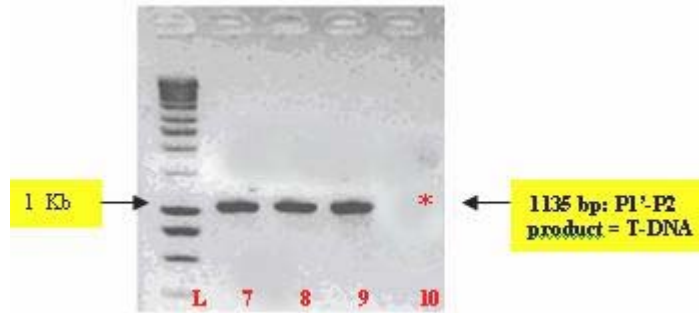


Fig.4. E.g. of T-DNA presence and absence (*) on a 1% agarose gel. The expected PCR product of 1135 bp in line 7, 8 and 9 obtained with the primer combination P1'-P2 for the SALK_011529 line indicates that at least one mutant allele is present. The absence in line 10 of the band indicates that the seedling is probably a homozygote wild-type.

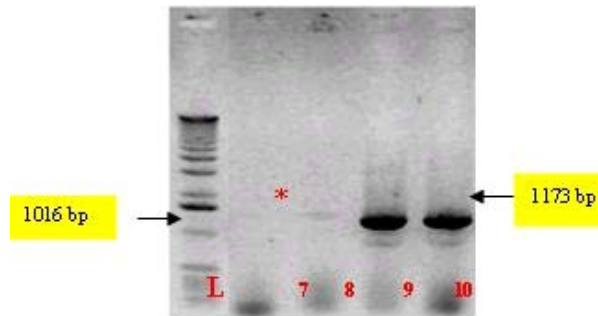


Fig.5. Example of a GSP-GSP (P1'-P3') amplification for the SALK_011529 line. On this 1% agarose gel is shown the presence or absence (*) of a 1173 bp PCR product: the occurrence of the band indicates the presence of at least one wild-type allele; instead the lack of the band indicates the presence of the T-DNA insertion which transforms the amplifiable region of 1173 bp in a non-amplifiable region (under these PCR conditions) of almost 6 Kb.

1.2.3 Summary and progeny analysis of AtELP1 alleles

The phenotypic scoring in F3 generation and genotyping results obtained from the PCR experiments are summarized in Table3a and Table3b. As preamble a legend for the primers and their codes is presented in Table2. Together with the phenotypic scoring, the genotype is presented: only in one case the genotype didn't match the phenotype scoring (line 15, nr. 6), indicating that the "narrow leaves" mutant phenotype is evident at a high degree and easy to score in these 2 AtELP1 alleles.

Table2. Legend	Primers	Primers code			
	P1	HineI-146			
	P1'	HineI-105	+	=	amplification
	P2	LBa1	-	=	no amplification
	P3	HineI-147			
	P3'	HineI-106	m/m	=	narrow leaves
			+/+ and +/m	=	wild-type

Table2. Primers code, PCR results and genotype annotation.

Table 3a. AtELP1: SALK_004690 (N504690)

Plant Nr.	Phenotype F3 GM+V	Label	P1P2	P1P3	Genotype F3	Phenotype F4 (GM+V)	Germinat. test GM+V+KM
Line 7							
1	mutant	1	+	-	m/m	mutant	resistant
2	mutant	2	+	-	m/m	mutant	/
3	mutant	3	+	-	m/m	mutant	resistant
4	mutant	4	+	-	m/m	.	/
5	mutant	5	+	-	m/m	mutant	resistant
6	wild-type	WT1	-	+	+/+	mutant	/
7	wild-type	WT2	+	+	+/m	-	/
8	wild-type	WT3	+	+	+/m	mutant	resist/sensit.
9	wild-type	WT4	-	+	+/+	wt heteroz.	/
10	wild-type	WT5	-	+	+/+	mutant	/

Table3a. Overview of the phenotypic/genotypic results and the germination analysis for the AtELP1 SALK_004690 allele. The F2 generation (line7) is presented with all the 10 derived F3 seedlings that have been selected, numerated and labelled (for the seed stock recognition) and from which DNA extraction was done. The presence and absence of a PCR product is indicated via + and – symbols. The scored phenotype is presented against the genotype conclusions in order to have an overview of the relation between the two. The name of the primers and the expected PCR product length are reported in the legend. The bold-marked plant number indicate which seeds have been sowed out on germination medium containing vitamins and kanamycin in order to test for the presence of at least one allele containing the T-DNA insert and the bared kanamycin resistance gene nptII.

Table 3b. AtELP1 alleles: SALK_011529 (N511529)

Plant Nr.	Phenotype F3 GM+V	Label	P1P2	P1P3	Genotype	Phenotype F4 GM+V	Germinat. test GM+V+KM
Line 10							
1	mutant	1	+	-	m/m	mutant	sensitive
2	mutant	2	+	-	m/m	mutant	sensitive
3	wild-type	WT1	+	+	+/m	wt heteroz?	/
4	wild-type	WT2	+	+	+/m	wt heteroz	sensitive
5	wild-type	WT3	-	+	+/+	wt homoz.	/
6	wild-type	WT4	-	+	+/+	wt homoz.	/
7	wild-type	WT5	+	+	+/m	wt heteroz	/
Line 14							
1	mutant	1	+	-	m/m	wild-type	/
2	mutant	2	+	-	m/m	mutant	sensitive
3	mutant	3	+	-	m/m	mutant	sensitive
4	mutant	4	+	-	m/m	mutant	sensitive
5	mutant	5	+	-	m/m	mutant	sensitive
6	mutant	6	+	-	m/m	/	/
7	mutant	7	+	-	m/m	/	/
8	mutant	8	+	-	m/m	/	/
9	mutant	9	+	-	m/m	/	/
10	mutant	10	+	-	m/m	/	/
11	mutant	11	+	-	m/m	/	/
12	mutant	12	+	-	m/m	/	/
13	mutant	13	+	-	m/m	/	/
14	mutant	14	+	-	m/m	/	/
15	mutant	15	+	-	m/m	/	/
16	mutant	16	+	-	m/m	/	/
17	mutant	17	+	-	m/m	/	/
18	mutant	18	+	-	m/m	/	/
19	mutant	19	+	-	m/m	/	/
20	mutant	20	+	-	m/m	/	/
21	mutant	21	+	-	m/m	/	/
22	mutant	22	+	-	m/m	/	/
23	mutant	23	+	-	m/m	/	/
24	mutant	24	+	-	m/m	/	/
25	mutant	25	+	-	m/m	/	/

Line 15							
1	wt-like	1	+	-	m/m	wt heteroz?	/
2	mutant	2	+	-	m/m	mutant	sensitive
3	mutant	3	+	-	m/m	mutant	sensitive
4	wild-type	WT1	+	+	+/m	wt heteroz.	sensitive
5	wild-type	WT2	-	+	+/+	wt homoz.	/
6	wt-like	WT3	+	-	m/m	mutant	sensitive
7	wild-type	WT4	-	+	+/+	wt homoz.	/
8	wild-type	WT5	-	+	+/+	wt homoz.	/

Table3b. Overview of the phenotypic/genotypic results and the germination analysis for the AtELP1 SALK_01529 allele. The plant line is presented with all the derived seedlings that have been selected numerated and labelled (for the seed stock recognition) and from which DNA extraction was done. The presence and absence of a PCR product is indicated via + and – symbols. The scored phenotype is presented against the genotype conclusions in order to have an overview of the relation between the two. The name of the primers and the expected PCR product length and the colour-associated genotypes are reported in the legend. The bold-marked plant number indicate which seeds have been sowed out on germination medium containing vitamins and kanamycin in order to test for the presence of at least one allele containing the T-DNA insert and the bared kanamycin resistance gene nptII.

1.2.4 Germination test: analysis on GM+V+Km of F4 seed population

To further investigate the T-DNA copy number some of the seeds obtained from the F3 population have been sowed on a selectable GM + V + Km (growth medium containing vitamins and in addition kanamycin, Table4). The nptII gene which confers the resistance to kanamycin is present in the T-DNA insert: plants with the inserted T-DNA will grow on the medium, plants without the T-DNA stop their growth and bleach at the dicotyledon emergence stage. The observations showed that seedlings of the SALK_004690 line 7 had a normal growth, but the SALK_011529 derived seedlings (line 10, 14 and 15) were affected in growth such as homozygote wild-type would be (Table4). The germination test gives also indications on the number of copy of T-DNA present in the genome: if only one copy is present the expected resistant mutants are ¼ of the population; in case there are more copies the ratio is much lower 1/16, 1/64, etc... Plant nr. 8 of line 7, which turned out to be a heterozygote for the mutation, gave 15 resistant seedlings out of 37 germinated seeds, indicating that with a high probability the copy number of the T-DNA is one in the genome.

Table4. Germination test for AtELP1 SALK-alleles

	Plant nr.	Resistant seedlings	Sensitive seedlings	Non-germinated seedlings
Line 7	1	18	0	2
	3	30	0	0
	5	10	0	1
	8	15	22	2
Line 10	1	0	9	0
	2	0	42	0
	4	0	32	0
Line 14	2	0	32	0
	3	0	20	0
	4	0	27	0
	5	0	14	8
Line 15	2	0	30	2
	3	0	29	3
	4	0	32	0

Table4. Germination test. The observed resistant or sensitive phenotypes are reported in this table together with non-germinated seeds. Seeds containing the T-DNA insert in a homozygous or hemizygous state bare also the nptII gene for kanamycin resistance.

1.2.5 Presence of the nptII region of the T-DNA checked by PCR

To test whether the T-DNA insertion was truncated in its 3' end, where the nptII is located, DNA has been extracted from some of these seedlings and amplified in the nptII region with specific primers (NptII1 and NptII2). DNA of AtELP1 line 7 and AtELP3 mutants was taken as control. The results showed that the nptII region in the controls was amplified but not in the AtELP1 line 10, 14 and 15 (data not shown) indicating that the T-DNA in SALK_011529 is truncated in its 3' end. Together with the Km germination test in which all seedlings were Km^S the data indicate that for the SALK_011529 line 10, 14 and 15 there is only one T-DNA copy which is truncated in the nptII gene.

1.2.6 Conclusion on AtELP1 alleles

At present, in addition to the *elp1-1* mutant allele (= *elo2*, “narrow leaves”) belonging to the *elongata* class (Berna *et al.*, 1999) identified as an allele of the AtELP1 gene (Nelissen, pers. comm.), it is possible to add 2 new alleles to this class (Table5): *elp1-2* (SALK_004690) and *elp1-3* (SALK_011529). The *elp1-1* EMS induced mutation present in Ler ecotype is located in the protein at position 1087 and transforms a normal codon (TGG) in a stop codon (TAG), causing a truncated protein of 1087 AA. instead of the normal 1319-long a.a. protein. The 2 new AtELP1 alleles present in the Columbia (Col-0) ecotype, *elp1-2* and *elp1-3* have a T-DNA insertion in position 449 and 951 respectively and possibly the insertion disrupts the protein architecture from that position because a mutant phenotype “narrow leaves” was caused by the insertion of the T-DNA in both alleles. The phenotype is similar to the one caused by the mutation in the DRL1 gene (Nelissen *et al.*, 2003). These alleles give further indication on the participation of AtELP1 and DRL1 in the functionality of the Elongator complex in the leaf organ growth.

Table5. AtELP1 alleles						
MIPS code	Allele	Ecotype	Mutagen	Mutation (a.a.)	Phenotype	References
At5g13680	<i>elp1-1</i> (=elo2)	Ler	EMS	1087	narrow leaves	Nelissen, H. (1999)
	<i>elp1-2</i> (=SALK_004690)	Col	T-DNA	449	narrow leaves	TAIR/SIGNAL
	<i>elp1-3</i> (=SALK_011529)	Col	T-DNA	951	narrow leaves	TAIR/SIGNAL

Table5. Alleles of AtELP1: the gene MIPS code, the allele name, the ecotype in which the allele is present and the mutagen (EMS, Ethyl Methane Sulfonate; T-DNA) that caused in a specific position the mutation are presented with the relative references.

1.3 Mutant alleles for AtELP2

Seeds of SALK_027091 and SALK_106485 present in the At1g49540 gene (Fig.6) have been ordered to perform the insertion analysis.

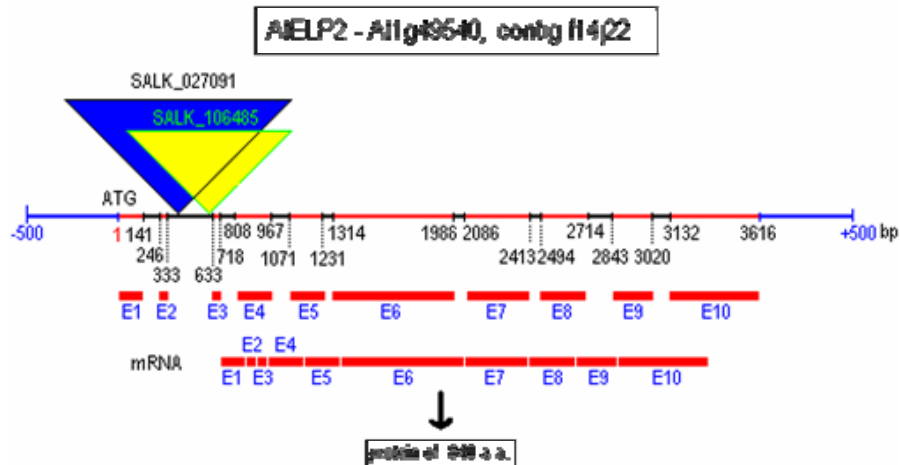


Fig6. AtELP2 structure and position of the 2 T-DNA insertions. The gene has 10 exons that encode a protein of 840 AA. The 2 SALK-lines on a colored triangle were selected for reverse genetics analysis.

1.4 Mutant alleles for AtELP3

T-DNA insertion lines for AtELP3 gene have been looked for in the SALK collection but no mutants were found for the At5g50320 locus. A search made at the INRA (Institut National de la Recherche Agronomique, Versailles) T-DNA Insertion Collection gave 1 mutant as result, a line which code is FST_219E08 (Fig.7). 100 T3 seeds were obtained from the INRA and additional information on them: the segregation number of the T2 population observed on a medium containing kanamycin was 3:1 (105 seedlings resistant: 37 sensitives, 6 non-germinated) and no peculiar phenotype was scored by the INRA searchers nor *in vitro* nor in greenhouse conditions.

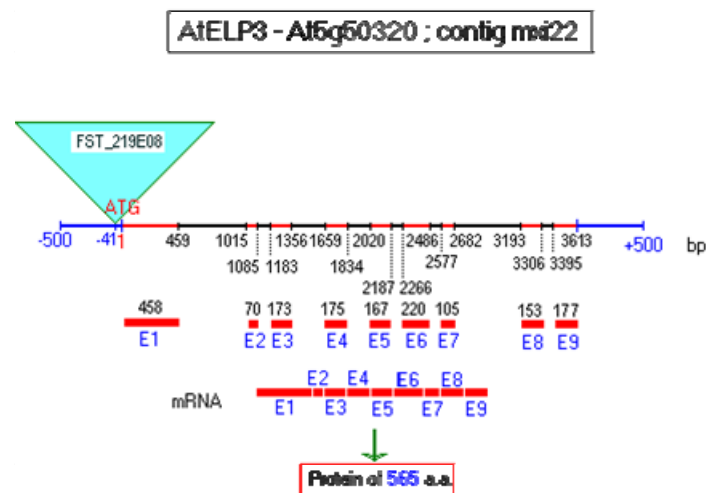


Fig.7. AtELP3 gene structure and position of the T-DNA insertion. The INRA code and the position of the mutation are presented. The gene is 3593 bp long and has 9 exons and 8 introns encoding a 559 AA protein. This FST_219E08 line has the insertion in the promoter region.

At the “collection of *Arabidopsis* T-DNA insertion lines produced at INRA Versailles” with the infiltration method (Bechtold et al., 1993), the A.th. ecotype used was Ws (Wassilevskija). The collection was generated using an *Agrobacterium tumefaciens* strain containing the binary vector pGKB5 (Bouchez et al., 1993) that carries the nptII gene, the bar gene and the GUS gene. The first confers kanamycin resistance, the second phosphinotrycin resistance (BASTA^R) and the last one situated at the right border of the T-DNA is necessary for promoter trapping.

1.4.1 AtELP3 FST_219E08 line: genotype and phenotype analysis of line 15 and 53

The AtELP3 seeds arrived from the INRA collection were sowed out on 4 GM+V+Km⁵⁰ (50 mg/L) plates and tested for the T-DNA presence via the resistance/sensitivity to kanamycin. 2 plates with Ws seeds were sowed as control. The phenotypic results of the germination test are shown in Table6.

Table6. Germination test for AtELP3 FST_219E08 line

N° plate	Resistants	Sensitives	Non-germinated	Tot. Seedlings
1	11	7	0	18
2	15	17	0	32
3	18	12	0	30
4	17	15	0	32
TOT.	61	51	0	112

Table6. Germination test on GM+V+Km⁵⁰ for the FST_219E08 INRA line.

The results showed the presence for 61 plants of the T-DNA in both homozygous or hemizygous state and a good germination rate. The 61 resistant seeds, containing the insertion were subsequently transplanted on soil-vermiculite and numbered from 1 to 61. Out of all these transplants 58 survived. DNA was extracted from all of them and the presence of T-DNA was checked via PCR. With a T-DNA specific primer (Tag5) and a GSP (Defle1) a 600 bp fragment was expected. DNA extracted from Ws plants was used as control. The results of the amplification experiments gave clear indications of T-DNA presence only for 12 plants: N° 15, 18, 19, 22, 23, 26, 27, 31, 50, 51, 52 and 53. 5 of the PCR products were sequenced and the T-DNA insertion was at the expected position as indicated from the INRA. 4 of these 12 plants gave no seeds. Seeds were harvested only from the following plants: N°15, 18, 19, 26, 27, 50, 52 and 53 (Fleury D. and Nelissen H.). The seeds were sowed out on GM+V and new DNA extraction was performed from all the lines. Line 15 and 53 were chosen to be further investigated and PCRs were carried out with the same specific primers as mentioned before. The presence of the T-DNA was confirmed for each line in a homozygous state by PCR. Finally, to confirm the genotype in a different way a germination test was done: seeds of this 2 lines were sowed on a selectable germination medium containing vitamins and kanamycin and phenotype scoring confirmed the presence of the T-DNA for all the seedlings germinated (Table7). The seeds were also sowed on a normal germination medium to score the phenotype and identify eventually a mutant phenotype.

Table7. Germination test for AtELP3 FST_219E08 line 15 and 53

Line	Resistant	Sensitives	Non-germinated	Tot. Seedlings
15	73	0	4	77
53	51	0	13	64

Table7. Germination test on GM+V+Km for FST_219E08 INRA line 15 and 53.

1.4.2 Conclusion

The molecular-genetic analysis of line FST_219E08 showed that the T-DNA insertion at position -41 in the promoter of the AtELP3 gene does result in a phenotype (Table8).

Table8. AtELP3 alleles						
MIPS code	Allele	Ecotype	Mutagen	Mutation (a.a.)	Phenotype	References
At5g50320	elp3-1 (elo3?)	Ler	EMS	? Hilde...	narrow leaves	Nelissen et al., 1999
	elp3-2 (=FST_219E08)	Ws	T-DNA	/	narrow leaves	INRA collection

Table8. Alleles of AtELP3: the gene MIPS code, the allele name, the ecotype in which the allele is present and the mutagen (EMS, Ethyl Methane Sulfonate; T-DNA) that caused in a specific position the mutation are presented with the relative references.

1.5 Mutant alleles for AtELP4

The elo1 mutant, belonging to the *A. th. elongata* class of leaf mutants (Berna *et al.*, 1999), has been identified as the first EMS-induced allele of AtELP4 (AtELP4-1): a donor splicing site is not recognized anymore in position 613 and intron 3 is expressed, with a resulting frame shift and a premature stop codon present in the intron. The isolation and sequencing of the AtELP4 cDNA in elo1 background confirmed that the spliced transcript lacked exon 4 (Nelissen *et al.*, unpublished). The resulting protein is 177 AA long and has 34 C-terminal random AA. At present, 3 different SALK-lines have been identified for AtELP4 (At3g11220) in the SIGnAL collection: SALK_079193, SALK_003541 and SALK_003548 (Fig.8).

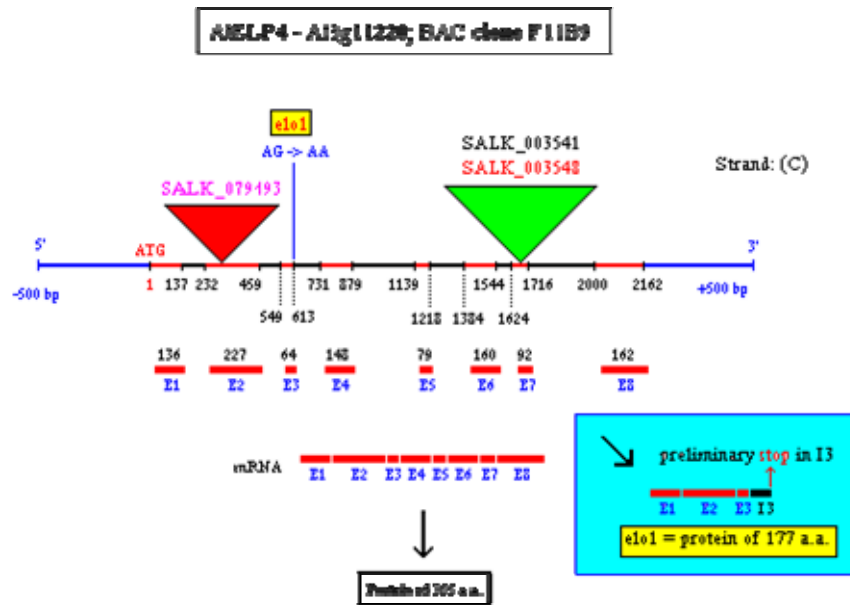


Fig.8 AtELP4 gene structure and position of the T-DNA insertions. The SALK codes and the position of the elo1 mutation are presented. The gene is 2161 bp long and has 8 exons and 7 introns encoding a 355 AA protein. In the elo1 mutants a donor splicing site between exon 3 and 4 is not recognized anymore (due to a point mutation, a G becomes an A) and I3 is expressed. I3 contains a stop codon that gives a truncated mutant protein of 177 AA. Two SALK-lines are located exactly in the same position (SALK_003541 and SALK_003548) in exon 7 and another is located in exon 2 (SALK_079193).

SALK_003548 seeds have been obtained from the NASC (Nottingham *Arabidopsis* Salk Center) and have been sowed out to scale up the seed stock. DNA extraction was done from 15 initial plants. The presence of the T-DNA has been tested with specific primers (Hinel-73, Hinel-74 and LBb1). 6 plants resulted clearly positive (1, 3, 5, 9, 11 and 15) for the T-DNA presence after PCR with the GSP-T-DNA specific primers (Hinel73/LBb1) (Table9). Nr 3, 5, 9 and 15 were heterozygous line for the T-DNA; 1 and 11 were homozygous for the T-DNA after the GSP-GSP amplification reaction. Only nr. 3 has been selected as a clear heterozygous plant and nr. 1, 11 as homozygous plants. The phenotype scoring was done on 30-40 plants for each line sowed out on soil, but no mutant “narrow leaves” phenotype was scored.

Table9. AtELP4: SALK_003548				
Plant Nr.	PIP2	PIP3	Phenotype	Genotype
1	+	-	Not evident	Homozygous
3	+	+	Not evident	Heterozygous
5	+	+	Not evident	Heterozygous
9	+	+	Not evident	Heterozygous
11	+	-	Not evident	Homozygous
15	+	+	Not evident	Heterozygous

Table9. Phenotypic and genotypic results for SALK_003548 line.

Seeds of the SALK_003541 were sowed out on GM+V medium and DNA (nr. 131-137) was extracted and analyzed with the same 2 primer combinations used for the previous SALK-line, since the T-DNA is present in the same genomic region. All of them contained the insertion. The results (Table10) showed a T-DNA band present in all the samples but also in the Wt control. A T-DNA specific PCR was done with nptII specific primers to find out whether the T-DNA was present in the genome and the results showed it was.

Table10. AtELP4: SALK_003541					
Plant Nr.	PIP2	PIP3	Phenotype	NptII region	Genotype
131	+?	+	Not evident	+	Heterozygous?
132	+?	+	Not evident	+	Heterozygous?
133	+?	+	Not evident	+	Heterozygous?
134	+?	+	Not evident	+	Heterozygous?
135	+?	+	Not evident	+	Heterozygous?
136	+?	+	Not evident	+	Heterozygous?
137	+?	+	Not evident	+	Heterozygous?
C	+?	+	Wild-type	-	Wild-Type?

Table10. Phenotypic and genotypic results for SALK_003541 line.

Also from SALK_079193 first and second line DNA was extracted (nr. 139-146, 147-155) and the same type of analysis was performed with hinel69/hinel70 as GSP-GSP primers and hinel69/LBb1 as GSP-T-DNA specific primers (Table11 and 12). Only nr 139 and 145 showed an heterozygous phenotype for the first line and nr. 150 for the second line.

Table11. AtELP4: SALK_0079193 (First line)				
Plant Nr.	PIP2	PIP3	Phenotype	Genotype
139	+	+	Not evident	Heterozygous
140	-	+	Not evident	Wild-type
141	-	+	Not evident	Wild-type
142	-	-	Not evident	/
143	-	+	Not evident	Wild-type
144	-	+	Not evident	Wild-type
145	+	+	Not evident	Heterozygous
146	-	+	Not evident	Wild-type
C	-	+	Wild-type	Wild-type

Table11. Phenotypic and genotypic results for SALK_079193 first line.

Table 12. AtELP4: SALK_0079193 (Second line)				
Plant Nr.	PIP2	PIP3	Phenotype	Genotype
147	-	+	Not evident	Wild-type
148	-	+	Not evident	Wild-type
149	-	+	Not evident	Wild-type
150	-	+	Not evident	Heterozygous
151	+	+	Not evident	Wild-type
152	-	+	Not evident	Wild-type
154	-	+	Not evident	Wild-type
155	-	+	Not evident	Wild-type
C	-	+	Wild-type	Wild-type

Table 12. Phenotypic and genotypic results for SALK_079193 second line.

Table 13. AtELP4 alleles						
MIPS code	Allele	Ecotype	Mutagen	Mutation (a.a.)	Phenotype	References
At3g11220	elp4-1 (=elc1)	Ler	EMS	143	Narrow Leav	Berna et al.,1999
	elp4-2 (=SALK_003548)?	Col	T-DNA	/	not evident	Tair/SIGNAL
	elp4-3 (=SALK_003541)?	Col	T-DNA	/	not evident	Tair/SIGNAL
	elp4-4 (=SALK_079193)?	Col	T-DNA	/	not evident	Tair/SIGNAL

Table 13. AtELP4 allele. Up to now only one allele has been identified in *A. thaliana*. The gene MIPS code, the allele name, the ecotype in which the allele is present and the mutagen (EMS, Ethyl Methane Sulfonate; T-DNA) that caused in a specific position the mutation are presented with the relative references.

1. 6 Mutant alleles for AtELP5

Seeds of SALK_143430 have been ordered to perform the insertion analysis in the At2g18410 gene, which was found to be the *A. th.* homologue of the Yeast ELP5 gene.

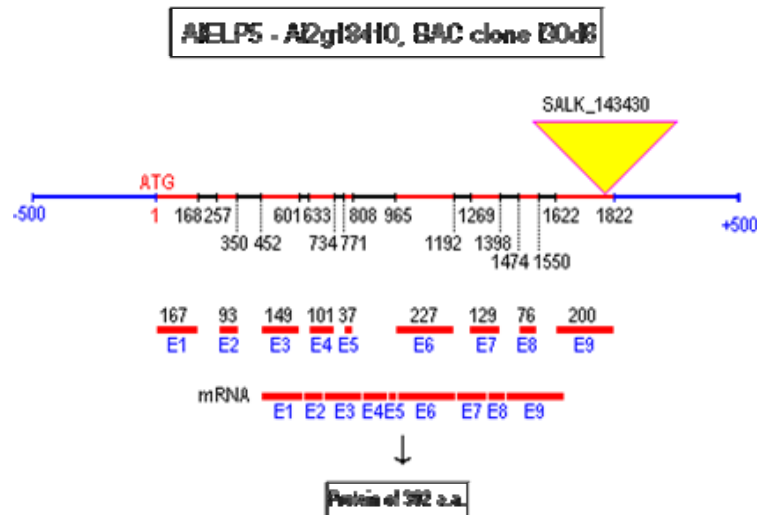


Fig 9. AtELP5 structure and position of the T-DNA insertion (SALK_143430) in the At2g18410 gene. The gene has 9 exons that encode a protein of 392 AA.

1.7 Mutant alleles for AtELP6

3 different SALK-lines have been identified in the AtELP6 locus (At4g10090) on the F28M11 BAC clone in the SIGNAL collection: SALK_027093 (N527093), SALK_100099 and SALK_028216 (Fig. 8).

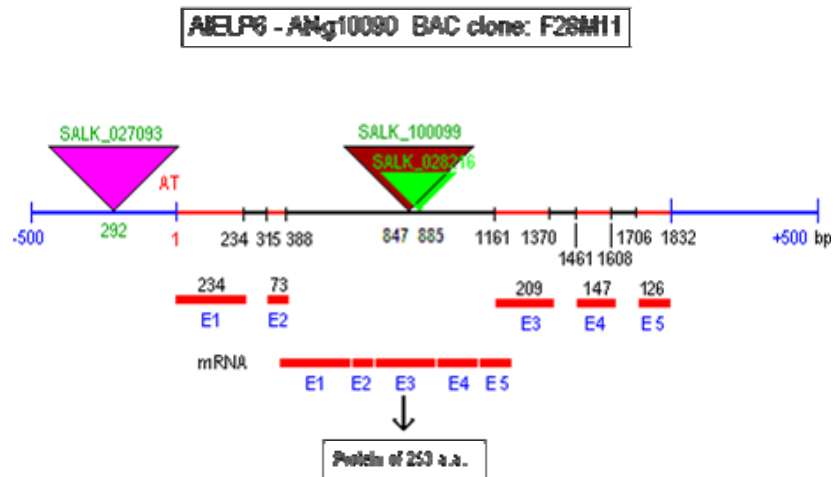


Fig.8. AtELP6 structure and position of the T-DNA insertions with their respective SALK- codes. The gene (At4g10090) is 1649 bp long, contains 4 exons and 3 introns and encodes for a small protein of 253 AA. One line (SALK_027093) has the T-DNA insertion in the promoter region, another in exon 3 (SALK_100099) and the last one in the third intron (SALK_028216). The SALK-100099 and SALK_027093 seeds are available at the RUG (Rijks Universiteit Gent).

SALK_100099 seeds obtained from the NASC (Nottingham *Arabidopsis* Salk Center) were sowed out on GM + V medium and transferred after 3 weeks on soil:vermiculite (3:1). The resulting generations were tested for the T-DNA presence. DNA was successfully extracted from all the plants with the fast Edwards protocol and PCR was performed with specific primers (Defle8, Defle9 and Lbb1) to test the presence of the T-DNA and the hetero- or homozygosity at the locus. With primer combination Defle8/Defle9 (GSP-GSP) the heterozygosity at the locus was tested. With primer combination Defle8/Lbb1 (GSP-T-DNA specific primers) the presence/absence of the T-DNA insertion was tested. All 4 samples were heterozygous plants (Table14). No mutant phenotype was scored.

Table14. AtELP6: SALK 100099				
Plant Nr.	PIP2	PIP3	Phenotype	Genotype
1	+	+	Not evident	Heterozygous
2	+	+	Not evident	Heterozygous
3	+	+	Not evident	Heterozygous
4	+	+	Not evident	Heterozygous
C	-	+	Not evident	Wild-type

Table14. Phenotypic and genotypic results for SALK_100099.

The same analysis was performed on the SALK-527093 line. DNA was extracted from several plants (nr. 159-170) and PCR was done with anfall1/anfal2 as GSP-GSP primer combination and Anfall1/Lbb1 as GSP-T-DNA primer combination. Results are shown in Table15.

Table15. AtELP6: SALK 527093				
Plant Nr.	PIP2	PIP3	Phenotype	Genotype
159	+	-	Not evident	Homozygous
161	+	+	Not evident	Heterozygous
162	-	+	Not evident	Wild-type
163	+	+	Not evident	Heterozygous
164	+	+	Not evident	Heterozygous
165	+	-	Not evident	Homozygous
166	-	-	Not evident	/
167	+	-	Not evident	Wild-type
168	+	-	Wild-type	Wild-type
169	+	+	Not evident	Heterozygous
170	+	-	Not evident	Homozygous
C	-	+	Wild-type	Wild-type

Table15. Phenotypic and genotypic results for SALK_527093.

Table16. AtELP6 alleles						
MIPS code	Allele	Ecotype	Mutagen	Mutation (a.a.)	Phenotype	References
At4g10090	elp6-1 (=SALK_100099)?	Col	T-DNA	/	not evident	Tair/SigNAL
	elp6-2 (=SALK_527093)?	Col	T-DNA	/	not evident	Tair/SigNAL

Table16. Alleles of AtELP6: the gene MIPS code, the allele name, the ecotype in which the allele is present and the mutagen (EMS, Ethyl Methane Sulfonate; T-DNA) that caused in a specific position the mutation are presented with the relative references.

1.8 General conclusions

By reverse genetics approaches, several genes presumably involved in the *A. th.* Elongator complex were analyzed for T-DNA insertions and the heterozygosity at the locus by means of PCR analysis to find new alleles for the *A. th.* homologues of the Yeast Elongator complex. Phenotype scoring and germination tests were done to further ascertain the mutant genotypes and phenotypes, but the “narrow leaf” phenotype of the Elongator mutations in the Ler background was not fully penetrant in the Col background (Table17). It means that the insertion of a T-DNA at a position in the gene resulting in a defective protein does not result in a phenotype or does result in a phenotype that is not always as clear in every mutant individual. It can be explained that some of the Elongator complex components may be redundant in Col. In literature, the FRIGIDA gene presents similar aspects (Johanson et al., 2000).

Table17. Summary of all the AtELP alleles							
MIPS code	Gene	Allele	Ecotype	Mutagen	Mutation	Phenotype	References
At5g13680	AtELP1	elp1-1 (=elo2)	Ler	EMS	1087	narrow leaves	Nelissen et al.(1999)
		elp1-2 (=SALK_004690)	Col	T-DNA	449	narrow leaves	TAIR/SigNAL
		elp1-3 (=SALK_011529)	Col	T-DNA	951	narrow leaves	TAIR/SigNAL
At1g49540	AtELP2	/	/	/	/	/	/
At5g50320	AtELP3	elp3-1 (elo3?)	Ler	EMS	/	narrow leaves	Berna et al.,1999
		elp3-2 (=FST_219E08)	Ws	T-DNA	/	narrow leaves	INRA collection
At3g11220	AtELP4	elp4-1 (=elo1)	Ler	EMS	143	narrow leaves	Berna et al.,1999
		elp4-2 (=SALK_003548)?	Col	T-DNA	/	not evident	Tair/SigNAL
		elp4-3 (=SALK_003541)?	Col	T-DNA	/	not evident	Tair/SigNAL
		elp4-4 (=SALK_079193)?	Col	T-DNA	/	not evident	Tair/SigNAL
At2g18410	AtELP5	/	/	/	/	/	/
At4g10090	AtELP6	elp6-1 (=SALK_100099)?	Col	T-DNA	/	not evident	Tair/SigNAL
		elp6-2 (=SALK_527093)?	Col	T-DNA	/	not evident	Tair/SigNAL

Table17. Summary on the SALK-lines analyzed.

2. Morphological comparison between first and third leaves of the DRL1 overexpression line 10B5 (in Ler background) and the wild-type Ler. PCN analysis on RON1 first and third leaves

2.1 Introduction

The DRL1 (Deformed Roots and Leaves1) protein is the *Arabidopsis thaliana* homologue of the Yeast TOT4/KTI12 protein associated with the Elongator complex. The recessive mutation at the DRL1 locus causes growth defects and general organ disorganization: at the anatomic and cyto-histological level shoot, root, inflorescence and flower meristems are affected (Nelissen et al., 2003). The leaf phenotype of the drl1-2 mutant, named “narrow leaves“, has been dissected at different morphological levels: compared to the wild-type Ler leaves the drl1-2 leaf has reduced lamina width and area and an increased lamina/petiole ratio or even an unclear transition between petiole and lamina. At a histological level the reduced lateral growth of the lamina has been correlated with a reduced (50%) Palisade Cell Number (PCN). DIC (Differential Interference Contrast) optics analysis showed a reduction in upper epidermis cell-size, but a significant increased palisade cell-size. In serial transversal sections the palisade cells were larger and more irregularly shaped and intercellular spaces were present all over the mesophyll; the lamina was thicker and the midvein less pronounced, which possibly indicates leaf ventralization. Marker gene analysis showed that the drl1-2 leaves had clear dorsal and ventral domains. In order to further investigate the drl1-2 leaf phenotype, a strong overexpression P35S::DRL1 construct was made (Clarke et al, unpublished results) and inserted in a T-DNA containing the BASTA herbicide sensitive marker in drl1-2 mutants for phenotype restoration. After Northern analysis the DRL1 overexpression line Nr.10, 20-fold overexpressing the insert, was selected for further morphological analysis. Subsequently, in order to obtain the overexpression line in wild-type Ler background the drl1-2 plants (♂), containing the p35S::DRL1 construct, were

crossed with Ler plants (♀). On a selectable (containing phosphinotrycin, ppt) medium plants containing the construct (homozygous wild-type for the *drl1* locus) were selected in the F2 population. F3 populations were subsequently germinated on ppt containing medium and a line was selected homozygous for the overexpression constructs, and homozygous wild-type for the *DRL1* locus. It has been named DRL1ox10B5. To investigate the phenotype resulting from an overexpression of the *DRL1* gene in a wild-type background seeds have been germinated in *in vitro* conditions and let grow for 30-40 days prior of harvesting.

2.2 Imaging analysis: morphological comparison between Ler and DRL1ox10B5 first and third leaves

8-12 expanded first and third leaves (L1 and L3) of 30-day-old and 40-day-old Ler and DRL1ox10B5 *in vitro* grown plants have been harvested and treated with 100% methanol O/N and cleared with 90% lactic acid for 2-3 days O/N and put on a slide for image analysis (Fig.9). Petiole, lamina and leaf length, lamina width and area of first and third leaves have been measured (Table 18-21) with the Scion Image software (version β-3b; Scion Corp., Frederick, MD) from digital pictures directly taken from binocular observations.

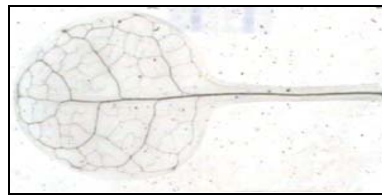


Fig9. A cleared leaf on a glass slide ready to be morphologically analysed under a binocular connected to a digital camera.

Table 18. Imaging results for L1 of 30-day-old plants				
Plant line	Parameter	Mean	St. dev.	
Ler L1	<i>petiole length</i>	2.88	0.57	
	<i>lamina length</i>	4.28	0.67	
	<i>lamina width</i>	4.08	0.45	
	<i>leaf length</i>	7.04	0.99	
	<i>lamina area</i>	13.25	9.32	
DRL1ox10B5 L1	<i>petiole length</i>	4.08	0.85	
	<i>lamina length</i>	4.35	0.36	
	<i>lamina width</i>	4.19	0.85	
	<i>leaf length</i>	8.43	0.99	
	<i>lamina area</i>	14.25	1.67	

Table 18. Imaging analysis: comparison of 5 leaf parameters between Ler and DRL1ox10B5 L1 of 30-day-old plants. Length and width are expressed in mm, the area in mm².

Table 19. Imaging results for L3 of 30-day-old plants				
Plant line	Parameter	Mean	St. dev.	
Ler L3	<i>petiole length</i>	4.24	0.7	
	<i>lamina length</i>	5.33	0.49	
	<i>lamina width</i>	5.21	0.47	
	<i>leaf length</i>	9.56	1.12	
	<i>lamina area</i>	21.88	3.44	
DRL1ox10B5 L3	<i>petiole length</i>	4.84	0.59	
	<i>lamina length</i>	6.28	0.8	
	<i>lamina width</i>	5.55	0.54	
	<i>leaf length</i>	11.11	1.2	
	<i>lamina area</i>	26.88	5.08	

Table 19. Imaging analysis: comparison of 5 leaf parameters between Ler and DRL1ox10B5 L3 of 30-day-old plants. Length and width are expressed in mm, the area in mm².

Table 20. Imaging results for L1 of 40-day-old plants				
Plant line	Parameter	Mean	St. dev.	
Ler L1	<i>petiole length</i>	3.28	0.35	
	<i>lamina length</i>	4.74	0.74	
	<i>lamina width</i>	4.4	0.53	
	<i>leaf length</i>	8.02	0.95	
	<i>lamina area</i>	15.67	3.94	
DRL1ox10B5 L1	<i>petiole length</i>	3.35	0.74	
	<i>lamina length</i>	5.24	0.56	
	<i>lamina width</i>	4.81	0.55	
	<i>leaf length</i>	8.77	1.08	
	<i>lamina area</i>	18.82	4.24	

Table 20. Imaging analysis: comparison of 5 leaf parameters between Ler and DRL1ox10B5 L1 of 40-day-old plants. Length and width are expressed in mm, the area in mm².

Table 21. Imaging results for L3 of 40-day-old plants				
Plant line	Parameter	Mean	St. dev.	
Ler L3	<i>petiole length</i>	5.47	0.62	
	<i>lamina length</i>	7.13	0.61	
	<i>lamina width</i>	6.14	0.36	
	<i>leaf length</i>	12.6	0.95	
	<i>lamina area</i>	33.08	4.58	
DRL1ox10B5 L3	<i>petiole length</i>	5.78	0.98	
	<i>lamina length</i>	7.56	0.55	
	<i>lamina width</i>	7.11	0.53	
	<i>leaf length</i>	13.34	1.25	
	<i>lamina area</i>	40.63	5.04	

Table 21. Imaging analysis: comparison of 5 leaf parameters between Ler and DRL1ox10B5 L3 of 40-day-old plants. Length and width are expressed in mm, the area in mm².

LER and DRL1ox10B5 first 30-day-old leaf: mean values

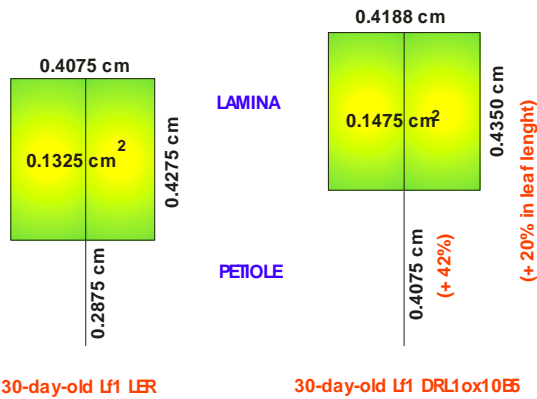


Fig.10. Comparison between the mean morphological values of 30-day-old Ler and DRL1ox10B5 first leaves (Lf1). In the “mean” mutant leaf the petiole length was 42% longer which gave a 20% longer leaf. Lamina width, length and area were not significantly different between mutant and wild-type leaves.

LER and DRL1ox10B5 third 30-day-old leaf: mean values

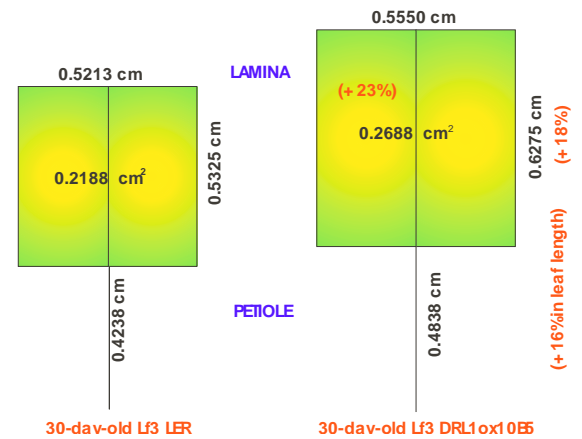


Fig.11. Comparison between the mean morphological values of 30-day-old Ler and DRL1ox10B5 third leaves (Lf3). In the longer (+16%) mutant leaves, due to a longer lamina length (+18%), the lamina area was found to be increased (+23%). The lamina width and the petiole length were not affected.

LER and DRL1ox10B5 first 40-day-old leaf: mean values

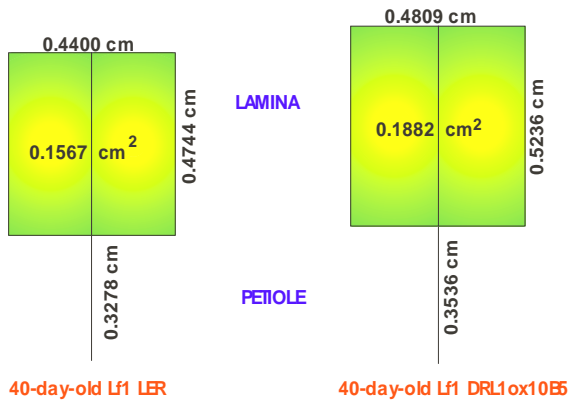


Fig.12. Comparison between the mean morphological values of 40-day-old Ler and DRL1ox10B5 first leaves (Lf1). After 40 days of growth the first leaves of the wild-type Ler (control) and the mutant DRL1ox10B5 were not significantly different.

LER and DRL1ox10B5 first 40-day-old leaf: mean values

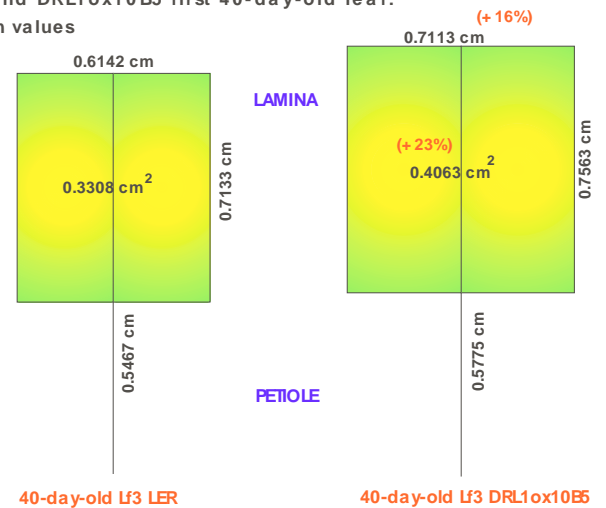


Fig.13. Comparison between the mean morphological values of 40-day-old Ler and DRL1ox10B5 third leaves (Lf3). The lamina width was found to be larger (+16%) in the mutants. Also the lamina area was increased (+23%) in the mutants as a result of the larger lamina.

The statistical significance of the mean differences ($p \leq 0.05$) was analyzed by t-test using the SPSS (Statistical Package for the Social Sciences, version 10.0.5, SPSS, Inc.; Chicago, IL) software on normally distributed data. The results showed that in plants grown for 30 days the only significant difference between DRL1ox10B5 and Ler first leaves is evident for the petiole length ($p=0,005$) and the leaf length ($p=0,010$) which were increased respectively about 42% and 20% (Fig.10). The length and width of the lamina does not differ significantly and the area is consequently similar too. Taking into consideration the DRL1ox10B5 third leaves (Fig.11) there was an increase in lamina length (+ 18%), which leads to an increased leaf length (+ 16%) and leaf area (+ 23%). In plants grown for 40 days the petiole, lamina and leaf length do not differ anymore in first and third leaves between the mutant and the wild-type (Fig.12 and 13). A significant difference between DRL1ox10B5 and Ler third leaves is only evident for the lamina width (+ 16%) and area (+ 23%): $p=0,000$ and $0,003$ respectively (Fig.12).

2.2.1 Discussion

If the mutant and wild-type leaves are analyzed taking into consideration their morphology at the two different time points under investigation (leaf growth after 30 and 40 days), the following results can be observed: first of all, it is evident that leaves in general continue to grow for all the morphological parameters under investigation (Fig.9-12), with the only exception of the petiole length in DRL1ox10B5 first leaves, which decreases in length (-13%) and, secondly, that third leaves of both the wild-type Ler and the mutant DRL1ox10B5 have a bigger lamina growth rate compared to the first leaves (Fig.14 and 15), with increments of more than 50% in the expansion of the lamina area compared to the 18-28% of first leaves in 10 days. Cutting a leaf at the basis of the petiole is not always precisely done and errors can easily occur. The results observed for the petiole and for the consequential leaf length will not be discussed. The discussion will be focused only on the lamina. In 10 days of extra growth, the area of the lamina of all the leaves analyzed increased significantly (Table13), due more to an increase in the proximo-distal direction (from 11-34%) than along the lateral axis (8-28%): for Ler first leaves an increase of 18% in surface was observed and for the DRL1ox10B5 leaves the increase raised up to 28% (Fig.13). More astonishingly the lamina area for Ler and DRL1ox10B5 third leaves increased 51% for both (Fig.14). Another observation made was that for the mutant third leaf the increase in lamina width is more prominent (+28%) than the increase in lamina length (+20%) in comparison with the wild-type (Table13), while in the mutant first leaf the situation is exactly the opposite and follows the general rule, being the increase in lamina length more prominent (+34%) than the one in lateral lamina growth (+18%). This points to a possible role for *drl1-2* in the lateral growth of the lamina, but only in late stages of growth and apparently only for third leaves. Already after 30 days it is possible to see differences between third leaves in lamina area values, which are kept after 40 days due to the same lamina growth rate (+51%), but what comes out of this experiment is that the final bigger leaf architecture in the mutant is achieved with an increment in the lateral growth rate instead of an increment along the proximal-distal axis. The mutant overexpression line 10B5 finally produces a phenotype that generates a third leaf with a bigger lamina, which is larger to an increased ratio lateral/longitudinal lamina growth, while the wild-type leaves have a smaller lamina and the growth still continues preferably along the proximo-distal axis and thus giving an opposite ratio.

Leaf type	Morphological parameter	Growth in 10 days
Ler Lf1	Petiole length	0,14
	Lamina length	0,11
	Lamina width	0,08
	Lamina area	0,18
	Leaf length	0,14
DRL1ox10B5 Lf1	Petiole length	-0,13
	Lamina length	0,2
	Lamina width	0,15
	Lamina area	0,28
	Leaf length	0,04
Ler Lf3	Petiole length	0,29
	Lamina length	0,34
	Lamina width	0,18
	Lamina area	0,51
	Leaf length	0,32
DRL1ox10B5 Lf3	Petiole length	0,19
	Lamina length	0,2
	Lamina width	0,28
	Lamina area	0,51
	Leaf length	0,2

Table22. Comparison in growth after 10 days between Ler and DRL1ox10B5 LF1 and LF3. 5 morphological parameters are shown with the changes in their values due to the growth of the plants. Different set of plants were germinated and let grow until the 2 chosen time-points. The petiole and the resulting leaf length were not taken into account for the discussion because of the “strange” result obtained for the petiole length in the first mutant leaf.

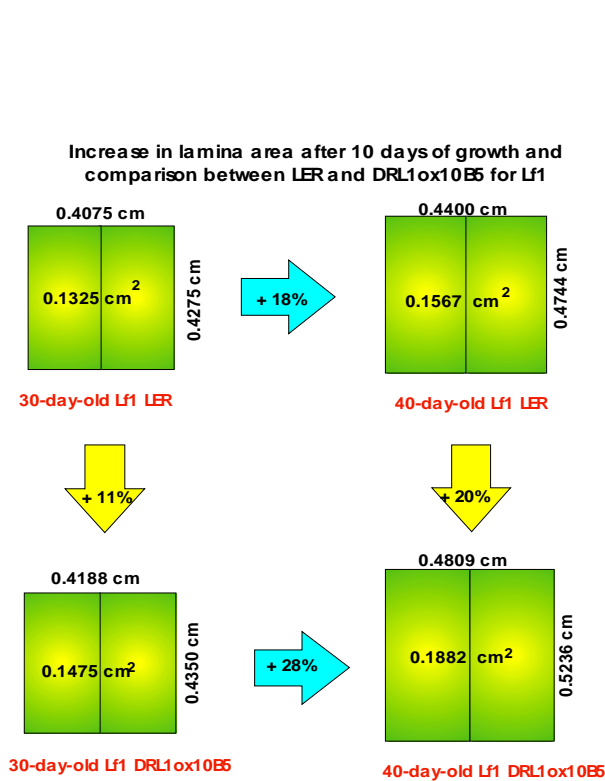


Fig.13. Increase in lamina area after 10 days (horizontal arrows) and difference between mutant and wild-type first mean leaf (vertical arrows). No significant differences are found between the mean first leaves after 30 or 40 days. The growth of the lamina is similar and for the first leaves no changes are to be seen anymore after 30 days.

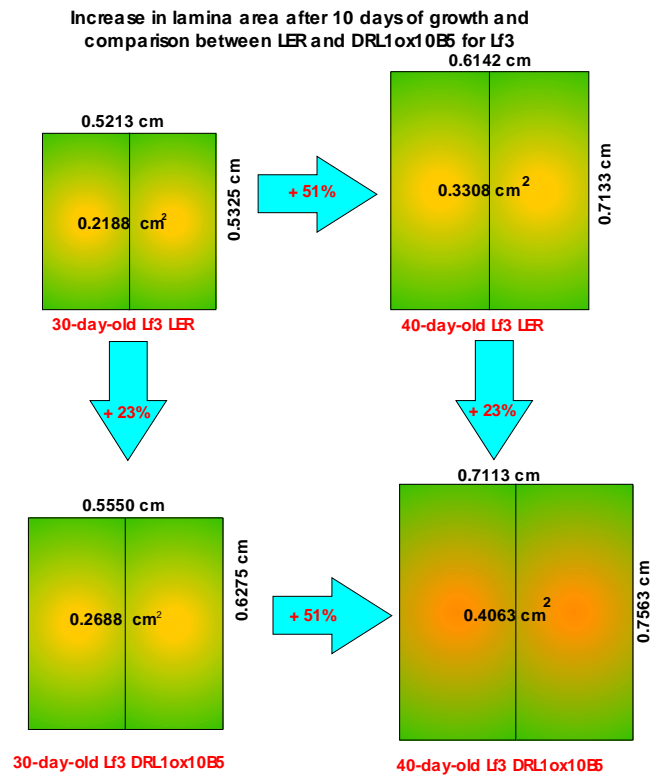


Fig.14. Increase in lamina area after 10 days (horizontal arrows) and difference between mutant and wild-type third mean leaf (vertical arrows). After 30 days the leaf lamina area is increased in the mutants (+23%). It remains the same also after 40 days because the lamina area growth rate is the same (+51%). What differs is the lamina length/width ratio between 40-day-old mutant and wild-type leaves, being this ratio >1 for wild-type third leaves and <1 for the third mutant leaves. 40-day-old mutants leaves have a relative “larger” and “smaller” lamina than 30-day-old, but both significantly increased in size if compared with the wild-type.

2.3 Leaf histology: determination of Palisade Cell Number (PCN)

5 μm transversal sections of 28-day-old DRL1ox10B5 and Ler first and third full-expanded leaves have been made with a Reichert Jung Ultracut microtome in order to determine with the aid of a binocular microscope the Palisade Cell Number (PCN) present at the widest part of the lamina. This parameter is an indicator of leaf blade lateral growth (Tsuge et al., 1996). Several leaves have been entirely sectioned from tip to petiole: one section every ten has been collected and put on a glass slide. The glass slides were subsequently stained with toluidine blue and mounted with DePex. The normally distributed data (Table5) have been analyzed for a statistical significant (P≤0.05) difference between the mean values with t-test using the SPSS software (Statistical Package for the Social Sciences, version 10.0.5, SPSS, Inc., Chicago, IL). The t-test for “Equality of Means” concerning the PCN showed that the first and third DRL1ox10B5 leaves are clearly different from first and third Ler leaves (p=0,000 in both cases): DRL1ox10B5 first and third leaves have a larger number of palisade cells: +31% and +16% respectively (Fig.13).

Leaf type	Leaf Nr.	Mean PCN	St.dev.
Ler Lf1	9	55,56	3,47
DRL1ox10B5 Lf1	15	72,93	2,66
Ler Lf3	12	82,05	12,11
DRL1ox10B5 Lf3	15	94,93	6,32

Table23. The mean PCN value and its standard deviation are indicated for first and third leaves of Ler and DRL1ox10B5.

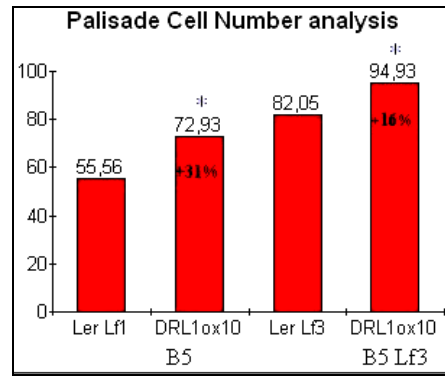


Fig.13. Graphic representation of the mean PCN values for first and third leaves of Ler and DRL1ox10B5. The symbol (*) indicates that there is a significant difference ($P \leq 0.05$) between the first two means and the second two.

2.4 Differential Interference Contrast (DIC) optic analysis

The cleared first and third DRL1ox10B5 and Ler first and third leaves prepared for the imaging analysis have been used to perform DIC (Differential Interference Contrast) optics analysis. This technique allows counting the number of cells of a determinate histological tissue layer and most importantly measuring the cell area from the adaxial side. The cells seen under a binocular can be drawn with a drawing tubus on a paper in a 14 cm circle, copied with a black marking pen on one or more transparent papers (Fig.11) in order to separate each overlapping cell (typical for the palisade layer) and scanned. With the use of Scion Image it is possible to outline each single cell (Fig.12) and to measure parameters, such as the area for example of each outlined cell. Statistics was done via the SPSS software on normally distributed data. In case of a skewed distribution, data were transformed using logarithmic values ($\ln x$).

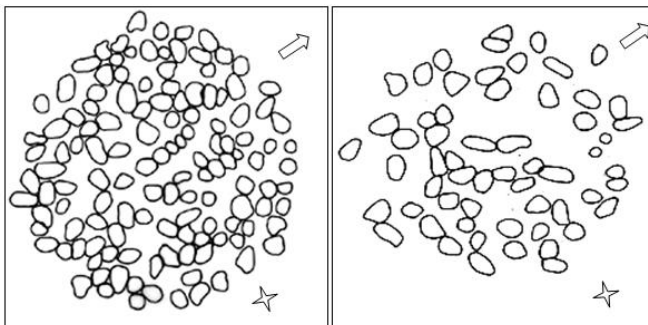


Fig14. DIC (Differential Interference Contrast) optics analysis. E.g. of a 2/3 draws of the palisade layer: the overlapping cells are separated on different transparent papers and marked with a black pen for a better scanning process. The arrow indicates the direction of the leaf tip and the star the position of the midvein.

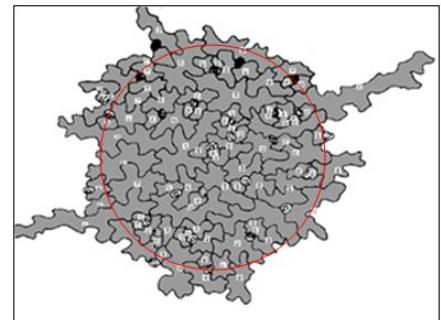


Fig15. DIC (Differential Interference Contrast) optics analysis. The upper epidermis layer has been drawn, copied on transparent paper, scanned and analyzed with the Scion Image software: every single cell has been outlined (grey colour) and number and the area has been measured. The red circle has a diameter of 14 cm and is initially drawn on a white paper. The microscope magnification is 20X and the image obtained in the microscope is also seen in transparency on the white paper. To correlate the microscope magnification with the drawn picture a ruler is also put at magnification 200X and drawn on the same white paper.

The measurements have been obtained only for Ler lfl1 upper epidermis and palisade cells (Table13) grown for 30 days and for DRL1ox10B5 and Ler Lf3 upper epidermis in 40-day-old leaves (Table14). The results presented in Table7, statistically analyzed with the SPSS software, after data normalization to obtain a distributed population, clearly point out that there is not a difference in cell size between mutant and wild-type of 40-day-old leaves.

Table24. DIC optics on Ler lfl			
Layer	Cell Nr	Mean Area	Mean St.Dev.
Palisade	1417	882	8
Upper epidermis	956	1499	43

Table24. DIC optics performed on 30-day-old first leaves on palisade and upper epidermis layers. The area is expressed in μm^2 .

Table25. DIC optics on DRL1ox10B5 and Ler lf3 upper epidermis						
Layer	Leaf type	Cell Nr	Mean Area (A)	Mean St.Dev. (S)	Log(A)	Log(S)
Upper epidermis	Ler Lf3	573	1706	68	7,01	0,04
	DRL1ox10B5 Lf3	523	1993	94	7	0,06

Table25. DIC optics performed on 40-day-old third leaves. The data are not normally distributed: they have been normalized via a logarithmic transformation in order to perform a t-test to check significant differences between the two populations. The area is expressed in μm^2 .

2.5 Conclusion

The 40-day-old third leaves cell area is the same as in wild-type. Drlox10B5 40-day-old plants have larger lamina due to an increase in cell number but not in cell size. This data should be confirmed with other measurements that will be done for the palisade layer cells of third leaves and possibly also for first leaves, palisade and upper epidermis.

2.6 Leaf histology: RON1 (ROTUNDA1) PCN analysis

5 μm transversal sections of 28-day-old RON1 (ROTUNDA1) and Ler first and third full-expanded leaves have been made with a Reichert Jung Ultracut microtome in order to determine with the aid of a binocular microscope the Palisade Cell Number (PCN) present at the widest part of the lamina. (Tsuge et al., 1996). Several leaves have been entirely sectioned from tip to petiole: one section every ten has been collected and put on a glass slide. The glass slides were subsequently stained with toluidine blue and mounted with DePex. The normally distributed data (Table26) have been analyzed for a statistical significant ($P \leq 0.05$) difference between the mean values with t-test using the SPSS software (Statistical Package for the Social Sciences, version 10.0.5, SPSS, Inc., Chicago, IL). The t-test for "Equality of Means" concerning the PCN showed that the first and third RON1 leaves are clearly different from first and third Ler leaves ($p=0,000$ in both cases): RON1 first and third leaves have a larger number of palisade cells: +36% and +25% respectively (Fig. 16).

Table26. Palisade Cell Number (PCN) analysis			
Leaf type	Leaf Nr.	Mean PCN	St.dev.
Ler Lf1	9	55,56	3,47
RON1 Lf1	14	75,33	5,24
Ler Lf3	12	82,05	12,11
RON1 Lf3	15	103,66	5,22

Table26. The mean PCN value and its standard deviation are indicated for first and third leaves of Ler and RON1.

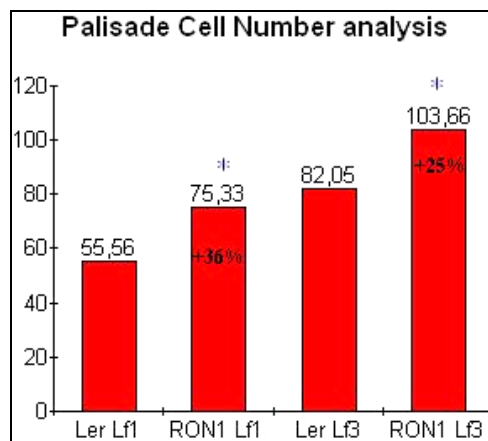


Fig.16. Graphic representation of the mean PCN values for first and third leaves of Ler and RON1. The symbol (*) indicates that there is a significant difference ($P \leq 0.05$) between the first two means and the second two.

3. Map Based Cloning (MBC): the TRN1 experience

3.1 Introduction

An AFLP-based (Amplified restriction Fragment Length Polymorphism) strategy (Vos et al., 1995) allowed chromosome landing in a C24 transgenic line at the *Arabidopsis* TORNADO1 (TRN1) locus (Cnops et al., 1996). The position of the recessive mutation was mapped at 5 cM from a T-DNA insertion. The TRN1 locus was “roughly” mapped with a standard marker set at the bottom half of chromosome 5 relative to visible and RFLP (Restriction Fragment Length Polymorphism) markers. To identify the locus to a relative small genomic region fine mapping was done using the AFLP technique. Recombinant classes within a 3-cM region were used to build a high resolution map in this region 300 primer combinations have been used to test about 26000 fragments for polymorphisms; 17 of these AFLP markers were identified in the 3-cM region around TRN1. These markers were mapped in this region using individual recombinants. 4 of these AFLP markers co-segregate with TRN1 whereas one maps at one recombinant below TRN1. The isolation and cloning of 3 of these markers was done and the markers identified 2 Yeast Artificial Chromosomes, CIC6C5 of 450 kb and CIC8H1 of 305 kb, containing the RFLP marker above and the AFLP marker below TRN1, demonstrating that these YACs span the TRN1 locus and that the chromosome landing was achieved, using the AFLP strategy (Fig.17). The MDF20 BAC clone was identified as the clone containing the TRN1 mutation. The At5g55540 gene in the MTE17 BAC clone has been indicated as the possible *trn1* locus from the Universitaet fuer Bodenkultur, Center for Applied Genetics, Vienna, in the so-called 9-29 *trn1* allele, which was isolated by T-DNA tagging: the T-DNA insertion was positioned in the At5g55540 gene (Luschnig, C., personal communication).

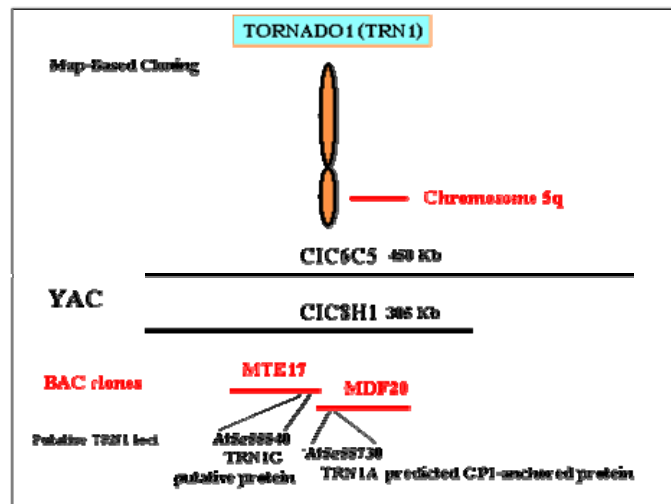


Fig.17. Position of the TRN1 candidate genes and results of the Map-Based Cloning approach to achieve chromosome landing and identify via fine mapping techniques the MDF20 as the BAC clone spanning the *trn1* mutation. In this clone the TRN1A locus (At5g55730) has been chosen as candidate gene. The MTE17 BAC clone is reported from the Universitaet fuer Bodenkultur, Center for Applied Genetics, Vienna (Luschnig, C., personal communication).

3.2 TRN1A (At5g55730) and TRN1G (At5g55540): two putative genes for the TORNADO1 mutation

TRN1 has not been cloned yet but fine mapping and new information obtained in collaboration with the Universitaet fuer Bodenkultur, Center for Applied Genetics, Vienna (Luschnig, C., personal communication) have restricted the search of the mutant locus to 2 BAC clones, MDF20 and MTE17. The first BAC clone contains 8 known and 20 putative genes; the second has 15 known genes and 12 putative. To find where the *trn1* mutation is located DNA was extracted from *trn1-1*, *trn1-3* mutant plants and C24 plants (Table15). The extraction was done using the CTAB protocol to obtain a good DNA quality from plants. The two genes, TRN1A (At5g55730) and TRN1G (At5g55540), were selected for different reasons. TRN1A is a predicted GPI-anchored protein (Glycosylphosphatidyl- inositol-anchored protein), which is part of regulatory molecules that determine the extent and direction of expansion in cell morphogenesis and could possibly explain the positive regulation of epidermal fate or the negative regulation of lateral root cap determinants in the inner protoderm derivatives observed for the TORNADO1 and TORNADO2 mutants (Cnops et al., 2000). TRN1G, instead, contains an ATP/GTP-binding site motif (P-loop) and has been proposed as a possible candidate by Prof. Luschnig: the TRN1-like phenotype has been identified at the Universitaet fuer Bodenkultur in plants segregating for the 9-29 phenotype. Mutagenesis was performed in these plants with pSKI15 on a mixed genetic background consisting of *eir1-1* (Col-0) and NoO. Two further backcrosses were made in Col-0 to select for Col-0 background. The seeds obtained were checked for the 9-29 phenotype. The TORNADO1-like phenotype strictly co-segregated with a T-DNA insertion which was found to be in the At5g55540 gene on the MTE17 clone. Moreover it was seen that there was a 3:1 segregation for BASTA resistance with all the resistant plants being either 9-29 (almost 1/3) or hemizygote for the 9-29 phenotype (almost 2/3). The BASTA resistance seems to co-segregate with 9-29 and can be used for the selection of hemizygotes.

Allele	Ecotype	Origin
trn1-1	C24	Cnops G., RUG
trn1-3	C24	RUG
9-29	Col-0	Luschnig
wt1	C24	RUG
wt2	Col-0	Internet

Table27. Trn1 alleles and wild-type used for DNA sequence analysis of TRN1A and TRN1G genes. DNA extraction has been performed from all these alleles with the exception of wt2, whose entire genome is available in internet. The alleles are to be found at the RUG (Rijks Universiteit Gent) or at the Universitaet fuer Bodenkultur.

3.2.1 Results

With specific primer combinations designed with the OLIGO4 software (Rychlik, 1989) the 2 candidate genes have been fully (TRN1A) and partially (TRN1G) sequenced to find possible point mutations in the mutants compared to the wild-type and the Col-0 ecotype complete genome, present on the web and freely accessible. 2 primer combinations (Trn1a3/4 and Trn1a5/6) were able to amplify all the genomic region of the putative locus TRN1A in the MDF20 BAC clone from nucleotide 48860 to 52029 (Fig.18) and 5 other primer combinations (Trn1g1/2, Trn1g3/4, Trn1g5/6, Trn1g7/8 and Trn1g9/10) almost all the putative locus G on the BAC clone MTE17 (Fig.20). The PCR products obtained were sequenced and the sequences were introduced into the Biology Workbench interface (<http://workbench.sdsc.edu/>), “for rapid access of biological databases and analysis tools”, in order to perform sequence alignments and find possible point mutations typical for each allele (Fig.19). The sequencing of the TRN1A PCR products clearly indicates that this locus is not the putative locus for the trn1 mutation in the trn1-1 and trn1-3 mutant alleles since there were no mutations present in the alignments (Fig.18). The PCR products were obtained with specific primer combinations (Trn1a3/4 and Trn1a5/6) and PCR conditions standard PCR conditions, as mentioned in Material and Methods, optimizing the reaction with the best OAT (Optimal Annealing Temperature). The sequencing of the TRN1G in the 3 amplified regions gave no mutation in none of the alleles compared to the wild-types (Fig.20). Two primer combinations didn't work as expected and new primers have been designed: Trn1g1 a,b,c,d,e,f and Trn1g7a,b. The first 3 primer combinations (Trn1g1a/b, c/d, e/f) are designed to include also the promoter region, in order to find out whether a possible mutation is present in the regulatory region of the gene.

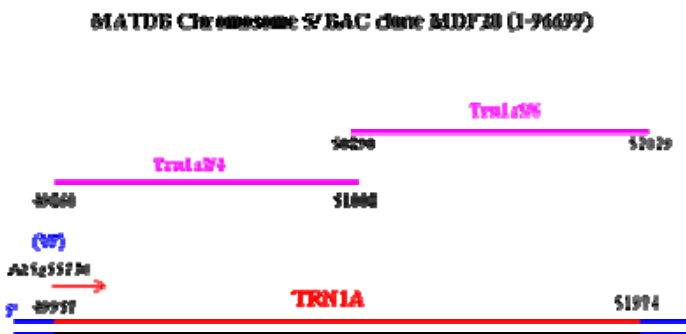


Fig.18. DNA amplification and sequence determination of the TRN1A gene. Trn1a3/4 and Trn1a5/6 amplified the entire putative TRN1A locus (At5g55730). The PCR products were sequenced and aligned.

ERN_A56_T13_1	GATAAGTGTACCAATACATTTATTAAGTGTACACAGGACATGCATATAATTTGAT
ERN_A56_T13_1_1	GATAAGTGTACCAATACATTTATTAAGTGTACACAGGACATGCATATAATTTGAT
ERN_A56_T13_4	GATAAGTGTACCAATACATTTATTAAGTGTACACAGGACATGCATATAATTTGAT
ERN_A56_T13_3	GATAAGTGTACCAATACATTTATTAAGTGTACACAGGACATGCATATAATTTGAT
ERN_A56_T13_3	GATAAGTGTACCAATACATTTATTAAGTGTACACAGGACATGCATATAATTTGAT
ERN_A56_T13_3	GATAAGTGTACCAATACATTTATTAAGTGTACACAGGACATGCATATAATTTGAT
ERN_A56_T13_5	GATAAGTGTACCAATACATTTATTAAGTGTACACAGGACATGCATATAATTTGAT
ERN_A56_C24_3	GATAAGTGTACCAATACATTTATTAAGTGTACACAGGACATGCATATAATTTGAT
ERN_A56_T11_1	GATAAGTGTACCAATACATTTATTAAGTGTACACAGGACATGCATATAATTTGAT
ERN_A56_T11_1	GATAAGTGTACCAATACATTTATTAAGTGTACACAGGACATGCATATAATTTGAT
ERN_A56_T13_2	GATAAGTGTACCAATACATTTATTAAGTGTACACAGGACATGCATATAATTTGAT
ERN_A56_T13_10	GATAAGTGTACCAATACATTTATTAAGTGTACACAGGACATGCATATAATTTGAT
ERN_A56_C24_4	GATAAGTGTACCAATACATTTATTAAGTGTACACAGGACATGCATATAATTTGAT
ERN_A56_T11_1	GATAAGTGTACCAATACATTTATTAAGTGTACACAGGACATGCATATAATTTGAT
ERN_A56_T11_1	GATAAGTGTACCAATACATTTATTAAGTGTACACAGGACATGCATATAATTTGAT
ERN_A56_T11_14	GATAAGTGTACCAATACATTTATTAAGTGTACACAGGACATGCATATAATTTGAT
Col_A56	GATAAGTGTACCAATACATTTATTAAGTGTACACAGGACATGCATATAATTTGAT

Fig.19. Example of an alignment done with Boxshade software (version 3.3.1, Kay Hofmann and Michael D. Baron). The sequences are obtained with specific primer combinations which amplified the TRN1A5/6 region. PCRs have been made in double or more on trn1-1, trn1-3 and C24 DNA. The Col-0 sequence has been retrieved from Internet. It is possible to see a polymorphism between C24 and Col-0 ecotypes (yellow colour).



Fig.20. Strategy for DNA amplification and sequence determination of the TRN1G gene. In all the alleles analyzed 3 primer combinations amplified 3 genomic regions (rose bars) of the At5g55540 gene (another putative TRN1 locus) under the PCR conditions and the Optimal Annealing Temperature (OAT). The PCR products were sequenced and aligned. 2 primer combinations didn't work as expected (green bars).

3.2.2 Conclusions

The DNA sequence data are conclusive for the TRN1A gene: there are no mutations in the different alleles meaning that the TRN1A gene cannot correspond to the TRN1 locus to be sequenced. Under the supervision of Dr. Cnops I amplified and sequenced a small genomic region in order to find the possible mutation causing the TRN1 phenotype: part of this region was excluded thanks to the sequencing and alignments results and the T-DNA tagged candidate allele of the TRN1 gene was analysed. I contributed to the sequencing of the gene in which the T-DNA was inserted. Before discovering the *trn1* locus a crossing program was started to perform an allelism test between heterozygous *trn1-1* plants and the 9-29 plants, so as to find out phenotypically and genotypically from the F1 wild-type:mutant ratio if the locus was the same or another.

3.3 Allelism test between *trn1-1* and 9-29

In order to define whether the mutated At5g55540 locus (in the 9-29 line) could be the possible unknown *trn1* locus a parallel experiment has been done: heterozygous *trn1-1* plants were crossed with heterozygous *trn1* 9-29 plants so as to find out from the F1 wild-type:mutant ratio if it was the same locus or another. If the locus is the same a 3:1 ratio between wild-type and mutants is expected in the F1 generation; if the loci are different no mutant phenotype is expected (Fig.21).

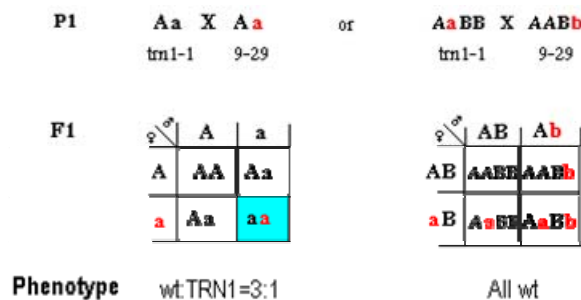


Fig.21. Allelism test between *trn1-1* and 9-29 plants. Two possible outputs can be obtained from this Allelism test: in case *trn1-1* and 9-29 are the same gene one plant out of four should have a mutant TRN1 phenotype; if the mutation is present in another locus no mutants are expected and all the plants of the F1 generation are wild-type.

4 crosses were made between *trn1-1* and 9-29 line plants and from the 4 siliques obtained 55 seeds were collected, vernalized for 1 week and sowed out on germination medium added with vitamins (GM + V). Phenotype scoring was done after germination: 5 plants did not germinate, 47 plants showed the wild-type and 3 the TRN1 phenotype. The 3 mutant plants were frozen for DNA preparation to test the presence of indel markers. In the TRN1 area only 1 indel polymorphic marker between C24 and Col-0 was found. The aim was to test polymorphism of indels between Col-0 and C24. In case F1 *trn1* mutants contain Col-0 X C24 indels, this would imply that they originated from crossings and thus 9-29 would be the *trn1-4* allele. In case F1 *trn1* mutants contain only Col-0 or C24 indels they originated from self-pollination. DNA was extracted from the 3 plants with the CTAB protocol and a touch-down PCR was done to amplify with specific primers (*trn1-in-9* and *trn1-in-10*) 2 different indel fragments of 109 bp (Col-0) and 115 bp (C24). The fragments were separated on a Nusieve agarose: agarose (3:1) gel but the 3 fragment present corresponded to the C24 band, indicating that the 3 plants came from a self-pollination in the *trn1-1* background.

4. Bioinformatics: AtELP1p homologue of *Saccharomyces cerevisiae* ELP1/TOT1/IKI3p

BLASTP (2.2.5) searches have initially been performed with the aid of the Biology WorkBench 3.2 interface (<http://workbench.sdsc.edu/>), “for rapid access of biological databases and analysis tools”, at the National Center for Biotechnology Information (NCBI; www.ncbi.nlm.nih.gov/blastp/db/) with the databases information they currently update and provide, in order to find the *Arabidopsis thaliana* homologue of the *Saccharomyces cerevisiae* known ELP1/TOT1/IKI3p Elongator-complex protein. The 1349 amino acid sequence of ELP1/TOT1/IKI3p has been blasted as query in the Non-Redundant Protein Sequence Database (NR; ftp.ncbi.nlm.nih.gov/blast/db/), which contains at present more than 1 250 000 sequences. The default search parameters (Blosum62 as matrix, 11 as GOP Gap Opening Penalty, 1 as GEP, Gap Extension Penalty and 0.85 as Lambda Ratio value) have been preserved. Throughout different species, 19 highly significant matches were obtained (E-value $\leq 9e^{-09}$, see table1): in *Arabidopsis thaliana* the only significant homologue with an E-value of $4e^{-43}$ was a putative protein [ID: At5g13680.1] with a query identity of 28% (134/465 AA), 51% of positive matches (238/465) and 8% gaps, in the 2/3 region of the protein. This putative protein has been named AtELP1p.

Performing alternatively the search in the GenBank Plant Sequences database, that contains more than 200 000 plant sequences and in the *Arabidopsis thaliana* Proteins database, containing more than 27 000 sequences, the previous results have been confirmed (E-value = $9e^{-44}$ and $2e^{-44}$). Subsequently, when the AtELP1p 1319 amino acid sequence was blasted as query in the NR database it was found that this protein is highly homologue (E-value from 0.0 to $3e^{-67}$) to all members of the Human IKAP (IkappaB Kinase complex-Associated Protein; [AL023589]) subfamily, which includes *Oryza sativa* (rice; [AP_005296]), *Mus musculus* (mouse; [AF367244]), *Schizosaccharomyces pombe* (yeast; [NC_003423]), *Encephalitozoon cuniculi* (fungus; [NC_003242]) and *Oryctolagus cuniculus* (rabbit; [AF388202]) as species.

The IKAP subfamily is part of the IKI3 family, containing the ELP1/TOT1/IKI3p founder and whose members are yet recognized as “components of the Elongator multi-subunit component of a novel RNA polymerase II holoenzyme for transcriptional elongation” (PFAM, Protein Families databases of Alignments and HMMs; [PF04762]). IKI3 members have also been found in *Caenorhabditis elegans* (worm; [NM_059123]) and *Drosophila melanogaster* (fruit fly; [NM_141841]). In addition, it was also found that a high homology ($E \leq 9e^{-65}$) was present between the query and the human Inhibitor of Kappa Light Polypeptide gene enhancer in B-cells (a kinase complex-associated protein; [BCO33094]) and its homologues in *Rattus norvegicus* (rat; [NM_080899]) and *Mus musculus* (mouse; [NM_026079]).

Searches for functional domains of AtELP1p have been performed at ProDom 2002.1 “whole database” (<http://prodes.toulouse.inra.fr/prodom/2002.1/html.php>), which contains more than 480 000 protein sequences and 365 000 family-domains. The output of the blast against known domains showed that in AtELP1p there are 2 “phosphorylation” domains, D2 and D4, interspersed between 3 unknown amino acid regions. Both domains are homologues with all the previous described members of the IKI3 family (10 matches).

A PROSITE search found many potential phosphorylation sites on serine/threonine residues by cAMP and cGMP-dependant protein kinases, by Casein kinases II or by Tyrosine kinases on tyrosine residues. In addition it also finds several possible N-glycosylation, myristilation and amidation sites and even a RGD cell attachment site.

5. Cloning of AtELP genes into the pGEM3z vector

The 2743 bp Promega’s pGEM[®]-3Z vector was extracted from the *E. coli* bacterial strain present in the VIB collection (code 4171) with the QIAGEN’s midi plasmid extraction protocol. 2 tubes were obtained and named pGEM3z1 and pGEM3z2. They were subsequently linearized with the restriction enzyme HincII, which creates blunt ends and finally dephosphorylated with the CIP (Calf Intestinal Phosphatase) enzyme. The concentration was determined with the spectrophotometer (Table28).

Table28. Vector preparation

Vector	Strain Code	Extraction	Abs	Lin-Deph	Dilution
		28/09/2003	[] ng/μl	[] ng/μl	[] ng/μl
pGEM-3Z	4171	pGEM-3Z-1	570	450	45
		pGEM-3Z-2	475	425	42,5

Table28. Vector extraction, linearization, dephosphorylation and quantification.

With the QIAGEN[®] One-Step RT-PCR kit several genes were amplified from Ler RNA preparation. Some of these AtELP genes have been amplified with primers that introduce the nucleotidic sequence for a codon stop (+ STOP), others without (- STOP). In the same time, these primers introduce also a partial nucleotidic sequence at both ends, which creates partial att recombinant sites. To complete these att sites a new PCR is made using the purified RT-PCR products as templates. The inserts obtained have at both ends the att sites which are recognized by the homologous sequences present in the GATEWAY entry clones. The concentration of the PCR products has been measured with a spectrophotometer and some dilution were made.

The Elongator complex: its function in leaf development and germination

Table29. One-Step RT-PCR and attPCR products				
Insert	One-Step	RT-PCR	Abs [] ng/µl	Abs [] ng/µl
	- Stop	+ Stop	- Stop	+ Stop
AtELP3	yes	yes	/	/
AtELP4	yes	yes	260	165
AtELP5	yes	yes	200	/
DRL1-2	yes	/	380/75/175	/
Insert	att PCR			
	Abs [] ng/µl	Abs [] ng/µl	Dilution	Dilution
	- Stop	+ Stop	- Stop	+ Stop
AtELP3	>400 (on gel)	>400 (on gel)	/	/
AtELP4	340	360	17	18
AtELP5	375	370	18,5	18,5

Table29. One-Step RT-PCR and attPCR products. In this table the AtELP gene obtained by One-Step RT-PCR are presented. On AtELP3, AtELP4 and AtELP5 further PCR with att upper and lower primers were made in order to obtain inserts with complete att sites. The absorbance (Abs) of the products was measured with the spectrophotometer.

In order to perform *in vitro* transcription to obtain RNA probes from AtELP1 and AtELP4 to be used for *in situ* hybridizations 2 primer combinations were designed (Table30) so as to amplify a 300 bp gene-specific sequence, which will be cloned into a suitable vector (pGEMT-easy).

Table30. Primers specific for AtELP1 and AtELP4				Tm
Anfal3	AtELP1 up. primer	5'GCGGGTGAGGAGATGGCT3'		64
Anfal4	AtELP1 low. primer	5'CATGGGCTTATGAAGACCTTAAGCA3'	U1+L1 314 bp	64
Anfal5	AtELP4 up. primer	5'GATACTAGGTGGTGGGTATCCTTT3'		59
Anfal6	AtELP4 low. Primer	5'GTCGGGGCCAGTAGGCTT3'	U4+L4 217 bp	64

Table30. Primer designed to amplify a gene-specific fragment of AtELP1 and AtELP4.

Materials and methods

1. Primers and PCR conditions

Primer Name	Primer Sequence	Gene
Hine1-105 UP	5CAGCAACGGTTCAAAGATGCG3'	AtELP1
Hine1-106 LP	5CCACTAGCACACTCCAAAAGCC3'	AtELP1
Hine1-146 UP	5'ATCCAACAAAAGCCACTGCC3'	AtELP1
Hine1-147 LP	5'TGCCTGOCACCCATATAG3'	AtELP1
Defle2 UP	TGAAAAATTTGAAGCTTTTCTCGGA	AtELP1
Defle3 LP	IGGGCTTATGAAGACCTTAAAGCATC	AtELP1
Defle4 LP	ICATGGGCTTATGAAGACCTTAAGCA	AtELP1
Defle1 UP	5'TAACACTTGAATGTAATTGGC3'	AtELP3
Defle9 LP	5'GCTAGCTCCACCAAACCTCA3'	AtELP3
Hine1-69 UP	5AATTTTATGCGAATTACG3'	AtELP4
Hine1-70 LP	5GACAAAAGTGACACTAACC3'	AtELP4
Hine1-73 UP	5'CTTCTCTAAAAGACTGC3'	AtELP4
Hine1-74 LP	5'CTCTTGTATAAGCTTTGG3'	AtELP4
Anfal-1 UP	5'CTAGAAATAAACTTAGGTTACA3'	AtELP6
Anfal-2 LP	5'AGACAAAACAGTAAAAGATT3'	AtELP6
Tag5 LP	5'CTACAAAATTGCTTTTCTTAT3'	T-DNA
NptIII UP	5'TGTTCCGGCTGTGACGGCAG3'	T-DNA
NptIII2 LP	5'TCGCAAGCAGGCATCGCCA3'	T-DNA
Tmla3 UP	5'CCGACTATTTAATTCGACAACC3'	TRN1A
Tmla4 LP	5'AATTTCCGTTGTTAAATGAGAA3'	TRN1A
Tmla5 UP	5'GCTTAAGAAACAGTCAACACCT3'	TRN1A
Tmla6 LP	5'ATCCCTCACCTTAAGCTCTTC3	TRN1A
Tmlb1 UP	5'GATACGATGGTGTGTGTGTTT3	TRN1A
Tmlb2 LP	5'ACAAGGGCTAGTTGAAAGATGCT3'	TRN1A
Tmlc1 UP	5'ATCGAGAGCCAGAGAAAGGTGT3'	TRN1A
Tmlc2 LP	5'GCCAGCTCTTTCTAATTC AACCC3'	TRN1A
Tmld1 UP	5'CTCGCCCTCTTTTGTGTTTTTT3'	TRN1A
Tmld2 LP	5'GCTOCCAAAAGTTCTTCTGTTTA3'	TRN1A

The Elongator complex: its function in leaf development and germination

Tmlg1 UP	5'CTTTACCTTCTCTCTCTG3'	TRN1G
Tmlg2 LP	5'AGTCCATCTCTTCCAATCTT3'	TRN1G
Tmlg3 UP	5'TGCTTTGTCCATTGAGTAGA3'	TRN1G
Tmlg4 LP	5'GTGTTTTGGGTTCTTTATTG3'	TRN1G
Tmlg5 UP	5'AAGGACGAGGAGACAAAGAT3'	TRN1G
Tmlg6 LP	5CCCTGGAATTTGGACTCTGTA3'	TRN1G
Tmlg7 UP	5TCGCAACGAGAACATTCAGA3'	TRN1G
Tmlg8 LP	5'TTCGGGGTTTTCGTCGTGTG3'	TRN1G
Tmlg9 UP	5'ACCTCCTCTCTGATGATGAT3'	TRN1G
Tmlg10 LP	5'CTGGTCTACTTTTTTCTTTG3'	TRN1G
Tmlg1a UP	5'ATTATGACAAAACAACTTACA3'	TRN1G
Tmlg1b LP	5'ACCTCCATTTCTCTGTTTATA3'	TRN1G
Tmlg1c UP	5'AGACAACCTCACTTCACTTTC3'	TRN1G
Tmlg1d LP	5'TCTCACATTCTCCACATAAGG3'	TRN1G
Tmlg1e UP	5'GGTGTGAGGATTTGCTTTGT3'	TRN1G
Tmlg1f LP	5'AGCCCAAATCATCAAAGTAAA3'	TRN1G
Tmlg7a UP	5'GGGAGAGGTGATTTACTTTGA3'	TRN1G
Tmlg7b LP	5'TATGGCTCAAGTCAGGTATCA3'	TRN1G

Table1. Name and related sequence of upper (UP) and lower (LP) primers and amplified gene. 18 to 27-long optimized upper and lower primers (Table1) have been designed with the OLIGO4 software (Hychlik et al.) in order to be specific, with no hairpin formation or possible dimerizations.

1.2 PCR profile and conditions

PCRs have been run with the Robocycler gradient 96 (Stratagene Europe) following the 2 PCR profiles: 3' or 2' at 94°C as initial denaturation step for 1 cycle; 30'' or 15'' at 94°C as denaturation step + 30'' at OAT as annealing step + 2' at 72°C or 68'' as elongation step for 25-35 cycles; 3' at 72°C or 68'' as final elongation step for 1 cycle (Table2 and 3).

Table2. PCR profile for Taq DNA Polymerase	
94°C for 3'	1 cycle
94°C for 30"	25-35 cycles
OAT for 30"	
72°C for 1' x Kb	1 cycle
72°C for 4'	

Table3. PCR profile for Taq DNA Polymerase	
94°C for 2'	1 cycle
94°C for 15"	25-35 cycles
OAT for 30"	
68°C for 1' x Kb	1 cycle
68°C for 10'	

Table2 and 3. PCR profiles. The two DNA Polymerases perform differently and have different efficiency and characteristics. The Platinum Pfx DNA Polymerase possesses a 3' to 5' exonuclease activity and is better suited for long fragment amplifications (> 2,5 kb). The Taq DNA Polymerase is a less expensive enzyme best suited for routine amplification reactions. Buffers are different for the 2 enzymes, but presence of Mg²⁺ ions are important for good quality reactions.

Primer combination	Optimal Annealing Temperature (OAT)
Hinel-105/Hinel-106	53°C
Hinel-146/Hinel-147	53°C
Hinel-105/LBa1	53°C
Hinel-146/LBa1	55°C
Hinel-69/Hinel-70	51°C
Hinel-73/Hinel-74	54°C
Defle1/Defle9	54°C
Defle1/Tag5	54°C
Nptl11/Nptl12	53°C
Trn1a1/Trn1a2	52°C
Trn1a3/Trn1a4	52°C
Trn1a5/Trn1a6	53°C
Trn1b1/Trn1b2	52°C
Trn1c1/Trn1c2	52°C
Trn1d1/Trn1d2	52°C
Trn1g1/Trn1g2	51°C
Trn1g3/Trn1g4	52°C
Trn1g5/Trn1g6	53°C
Trn1g7/Trn1g8	54°C
Trn1g9/Trn1g10	52°C
Trn1g1a/Trn1g1b	47°C
Trn1g1c/Trn1g1d	52°C
Trn1g1e/Trn1g1f	53°C
Trn1g7a/Trn1g7b	53°C
Defle2/Defle3	56°C
Defle2/Defle4	56°C
Anfal-1/Anfal-2	48°C

Table4. Primer combinations and their OAT.

2. Plant germination and growth conditions

The Elongator complex: its function in leaf development and germination

2.1 Plant germination medium (GM): the *in vitro* conditions

1 L of plant germination medium (GM), (Valvekens et al., 1988) has the following composition: 4.3g/L of Murashige & Skoog salts (ICN Biomedicals Inc.) containing micro and macro nutrients and Fe-EDTA, 100 mg/L of myo-inositol, 500 mg/L of MES (2-[N-morpholino] ethane sulfonic acid), 1% sucrose (10g/L), 0.85% plant tissue culture agar (Lab M) and distilled water up to volume. The Difco Bacto agar is usually added in the solution after it has reached pH 5.7 with 1M KOH. Autoclavation at 121°C for 15' is necessary before the pouring of the medium into the germination plastic plates. Vitamins (thiamine 10 mg/L, pyridoxine 1 mg/L and nicotinic acid 1 mg/L) are to be added when needed before autoclaving; kanamycin (50 mg/L) is to be added after autoclaving. It is important to work in sterile conditions (in a laminar flow bench) to avoid fungi and bacterial contaminations in the plates.

2.2 Seed sowing: *in vitro* growth conditions

Seeds are incubated 2' in technical (denatured) ethanol 97% and after ethanol has been removed 12' in 5% hypochlorite solution containing 1% Tween20. After the sterilisation, seeds are washed and rinsed several times with distilled water and sowed in 150 x 25 mm Petri dishes in an appropriate germination medium under the laminar flow bench in order to avoid contamination. Plates are sealed with gas-permeable medical tape and kept O/N at 4°C prior to be transferred to the germination chamber.

2.3 Plant growth: *in vivo* conditions

Plants are grown under non-sterile conditions in a soil:vermiculite (3:1) mixture in a 16-h-light/8-h-dark regime at 22°C, with light intensity of 100 $\mu\text{mol} \cdot \text{m}^{-2} \cdot \text{sec}^{-1}$ and 60% RH.

3. Protocols for plant DNA extraction

3.1 Fast DNA extraction: the Edwards protocol

The extraction buffer is prepared using 200 mM Tris-HCl pH 7.5, 250 mM NaCl, 25 mM EDTA and 0.5 % SDS. 0.5 mg of tissue is collected from the seedlings and put in 2ml Eppendorf tubes floating on liquid nitrogen. In the tubes some metal balls are put and the disruption of the tissue is mechanically done with a high frequency shaking Retsch instrument. 400 μL of extraction buffer is added and a centrifugation of 2' at 13000 rpm is done. The supernatant is transferred to a new Eppendorf tube and 1 volume of isopropanol is added at room temperature for 10' for the DNA precipitation step. Subsequently, a new centrifugation at 13000 rpm for 10' is done. The pellet is kept and washed with 70% ethanol. After the last centrifugation of 2' the ethanol is poured off and the pellet is left drying for a while. 50-100 μL of distilled water is added. A 1% agarose gel is prepared to check the presence of the extracted DNA.

3.2 Plant DNA extraction: CTAB mini preparation (Tel-Zur et al., 1999)

This DNA extraction protocol needs a double buffer preparation: the "extraction buffer" is prepared at 4°C with 0.1 M Tris-HCl at pH 8.0, 0.5 M NaCl, 0.05M EDTA at pH 8, distilled water and 14.3 M β -mercapto-ethanol, to be added before use; the "CTAB (cetyltrimethylammonium bromide) buffer" contains 0.2 M Tris-HCl at pH 7.5, 2 M NaCl, 0.05M EDTA at pH 8 and 2% (W/V) CTAB. The CTAB has to be previously heated to be dissolved in sterile water. Tissue (50-60 mg freshweight) is grinded with metal balls in a high frequency shaking Retsch instrument in 2 ml Eppendorfs kept on liquid nitrogen. 1 ml of extraction buffer is added in each tube followed by 50 μl of 10% SDS which denatures the peptides in the cell wall and advances the disruption. The tubes are incubated for 30' at 65°C, swirled periodically and centrifuged at 14000 rpm for 10'. The supernatant is then transferred to a fresh tube and 1 volume of isopropanol is added for DNA precipitation. The tubes are kept on ice for 10-30'. A new centrifugation is done for 10' and the supernatant is discarded. The pellet is dissolved in 400 μl of TE (10 mM Tris-HCl at pH 8.0 + 1 mM EDTA at pH 8.0) for a few minutes at 65°C (if needed). Adding 1 μl of RNase (10 mg/ml) at 37°C is a good optional step to degrade RNA and keep only the DNA. 400 μl of CTAB buffer are added at this stage in each tube and incubation at 65°C for 15' is necessary. Subsequently, 800 μl of chloroform/isoamylalcohol (24:1) are added and 5' centrifugation at 14000 rpm is done. The aqueous phase is transferred to fresh tubes. If needed the extraction with the CTAB buffer can be repeated. 1.4 ml 96% ethanol is added in the aqueous phase and 15' incubation is done at room temperature. At this stage it is possible to leave O/N the tubes at -20°C. A 10' centrifugation at 14000 rpm is done to obtain a pellet that is washed after with 1 ml in each tube of 70% ethanol. A final 5' centrifugation at 14000 rpm is done and the supernatant is removed leaving the pellet as dry as possible. The DNA-pellet is finally dissolved in 50-100 μl TE or distilled water. The "quality-quantity" of the DNA is checked on a 0.8% agarose gel in TAE buffer, run at 50 volts and stained with Ethidium Bromide.

4. Leaf histology: fixation, infiltration, embedding, sectioning, staining, mounting and imaging

30 and 40-day-old fully expanded first and third leaves of Ler and DRL1ox10B5 plants have been harvested and immediately fixed in FAA (90% EtOH, 5% acetic acid, 5% formaldehyde) at 4°C O/N. Afterwards, they have been dehydrated with increasing concentrations of EtOH: 2 x 30' EtOH 50%, 2h EtOH 50%, 2h EtOH 70%, 2h EtOH 80%, O/N EtOH 80%, 2 x 2h EtOH 90% and ultimately O/N EtOH 95%. The infiltration step consisted in a gradually permeation of Histoiresin in the tissue and was achieved by putting first the leaves for 4h in a mix 50% EtOH + 50% Histoiresin, followed by another mix 30% EtOH + 70% Histoiresin for 4h and finally in 100% Histoiresin for 4h. After 30' of vacuum infiltration to plunge the tissue into the Histoiresin solution the leaves were shaken at room temperature for 2 or 3 days. The leaves were then immersed in a new basic resin solution containing a 1% temperature-sensitive activator and left shaking O/N. Leaves were finally oriented in beds which were half-filled with the resin solution, covered with new resin and left polymerizing at 45°C for at least 2 h.

The histology analysis has been performed on 5 μm sections collected on glass slides and obtained with a Reichert Jung Ultracut Microtome using home-made glass knives. The Histoiresin leaf-containing blocks obtained after polymerization were oriented on a glass cube and fixed on it with super-glue. These blocks were entirely sectioned in order to obtain serial sections of the leaf from the tip to the petiole. One

The Elongator complex: its function in leaf development and germination

section every 10 was taken. The glass slides were afterwards stained for 8' with 0.05% toluidine blue in phosphate buffer 0.1 M pH 6.8 and mounted with DePex. Photographs were taken with an Olympus CAMEDIA digital camera C-3040 zoom 3.3 megapixel at the same magnification.

5. Pollination: the crossing program between “male” and “female” plants

Seeds of *Arabidopsis thaliana* are germinated in *in vitro* growth conditions for 2-3 weeks prior to transplantation in soil. Plants are selected for the crossing program as soon as the flowering starts (usually after 3 weeks). The stamens of the “male” plants containing the pollen are taken under a stereomicroscope with sterile tweezers and used to pollinate the stigma of “female” plants (one or more). The buds containing the gynaeceum are opened, petals and sepals are gently taken off and the stigma with its papillae is exposed. Pollen sticks on the papillae when the stamens are gently passed on them. The location of the future silique formation is indicated with a nylon marker and the harvesting of the mature (yellow) siliques is done in a little sterile plate which will be vernalized for one week at 4°C.

6. Statistical Package for the Social Science (SPSS)

All the morphological data collected from Image analysis (leaf morphology analysis) and from microscope observations (Palisade Cell Number analysis) have been evaluated statistically with the SPSS software (Statistical Package for the Social Sciences, version 10.0.5, SPSS, Inc., Chicago, IL). In order to find out whether the distribution was normal or skewed to left or right, a “descriptive statistics” was performed; in case the distribution was found skewed, a logarithmic transformation was done so as to transform a skewed distribution into a normal distribution and perform a t-test (Sokal R., and Rohlf F.J. 2000, Biometry W.H. Freeman and company edition) between two set of data (e.g. mutant vs. wild-type). A significance value p is calculated using “compare means”. This value related to the null hypothesis H_0 , which is the hypothesis under test, gives a statistically indication whether to accept the hypothesis or reject it. In our case the hypothesis was “the two mean values are the same”: the H_0 is rejected if $p \leq 0.05$ (it is highly improbable, less than 5%, that the two means are the same). By the means of “graphs” it is possible to have a representation of the means and their standard deviation.

7. Vector and bacterial strain used for the cloning of the AtELP genes

The 2743 bp Promega's pGEM[®]-3Z vector was used for the cloning of the 6 AtELP genes and the DRL1 gene. It is a “standard subcloning vector good for highly efficient synthesis of RNA *in vitro*” and for “blue/white screening of recombinants”, containing a Multiple Cloning Region (MCR) and two RNA polymerase promoters, SP6 and T7 next to the MCR, from which *in vitro* transcription is possible on both strands, in opposite directions.

The MCR is located into the lacZ α -peptide locus, which encodes for the β -galactosidase. This protein is able to convert IPTG or X-GAL as substrate into a product which confers a blue colour to the bacterial cells of a colony. The Promega code of the bacterial strain used for the cloning procedure is JM109 and its characteristic is to have a lacZ Δ M15 genotype, not producing a functional β -galactosidase. This strain can be complemented with the pGEM[®]-3Z vector carrying a functional lacZ locus: this is only possible if no insertion takes place in the MCR. Blue colonies are obtained. If the insert is cloned into the lacZ site, the β -galactosidase is not working and the substrates are not converted into a coloured product: the colonies stay white. The screening of the recombinants can be done by plating the transformed bacteria on selective media containing IPTG or X-GAL. This vector is also present in the VIB collection with the code name 4171.

8. RNA isolation

Arabidopsis th. tissue is homogenized in TRIzol (1 ml for each 50-100 mg of tissue) and incubated at room temperature for 5'. 0,2 ml of chloroform are added for each ml of TRIzol and the tubes are vigorously shaken and incubated for 2-3'. Samples are centrifuged at 12000 g for 15' at 4°C. 3 phases are evident: the liquid upper phase is taken into a fresh tube. 0,5 ml of isopropyl alcohol are added for each ml of TRIzol used to homogenized the tissue and the samples are incubated at room temperature for 10'. A new centrifugation is done at max 12000 g for 10' at 4°C. Supernatant is removed and the pellet is washed with 75% ethanol (1 ml of ethanol for each initial TRIzol ml). The tube is vortexed and centrifuged at max 7500 g for 5' at 4°C. The pellet is finally dried and then dissolved in 40 μ l DEPC-treated water O/N on ice.

9. One-step RT-PCR

The one-step RT-PCR is performed with the QIAGEN[®] One-Step RT-PCR kit. Initially, a “master mix” is prepared adding the following components: 10 μ l of provided 5x QIAGEN OneStep RT-PCR Buffer, 2 μ l of provided dNTP mix (each containing 10 mM of each dNTP), 2 μ l of provided QIAGEN OneStep RT-PCR enzymes, 1-1,5 μ l of primer A and B (10 μ M each), 5-10 units/reaction of Rnase inhibitor and Rnase-free water up to final volume 50 μ l. 1 pg-2 μ g/reaction of RNA template is added to the individual tubes at the end of the mix preparation. The RT-PCR profile has an initial 30' step at 50°C for the reverse-transcription reaction, 15' at 95°C to activate the HotStarTaq DNA Polymerase and the inactivation of the Omni- and Sensiscript Reverse Transcriptases and the initial denaturation of the cDNA fragments. A 3-step cycling PCR reactions performed for 35 cycles is made to amplify the proper cDNA: 0,5-1' at 94°C as denaturation step, 0,5-1' at OAT (50-68°C max) as annealing step and 0,5-1' at 72°C as elongation step, with a final elongation step for 10' at 72°C. The products are show on an agarose gel 0,8% in TAE 0,5 X.

Table5. RT- PCR profile	
50°C for 30'	1 cycle (for cDNA formation)
95°C for 15'	1 cycle
94°C for 0,5-1'	25-35 cycles
OAT (50-68) for 0,5-1'	
72°C for 1' x Kb	
72°C for 10'	1 cycle

Table5. RT-PCR profile. This profile has been used to select and amplify AtELP genes as inserts to be used for the cloning procedure. Conditions can be changed as follow if no products are present: 45°C as initial reverse-transcription reaction, 10' at 94°C for the denaturation step in the 3-step cycling and addition of a provided Q-solution to the master mix, to be used in parallel with a master mix without Q-solution.

Table6. Primers for the cloning						
Name	Gene	Primer	Sequence	U/L comb.	OAT	Size
Deher16	ELP1	upper	AAAAAGCAGGCTCCATGAAAAATTGAAGCTTTT			
Deher17	ELP1	L-STOP	AGAAAGCTGGGTCTGGGCTTATGAAGACCTTAA	16+17	58,8	3960bp
Deher18	ELP1	L-STOP	AGAAAGCTGGGTCTCATGGGCTTATGAAGACCT	16+18	58,9	3960bp
Deher19	ELP2	upper	AAAAGCAGGCTCCATGTCCAGAAAAACACAAAAGT			
Deher20	ELP2	L-STOP	AGAAAGCTGGGTCAAACCTTGAAGTTAAAAACTC	19+20	57,6	2520bp
Deher21	ELP2	L-STOP	AGAAAGCTGGGTCTCAAACCTTGAAGTTAAAAA	19+21	57,7	2523bp
Deher22	ELP3	upper	AAAAGCAGGCTCCATGAACGGCGAGCTGAAAAA			
Deher23	ELP3	L-STOP	AGAAAGCTGGGTCAAAGAAGATGCTTCACCATGT	22+23	58,6	1698bp
Deher24	ELP3	L-STOP	AGAAAGCTGGGTCTCAAAGAAGATGCTTCACCATG	22+24	59,1	
Deher25	ELP4	upper	AAAAGCAGGCTCCATGGCTGCACCAAACGTT			
Deher26	ELP4	L-STOP	AGAAAGCTGGGTCAAATCTAGTGCTCCGGATTTG	25+26	58,8	1068bp
Deher27	ELP4	L-STOP	AGAAAGCTGGGTCTCAAATCTAGTGCTCCGGAT	25+27	58,6	
Deher28	ELP5	upper	AAAAGCAGGCTCCATGGCGGAATCGATTTT			
Deher29	ELP5	L-STOP	AGAAAGCTGGGTCAATGTCCAAATCATCATCAGGA	28+29	58,9	1179bp
Deher30	ELP5	L-STOP	AGAAAGCTGGGTCTTAAATGTCCAAATCATCATCA	28+30	57,8	
Deher31	ELP6	upper	AAAAGCAGGCTCCATGGATCGTTCTTTGAATCT			
Deher32	ELP6	L-STOP	AGAAAGCTGGGTCAATTAATGATTTGAGGAAAAA	31+32	56,5	762bp
Deher33	ELP6	L-STOP	AGAAAGCTGGGTCTCAATTAATGATTTGAGGAA	31+33	56,5	
Specific primer without gateway extension						
Defle2	ELP1	upper	atgaaaaattgaagctttctcggag			
Defle3	ELP1	L-STOP	tgggcttgaagaccttaagcctc	2+3	55,8	
Defle4	ELP1	L-STOP	tcattgggcttgaagaccttaagcctc	2+4	56,3	
Defle5	ELP2	upper	atgtcagaaaacacaaaagctgaagc			
Defle6	ELP2	L-STOP	aaacttgaagttaaaaactctcacaca	5+6	54,9	
Defle7	ELP2	L-STOP	tcaaaaacttgaagttaaaaactctcaca	5+7	55	

Table6. Primers with and without gateway extensions used for the cloning. Some primer combinations amplify fragments with stop codon (+ stop) and other without (- stop). The upper/lower primer combination, the Optimal Annealing Temperature (OAT) and size of the amplified fragments are reported. The partial att sequence is reported in bold for the upper and lower primers.

10. The cloning procedure: extraction, linearization and dephosphorylation of the vector, ligation, transformation and selection of the transformed colonies

10.1 Extraction of the plasmid from a bacterial strain with the QIAGEN Plasmid Purification Kit

Prior to extraction 1 colony has to be inoculated in 100 ml of LB⁺ + amp⁵⁰ liquid medium and let grow O/N at 37°C. The culture is then divided in 2 centrifuge tubes which have to be equilibrated. An initial centrifugation at 7000 rpm leaves a pellet which will be dissolved into the QIAGEN P1 buffer. It is good to vortex a bit. 4 ml of buffer P2 are added to the tube and also 4 ml of ice-cold buffer P3. Another centrifugation at 14000 rpm follows. The supernatant is filtrated through Miracloth paper in a 50 ml Falcon. The QIAGEN columns have to be equilibrated with QBT buffer and then the supernatant has to be put in the columns. The columns have to be washed after with 10 ml of QC buffer and afterwards the plasmid is eluted with 5 ml of QF buffer. 3,5 ml of isopropanol are added to the solution and a centrifugation at 7000 rpm for 30' is needed to precipitate the pellet, which finally is washed with 70% ethanol, centrifuged at 7000 rpm and air-dried before being dissolved in sterile water. The extraction result is checked on a 0,8% agarose gel: usually 2-3 bands are present because of the supercoiled structures of the circular plasmid.

10.2 Vector restriction

A restriction mix is prepared by adding 3µl of the restriction enzyme 10X buffer, 3µl of spermidine 40 mM, 2 µg of plasmid (5-10 µl), 20 u of the restriction enzyme and water up to a final volume of 30 µl. The mix is incubated for 2 h at 37°C. Afterwards the enzyme is inactivated at 65°C for 20' and the linearization is checked on a 0,8% agarose gel: 1 band only is expected.

10.3 Vector dephosphorylation

The vector is dephosphorylated by means of 2 µl of Calf Intestinal Phosphatase (CIP, Boehringer Mannheim) which is added to the restriction mix with 2 µl of its buffer (CIP 10X buffer) and water up to a final volume of 50 µl. The final mix is incubated for 1 h 20' at 37°C and afterwards the enzyme is deactivated at 65°C for 15'.

10.4 Purification of the vector from the restriction-dephosphorylation mix

To purify the vector ½ a volume of 7,5 M (or 5M) Ammonium Acetate and 2 volumes of EtOH 100% are added to the mix, which is afterwards incubated O/N at -20°C or 30' at -80°C. The mix is then centrifuged at 14000 rpm for 15'. The supernatant is removed and the pellet is washed with 70% EtOH. A new centrifugation at 14000 rpm is done and the pellet is air-dried and dissolved in 50-100 µl of sterile water. The concentration of the vector is then measured with a spectrophotometer. The optimal dilution of the vector should be around 30-50 ng/µl.

10.5 Ligation between vector and insert

When performing the ligation it is important to know the size of the vector and whether the DNA ends of the insert are blunt or sticky. The size is important because the ng of insert should be equal to the ng of vector * the size of the insert /size of the vector. Different insert:vector ratios are tested (1:1, 1:3, 3:1). The T4 DNA Ligase (Invitrogen) is used to perform the ligation. For blunt end inserts, made with the Platinum Pfx DNA Polymerase, the following ligation mix is made by adding 15-60 ng of vector and 45-180 ng of insert (insert:vector ratio = 3:1) to 4 µl of 5X Ligase Reaction Buffer, 1 unit of T4 DNA Ligase (1 µl) and nuclease-free water up to a final volume of 20 µl. The

The Elongator complex: its function in leaf development and germination

ligation mix is then incubated for 16-24 h at 14°C. For an optimal transformation, the ligation reaction mix should subsequently be diluted at least 5 times.

10.6 Heat-shock transformation of competent cells

The optimal temperature to perform heat-shock transformation is 42°C. Competent cells (*Escherichia coli*, JM109) are removed from -70°C and thawed on ice for 5'. 1-5 µl of insert (10 ng of DNA) are added to 40-100 µl of competent cells. Heat-shock is performed in a water-bath set at 42°C for 1'-1'30". Cells are then immediately put on ice for 2'. 300-900 µl of cold SOC medium (or in alternative LB⁺ liquid medium) are added in each tube, which is afterwards incubated for 1h at 37°C on a shaker at 225 rpm. For each transformation reaction, the cells are diluted 10 and 100 times. The undiluted and diluted tubes are plated on LB⁺ + agar + amp⁵⁰ + IPTG (isopropyl-β-thiogalactopyranoside) + Xgal (5-bromo-4-chloro-3-indolyl-beta-D-galactopyranoside, the colour indicator for β-galactosidase activity) and incubated O/N at 37°C. The plates are then put at 4°C to perform the blue/white coloration. The white colonies are the transformed ones containing the insert. These colonies are plated individually on new plates and incubated O/N at 37°C. Colony-PCR is then performed with gene specific primers or SP6/T7 primers, in order to identify the insert. The size of the insert is checked on gel and after purification the PCR product is sequenced. The colony-PCR uses the colony as DNA template.

10.7 Preparation of the "white and blue" selection plates

LB⁺ + agar + amp⁵⁰ plates are taken from the 4°C storage room and dried under the laminar flow bench for 30'. The "white and blue" selection mix is prepared by adding 4µl of IPTG in 40 µl of Xgal/plate. These 2 products are stored at -20°C and in the dark. The mix is plated under the laminar flow bench and the plates are dried for 15'.

References

- Bechtold, N., Ellis, J. and Pelletier, G. (1993). "In planta *Agrobacterium* mediated gene transfer by infiltration of adult *Arabidopsis thaliana* plants." C.R. Acad. Sci. Paris, Life Sciences, **316**, 1194-1199.
- Bernà, G., Robles, P., and Micol, J.L. (1999). "A mutational analysis of leaf morphogenesis in *Arabidopsis thaliana*." Genetics, **152**, 729-742.
- Bouchez, D., Camilleri, C. and Caboche, M. (1993). "A binary vector based on Basta resistance for in planta transformation of *Arabidopsis thaliana*". C.R. Acad. Sci. Paris, Life Sciences, **316**, 1188-1193.
- Cnops, G., Den Boer, B., Gerats, A., Van Montagu, M., and Van Lijsebettens, M., (1996). "Chromosome landing at the *Arabidopsis* TORNADO1 locus using AFLP-based strategy." Mol. Gen. Genet., **253**, 32-41.
- Cnops, G., Wang, X., Linstead, P., Van Montagu, M., Van Lijsebettens, M., and Dolan, L. (2000). "TORNADO1 and TORNADO2 are required for the specification of radial and circumferential pattern in the *Arabidopsis* root." Development, **127**, 3385-3394.
- Edwards, K., Johnstone, C. and Thompson, C. (1991). "A simple and rapid method for the preparation of plant genomic DNA for PCR analysis." Nucl. Ac. Res., **19** (6), 1349.
- Johanson, U., West, J., Lister, C., Michaels, S., Amasino, R. and Dean, C. (2000). "Molecular Analysis of FRIGIDA, a Major Determinant of Natural Variation in *Arabidopsis* Flowering Time." Science, **290**, 344-347.
- Rychlik, W., Spencer, W.J., and Rhoads, R.E. (1990). "Optimization of the annealing temperature for DNA amplification in vitro." Nucleic Acids Res., **18**, 6409-6412.
- Nelissen, H., Clarke, J., H., De Block, M., De Block, S., Vanderhaeghen, R., Zielinski, R., E., Dyer, T., Lust, S., Inzé, D. and Van Lijsebettens, M., (2003). "DRL1, a homolog of the Yeast TOT4/KTI12 protein, has a function in meristem activity and organ growth in plants." The Plant Cell, **15**, 639-654.
- Tel-Zur, N., Abbo, S., Myslabodski, D. and Mizrahi, Y. (1999). "Modified CTAB procedure for DANN Isolation from epiphytic cacti of the genera *Hyllocereus* and *Selenicereus* (Cactaceae)." Plant Molecular Biology Reporter, **17**, 249-254.
- Tsuge, T., Tsukaya, H., and Uchimiya, H. (1996). "Two independent and polarised processes of cell elongation regulate leaf blade expansion in *Arabidopsis thaliana* (L.) Heynh." Development, **122**, 1589-1600.
- Valvekens, D., Van Montagu, M., and Van Lijsebettens, M., (1988). "*Agrobacterium tumefaciens*-mediated transformation of *Arabidopsis thaliana* root explants by using kanamycin selection." Proc. Natl. Acad. Sci. USA, **85**, 5536-5540.
- Vos, P., Hogers, R., Bleeker, M., Reijans, M., Lee, T., Van de Horne, M., Frijters, A., Pot, J., Peleman, J., Kuiper, M. and Zabeau, M. (1995). "AFLP: a new technique for DNA fingerprinting". Nucleic Acids Res., **23**, 4407-4414.

Publications, posters and workshops

Publications

Elongator has a function in plant growth and development in response to environmental conditions

Nelissen, H., Fleury, D., Granier, C., Bruno, L., Falcone, A., Bitonti, B., Delaure, S., Cammue, De Block, M., Inzé, D. and Van Lijsebettens, M.
Plant Cell, in preparation.

Cytological Investigations of the *Arabidopsis thaliana* elo1 Mutant Give New Insights into Leaf Lateral Growth and Elongator Function

Andrea Falcone, Mieke Van Lijsebettens and Maria Beatrice Bitonti.
Annals of Botany, November 2006, submitted

Il saccarosio nell'espansione fogliare laterale: un'analisi morfometrica e citoistologica del mutante *ELO1* di *Arabidopsis thaliana*

Falcone, A., Van Lijsebettens, M and Bitonti, MB
Informatore Botanico Italiano, 2005, 37 (1, parte B), pp. 714-715

Posters

Il saccarosio nell'espansione fogliare laterale: un'analisi morfometrica e citoistologica del mutante *ELO1* di *Arabidopsis thaliana*

Falcone, A., Van Lijsebettens, M and Bitonti, MB
Società Botanica Italiana, 20-23 Settembre 2005, Roma, Italia

Genome wide expression analysis to investigate function of Elongator genes in *Arabidopsis* leaf development

Fleury-Herve D., Nelissen H, Falcone A, Inze D, Van Lijsebettens M
Plant & Animal Genomes, XII Conference January 10-14, 2004, Town & Country Convention Center, San Diego, CA, USA.

Functional analysis of Elongator in plant development

Nelissen, H., Fleury, D., Falcone, A., Inze, D. and Van Lijsebettens, M
Plant Genetics 2003 Mechanisms of Genetic Variation, October 22-26, 2003, Snowbird, Utah.

Genetic factors that determine leaf size and shape in *Arabidopsis*

Nelissen H., Cnops G., Fleury D., Petrarulo M., Falcone A. and Van Lijsebettens M.
Società Botanica Italiana, Riunione Congiunta Gruppi di Lavoro Biologia Cellulare e Molecolare - Biotecnologie e Differenziamento, 2-4 Luglio 2003, Falerna, Italia

Workshops

Introduzione alla Genomica e Proteomica con Elementi di Bioinformatica

ENEA, Scuola Estiva C.R. TRISAIA, 21-25 Giugno 2004

**Relazione finale del Collegio dei docenti
sull'attività svolta dal dott.re Andrea FALCONE**

Durante il corso di dottorato in Biologia Vegetale il dott.re Andrea FALCONE ha analizzato, nel sistema modello *Arabidopsis thaliana*, alcuni aspetti citofisiologici del ruolo svolto dal complesso Elongator, coinvolto nell'elongazione della trascrizione, prendendo in esame la germinazione dei semi e lo sviluppo della foglia. I risultati di tale lavoro, programmato all' inizio del corso con il docente guida, prof. Maria Beatrice Bitonti, sono oggetto della tesi di dottorato, dal titolo "The Elongator complex and its function in leaf development and germination".

Il lavoro è stato svolto in parte presso il Department of Plant System Biology, Flanders Interuniversity Institute of Biotechnology (Gent, Belgium), sotto la supervisione della Prof. Mieke Van Lijsebettens, in qualità di vincitore di una borsa annuale del Marie Curie Training Site Fellowships (HPMT-CT-2000-00088). Nel corso di tale periodo il dott.re A. Falcone, accanto ad un'indubbia crescita culturale, ha sviluppato notevole padronanza nell'uso di svariati approcci metodologici, volti a individuare nuovi alleli per gli omologhi del Complesso Elongator di lievito in *Arabidopsis thaliana*. Altri studi hanno invece riguardato i mutanti foliari DRL1ox10B5 (una linea che overesprime DEFORMED ROOTS AND LEAVES1), RON1 (ROTUNDA1) e TRN1 (TORNADO) sempre di *Arabidopsis thaliana*.

Al suo rientro presso l'Università della Calabria, il dott.re A. Falcone, con pregevole e spiccata autonomia progettuale, che lo ha portato talvolta a privilegiare alcuni specifici aspetti del lavoro da sviluppare, ha programmato e portato avanti lo studio delle relazioni tra sviluppo della foglia, condizioni di crescita e ruolo del Complesso Elongator in *Arabidopsis thaliana*. Attraverso un approccio multiparametrico, che ha previsto test di germinazione, analisi morfometriche e ultrastrutturali su piante wild type e sul mutante *elo1*, il dott.re A. Falcone è pervenuto ad originali risultati, relativi alla prima caratterizzazione citofisiologica ed ultrastrutturale del mutante stesso, ed interessanti ed innovative indicazioni sul ruolo di Elongator .

Dotato di forte capacità interpretativa dei dati ottenuti, frutto anche di un costante ed approfondito studio della letteratura scientifica sul tema di ricerca, cui lo stesso si è dedicato con particolare cura e sicuro profitto, il dott.re A. Falcone, in collaborazione con il gruppo dell'Università di Gent, ha inoltre portato avanti l'analisi del pattern dei geni differenzialmente espressi nei mutanti elo, identificati da tale gruppo, giungendo ad

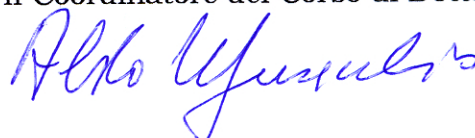
elaborare un modello funzionale per il complesso Elongator, correlato alla disponibilità di saccarosio e stadio-specifico.

I risultati del proficuo lavoro svolto dal Dott.re A. Falcone nel corso del dottorato hanno portato alla stesura di un manoscritto sottoposto per la pubblicazione su rivista internazionale del settore, mentre è in corso la stesura, in collaborazione con il gruppo di Ghent, di un secondo manoscritto relativo all'analisi dei profili di espressione genica, che mira a rivista con elevato impact factor IRC. Nel corso dei tre anni i risultati preliminari sono stati inoltre oggetto di pubblicazione di un lavoro breve su rivista nazionale e di comunicazione a Congressi Nazionali ed Internazionali.

Su tali basi il collegio dei docenti esprime piena soddisfazione per quanto il dott. re Andrea FALCONE ha realizzato nel corso del dottorato e vivo apprezzamento per la indubbia crescita scientifica raggiunta.

A nome del Collegio dei docenti

Il Coordinatore del Corso di Dottorato

Handwritten signature in blue ink, appearing to read "Aldo Fusco".

Extras



Gent 29th October 2003

Evaluation of Andrea Falcone (1st year PHD student)

Andrea Falcone has been working in the Department of Plant Systems Biology (Ghent University, Belgium) for one year (15/11/2002 till 7/11/2003). He studied leaf development in the model plant *Arabidopsis* by mutational analysis. The focus of his work was on DNA methods, bio-informatics, Mendelian genetics, tissue culture, DIC microscopy and image analysis. Skills in several computer programs were acquired such as SPSS, Scion image, WORKBENCH, BLAST, CLUSTAL. He got notice of the TAIR *Arabidopsis* database and can autonomously use it for his research. Andrea is very dedicated to the work. He is fast learning and very precise. He functions very autonomously and takes a lot of initiative. He is also very precise in the registration of the results in the notebook, and he is strong in the interpretation of the results. He is able to make a daily and more long-term planning for the work and he is also very much aware of the literature. He has a lot of background knowledge which he integrates with the experimental results or with the design of new experimental setup. Andrea functions very well in a research unit, he has a lot of social skills and takes responsibility in good laboratory practice.

Andrea has a lot of potential and he is determined to become a good scientist.

Prof. Dr. Mieke Van Lijsebettens